

Evaluating the Methodology and Performance of Jetting and Flooding Granular Backfill Materials

Dante Fratta, Associate Professor

University of Wisconsin-Madison

WisDOT ID no. 0092-11-03

November 2014



RESEARCH & LIBRARY UNIT



WISCONSIN HIGHWAY RESEARCH PROGRAM

WISCONSIN DOT
PUTTING RESEARCH TO WORK

DISCLAIMER

This research was funded through the Wisconsin Highway Research Program by the Wisconsin Department of Transportation and the Federal Highway Administration under Project 0092-11-03. The contents of this report reflect the views of the authors who are responsible for the facts and accuracy of the data presented herein. The contents do not necessarily reflect the official views of the Wisconsin Department of Transportation or the Federal Highway Administration at the time of publication.

This document is disseminated under the sponsorship of the Department of Transportation in the interest of information exchange. The United States Government assumes no liability for its contents or use thereof. This report does not constitute a standard, specification or regulation.

The United States Government does not endorse products or manufacturers. Trade and manufacturers' names appear in this report only because they are considered essential to the object of the document.

Technical Report Documentation Page

1. Report No.	2. Government Accession No	3. Recipient's Catalog No	
4. Title and Subtitle EVALUATING THE METHODOLOGY AND PERFORMANCE OF JETTING AND FLOODING GRANULAR BACKFILL MATERIALS		5. Report Date November 2014	6. Performing Organization Code
7. Authors Dante Fratta and Jeff Newgard		8. Performing Organization Report No.	
9. Performing Organization Name and Address University of Wisconsin-Madison 21 N. Park St., Suite 6401 Madison, WI 53715-1218		10. Work Unit No. (TRAIS)	11. Contract or Grant No. 0092-11-03
12. Sponsoring Agency Name and Address Wisconsin Department of Transportation Research & Library Unit 4802 Sheboygan Ave. Rm 104 Madison, WI 53707		13. Type of Report and Period Covered	
		14. Sponsoring Agency Code Wisconsin Highway Research Program (WHRP)	
15. Supplementary Notes			
16. Abstract Compaction of backfill in confined spaces on highway projects is often performed with small vibratory plates, based solely on the experience of the contractor, leading to inadequate compaction. As a result, the backfill is prone to erosion and often exhibits excessive settlements, causing loss of support beneath pavements. The scope of this project includes developing standard specifications for two alternative hydraulic compaction methods, flooding and jetting, which additionally are suitable in confined spaces. During flooding, or compaction by drainage, the backfill layer is saturated with water from the surface and allowed to drain. During jetting, a probe emitting a high pressure jet of water is inserted into the layer, and the backfill is allowed to drain. In slurry flooding, a slurry mix is flood into place and it is allowed to drain so the lift gains strength. In these cases the energy of the flowing water and residual suction upon drainage increase the effective stress and move the grains into a denser arrangement. The results in the lab indicate that for compaction by drainage applications, uniform, rounded soils achieve the highest relative density due to their minimal particle interlocking upon deposition and subsequent high drainage capacity. Meanwhile during jetting applications, soils liquefy locally around the jet of water, and their compactness upon drainage is highly dependent on the hydraulic gradient, or the energy with which water drains from the pore space. Greater hydraulic gradient during the drainage phase of jetting has been observed to produce more compact soil structure.			
17. Key Words Backfill, flooding compaction, jetting compaction, laboratory testing, field testing		18. Distribution Statement No restriction. This document is available to the public through the National Technical Information Service 5285 Port Royal Road Springfield VA 22161	
18. Security Classif.(of this report) Unclassified	19. Security Classif. (of this page) Unclassified	20. No. of Pages 163	21. Price

TABLE OF CONTENTS

FRONT PAGE.....	1
DISCLAIMERS.....	2
TECHNICAL REPORT DOCUMENTATION PAGE.....	3
TABLE OF CONTENTS.....	4
LIST OF FIGURES	6
LIST OF TABLES.....	9
EXECUTIVE SUMMARY	11
1. INTRODUCTION.....	12
2. LITERATURE REVIEW	15
2.1 'BUMP AT THE END OF THE BRIDGE' PROBLEM.....	15
2.2 COMPACTION AROUND UTILITIES AND MSE RETAINING WALLS	18
2.3 TRADITIONAL COMPACTION METHODS	20
2.3.1 Rubber-tired Roller.....	21
2.3.2 Dynamic Compaction	21
2.3.3 Vibration Compaction.....	22
2.3.4 Hydraulic Fills.....	24
2.4 RECOMMENDATIONS FOR JETTING AND FLOODING	26
2.5 INDUSTRY SPECIFICATIONS.....	27
2.6 SUMMARY OF LITERATURE REVIEW	34
3. CHARACTERIZATION OF TESTED MATERIALS AND FIELD METHODS	35
3.1 PARTICLE SIZE DISTRIBUTION	35
3.2 SPECIFIC GRAVITY	38
3.3 MAXIMUM AND MINIMUM VOID RATIO	39
3.4 PARTICLE SHAPE.....	41
3.5 PROCTOR COMPACTION	45
3.6 FIELD METHODS	47
4. LAB RESULTS AND DISCUSSION	50
4.1 LABORATORY TESTING DESCRIPTION	50
4.2 COMPACTION BY DRAINAGE IN THE LIQUEFACTION TANK.....	51
4.2.1 Flooded Deposition	51
4.2.2 Wet Deposition.....	57
4.2.3 Dry Deposition at Low and High Energy.....	62

4.2.4	Sensitivity Analysis.....	69
4.2.5	Compaction by Drainage Conclusions.....	70
4.3	COMPACTION BY JETTING IN THE TANK.....	71
4.3.1	Test Setup.....	71
4.3.2	Initial Observations and Hypotheses	71
4.3.3	Comparison of Deposition Method and Material Type	72
4.3.4	Comparison of Drainage Energy	74
4.3.5	Jetting Conclusions	77
4.4	RIGID WALL-FALLING HEAD CONDUCTIVITY TESTING	80
4.5	COMPACTION BY JETTING IN THE PLASTIC CONTAINERS.....	87
4.6	TESTS OF WISDOT BACKFILL MATERIALS	94
5.	FIELD RESULTS AND DISCUSSION	97
5.1	COMPACTION BY DRAINAGE AT HIGHWAY 51 SITE.....	97
5.2	COMPACTION BY SLURRY FLOODING AT HIGHWAY 51 SITE.....	105
5.3	COMPACTION BY JETTING AT GREENFIELD AVENUE	114
6.	HYDRAULIC MODELING OF FIELD SCALE JETTING TESTS	120
6.1	CONTEXT AND JUSTIFICATION OF MODELING	120
6.2	DETAILS OF MODFLOW WITH GROUNDWATER VISTAS	122
6.3	STEADY STATE MODELS FOR COMPACTION BY DRAINAGE	123
6.4	TRANSIENT MODELS FOR JETTING	130
6.5	MODELING CONCLUSIONS	149
7.	CONCLUSIONS.....	151
	REFERENCES	154
	APPENDIX.....	156
A.1	Void Ratio Calculation for Flooded Deposition.....	157
A.2	Void Ratio Calculation for Wet Deposition	160
A.3	Conclusions from Measurement Analysis	162

LIST OF FIGURES

Figure 1.1. Backhoe Outfitted with Vibrating Plate Compacting Fill.

Figure 2.1. Most Erodible Soils. Note that coarse, gravel size backfill is preferred to increase drainage behind bridge abutments (modified after Briaud et al. 1997).

Figure 2.2. Equipment for Deep Vibratory Compaction.

Figure 3.1. Particle Size Distribution Curves for Clean Sands.

Figure 3.2. Particle Size Distribution Curves for Coarser Materials.

Figure 3.3. Particle Size Distribution Curves for Materials at Highway 51 Project Site.

Figure 3.4. Krumbein Roundness Chart for Visual Characterization of Particle Shape.

Figure 3.5. Microscope Image of Limestone Screenings.

Figure 3.6. Microscope Image of Patio/Paver Base.

Figure 3.7. Microscope Image of Silica Sand.

Figure 3.8. Microscope Image of Bedding Sand.

Figure 3.9. Microscope Image of Clean Sand.

Figure 3.10. Microscope Image of Foundry Mix.

Figure 3.11. Microscope Image of Leveling Sand.

Figure 3.12. Microscope Image of Foundry Sand.

Figure 3.13. Standard proctor Compaction Curve for Silty Sand.

Figure 3.14. Compaction Curves for Sandy Backfill.

Figure 3.15. Nuclear Density Gauge, Soil Stiffness Gauge, and Dynamic Cone Penetrometer.

Figure 4.1. Flooded Deposition in the Tank.

Figure 4.2. Wet Deposition in the Tank.

Figure 4.3. Low Energy, Dry Deposition in the Tank during Round 1.

Figure 4.4. Low Energy, Dry Deposition in the Tank during Round 2.

Figure 4.5. High Energy, Dry Deposition in the Tank.

Figure 4.6. Summary of Compaction by Drainage in the Liquefaction Tank.

Figure 4.7. Hydraulic Jetting in the Tank.

Figure 4.8. Results From Jetting Tests Under the Vacuum in the Liquefaction Tank.

Figure 4.9. Conductivity versus Void Ratio Relationships for Plastic Container Materials.

Figure 4.10. Conductivity versus Void Ratio Relationships for Liquefaction Tank Materials.

Figure 4.11. Drain Tile Constructed from PVC Pipe. Setup with Central Drainage Column.

Figure 4.12. Voids Left Over After Jetting a Regular Grid.

Figure 4.13. Soil Relative Compaction with respect to Jetting Application.

Figure 4.14. Soil Stiffness with respect to Jetting Application.

Figure 4.15. Silty Sand in Viscous State Upon Completion of Jetting.

Figure 4.16. Wisconsin DOT Backfills Subjected to Both Jetting and Compaction by drainage in the Tank.

Figure 5.1. Bridge plans from Highway 51 at Bear Tree Parkway.

Figure 5.2. Flooding the Backfill to Initiate Compaction by Drainage.

Figure 5.3. Ponding Observed on the Backfill Surface During Flooding.

Figure 5.4. Compaction Results at the Highway 51 Site.

Figure 5.5. DCP in Action. Close-up of Fissured Flooded-Compacted Backfill.

Figure 5.5. Perspective of Fissured Flooded-Compacted Backfill. Drain Tile at Abutment.

Figure 5.6: Geographic location of the Highway 51 and Bear Tree Rd. Bridge for the slurry flooding compaction field test (Map source: Google Maps).

Figure 5.7: Properties of the slurry as presented by the contractor in the field.

Figure 5.8: Construction of the backfill using slurry flooding compaction technique.

Figure 5.9. Complete flooding of the backfill. Please note that the stone are now visible soon after the completion indicating the drainage characteristics of the solid material in the slurry.

Figure 5.10: Approximate location (red dots) of the nuclear density gauge, Geogauge, and dynamic cone penetration testing in both slurry and control compaction.

Figure 5.11: Compaction equipment used in the controlled backfill.

Figure 5.12. Dynamic cone penetration results on the control back fill the plot shows an equivalent measurement of shear strength as measured as blow per cm of DPC penetration. Points 1, 2 and 3 are next to the abutment while Point 4 is 5 m away.

Figure 5.13. Dynamic cone penetration results on the slurry flooding compaction 45 minutes after placement: the plot shows an equivalent measurement of shear strength as measured as blow per cm of DPC penetration.

Figure 5.14. Dynamic cone penetration results on the slurry flooding compaction 1 day after placement: the plot shows an equivalent measurement of shear strength as measured as blow per cm of DPC penetration.

Figure 5.15. Dynamic cone penetration results on the slurry flooding compaction on a mature lift: the plot shows an equivalent measurement of shear strength as measured as blow per cm of DPC penetration.

Figure 5.16. Cross Section of Pavement Structure at Greenfield Avenue.

Figure 5.17. Pictures of Jetting Operation at Greenfield Avenue.

Figure 5.18. Sandy Soils Subjected to Compaction by Drainage in the Tank in the Lab.

Figure 6.1. Jetting Case 1: Single Injection Well in Layer 2.

Figure 6.2. Mass Balance Dialog for Jetting Case 1.

Figure 6.3. Jetting Case 2: Single Injection Well in Layer 2 with Low Conductivity Native Soil.

Figure 6.4. Mass Balance Dialog for Jetting Case 2.

Figure 6.5. Jetting Case 3: Single Injection Well in Layer 2 with Low Conductivity Backfill.

Figure 6.6. Mass Balance Dialog for Jetting Case 3.

Figure 6.7. Flooding Case with Ten Injection Wells Near the Surface.

Figure 6.8. Jetting Case 4.

Figure 6.9. Grid for Jetting Case 4.

Figure 6.10. Hydrograph of Pressure Head at the Monitoring Well for Jetting Case 4.

Figure 6.11. Backfill-Native Soil Interface.

Figure 6.12. Jetting Case 5.

Figure 6.13. Grid for Jetting Case 5.

Figure 6.14. Hydrograph of Pressure Head at the Monitoring Well for Jetting Case 5.

Figure 6.15. Mass Balance Dialog for Jetting Case 5.

Figure 6.16. Jetting Case 6.

Figure 6.17. Hydrograph of Pressure Head at the Monitoring Well for Jetting Case 6.

Figure 6.18. Mass Balance Dialog for Jetting Case 6.

Figure 6.19. Mass Balance Hydrograph for Case 7.

Figure 6.20. Grid for Jetting Case 7-9.

Figure 6.21. Jetting Case 8 at 500 Seconds.

Figure 6.22. Jetting Case 8 at 800 Seconds.

Figure 6.23. Jetting Case 8 at 1200 Seconds or 20 Minutes After Initiation of Jetting.

Figure 6.24. Mass Balance Hydrograph for Case 9.

Figure 6.25. Hydrograph of Pressure Head at the Monitoring Well for Case 9.

Figure 6.26. Jetting Case 9 at 54 Minutes.

LIST OF TABLES

Table 2.1. Gradation Limits of Select Backfill Material.

Table 2.2. Acceptable Gradation of Floodable Backfill Materials.

Table 3.1. Specific Gravity of Soils.

Table 3.2. Minimum and Maximum Index Void Ratios of Lab-Tested Materials.

Table 4.1. First Round of Tests for Flooded Deposition in the Liquefaction Tank.

Table 4.2. Second Round of Tests for Flooded Deposition in the Liquefaction Tank.

Table 4.3. First Round of Tests for Wet Deposition at Slightly Wet in the Liquefaction Tank.

Table 4.4. Second Round of Tests for Wet Deposition at Very Wet in the Liquefaction Tank.

Table 4.5. Changes to Water Content and Relative Density Between Round 1 and Round 2.

Table 4.6. First Round of Tests for Dry Deposition at Low Energy in the Liquefaction Tank.

Table 4.7. Second Round of Tests for Dry Deposition at Low Energy in the Liquefaction Tank.

Table 4.8. First Round of Tests for Dry Deposition at High Energy in the Liquefaction Tank.

Table 4.9. Second Round of Tests for Dry Deposition at High Energy in the Liquefaction Tank.

Table 4.10. Changes to Water Content and Relative Density Between Round 1 and Round 2.

Table 4.11. First round of Tests: Jetting Selected Materials Deposited at High Energy in the Tank.

Table 4.12. Second Round of Tests: Jetting Selected Materials Deposited Wet in the Tank.

Table 4.13. Third Round of Tests: Jetting Selected Materials Under Greater Hydraulic Gradient.

Table 4.14. Fourth Round of Tests: Jetting Selected Materials Under Vacuum.

Table 4.15. Fifth Round of Tests: Jetting Selected Materials Under Vacuum.

Table 4.16. Comparison of Relative Density of Soils Subjected to Varying Drainage Energies.

Table 4.17. Comparison of Conductivity and Void Ratio Between Trial 3 and Trial 4.

Table 4.18. Additional Conductivity Results for Finer Soils seen at Highway 51 Project Site.

Table 4.19. Void Ratio and Conductivity for Trial 1.

Table 5.1. Summarizes the nuclear density gauge results on the control compaction

Table 5.2. Summarizes the nuclear density gauge results on the slurry flooding compaction

Table 5.3. Summarizes the GeoGauge results on the control compaction

Table 5.4. Summarizes the GeoGauge results on the slurry flooding compaction

Table A.1. Phase Calculations as Presented in Section 4.

Table A.2. Measurements Made During Silica Sand, Flooded Deposition Test.

Table A.3. Reasonable Estimate of Errors Made During Silica Sand, Flooded Deposition Test.

Table A.4. Measurements Made During Silica Sand, Wet Deposition Test.

Table A.5. Reasonable Estimate of Errors Made During Silica Sand, Wet Deposition Test.

EXECUTIVE SUMMARY

Compaction of backfill in confined spaces on highway projects is often performed with small vibratory plates, based solely on the experience of the contractor, leading to inadequate compaction. As a result, the backfill is prone to erosion and often exhibits excessive settlements, causing loss of support beneath pavements. The scope of this project includes developing standard specifications for two alternative hydraulic compaction methods, flooding and jetting, which additionally are suitable in confined spaces. During flooding, or compaction by drainage, the backfill layer is saturated with water from the surface and allowed to drain. During jetting, a probe emitting a high pressure jet of water is inserted into the layer, and the backfill is allowed to drain. In slurry flooding, a slurry mix is flood into place and it is allowed to drain so the lift gains strength. In these cases the energy of the flowing water and residual suction upon drainage increase the effective stress and move the grains into a denser arrangement. The results in the lab indicate that for compaction by drainage applications, uniform, rounded soils achieve the highest relative density due to their minimal particle interlocking upon deposition and subsequent high drainage capacity. Meanwhile during jetting applications, soils liquefy locally around the jet of water, and their compactness upon drainage is highly dependent on the hydraulic gradient, or the energy with which water drains from the pore space. Greater hydraulic gradient during the drainage phase of jetting has been observed to produce more compact soil structure.

SECTION 1 – INTRODUCTION

Achieving uniform compaction of granular backfill materials on highway projects is especially important near structures such as bridge abutments, mechanically-stabilized earth (MSE) wall faces, and around sewer lines or utility repairs. Inadequate compaction produces weak backfill that is prone to erosion, leading to excessive settlements, and consequently causing loss of support beneath pavements. Compaction describes the process of rearranging solid particles and removing air voids within the soil. When soils are compacted to a denser state, they will exhibit higher strength, lower compressibility, and lower permeability (Drnevich et al., 2007). If the soils are not properly compacted, they will have poor strength properties. This often results in large settlements, poor shear strength, liquefaction (in saturated coarse grained soils) and subsequent washout of materials (White et al., 2007).

However, large equipment, such as steel drum vibratory rollers, cannot operate near bridge abutments, mechanically-stabilized earth (MSE) wall faces, and around sewer lines or utility repairs due to practical considerations. For example, excessive compactive effort or use of heavy equipment near MSE walls could cause face movement or structural damage to the panels (Berg et al., 2009), or deform and break culverts and pipes. This is particularly dangerous when operating heavy compaction equipment above sewer lines. The equipment creates an unsafe load concentration in the pipe (Moser et al., 2008). For these reasons, equipment such as small single or double drum, walk-behind vibratory rollers or handheld vibratory plate compactors are often used for compaction within 1 m (3 ft.) of bridge abutments and MSE walls (Berg et al., 2009). Above sewer lines, “compaction” is commonly performed sporadically throughout the fill using a vibrating plate on the end of a backhoe (Schaefer et al., 2005), as seen in Figure 1.1. These methods tend to have little standardization by specification, and are instead performed based on the experience of the contractor. One of the worst construction practices is to try compacting backfill by driving trucks or dozers above sewer

trenches or near wall faces; this should never be permitted, as it will lead to gross misalignments and settlement problems (Berg et al., 2009).



Figure 1.1. Backhoe Outfitted with Vibrating Plate Compacting Fill. Often this type of operation is performed hastily before an inspector can arrive at the site to check the quality of the compaction.

This lack of standardization can result in non-uniform compaction near the structures and subsequent poor structural performance of the soils. Meanwhile, current inspection methods are often inadequate to detect non-uniform compaction. The use of the nuclear density gauge, while quick and reliable, offers only a spot check for dry density and moisture content of compacted backfill material (Schaefer et al., 2005). Other quality control methods to check compaction, such as the dynamic cone penetrometer test, or time domain reflectometry, have shown promise in research studies, but have not been adopted in state highway inspection specifications (Drnevich et al., 2007).

The scope of this project includes developing standard specifications for two alternative hydraulic compaction methods, flooding and jetting, which are well-suited to use in confined spaces. During flooding, or compaction by drainage, the backfill layer is saturated with water from the surface and allowed to drain. During jetting, a probe emitting a high pressure jet of water is inserted and removed from the layer in a specified grid, and the backfill is allowed to

drain. In both cases the energy of the flowing water and residual suction upon drainage increase the effective stress and move the grains into a more compact arrangement.

This report details all the results and experiences surrounding the investigation of jetting and flooding, and is organized into the following five sections:

- (1) Review of traditional compaction methods and best practices in flooding and jetting
- (2) Characterization of coarse-grain materials used in this study by lab index tests
- (3) Flooding and jetting experiments in the lab
- (4) Observations and lessons learned at Highway 51 and Greenfield Avenue project field sites
- (5) Numerical modeling of a jetting application to improve performance

The Highway 51 project site is located in DeForest, Wisconsin and consists of four bridge abutments at a divided four lane state highway. One of the abutments serves as a control, to be compacted by traditional means. The other three abutments are compacted by drainage only or jetting. The backfill at this site is a natural sand qualifying as structural fill (Section 209, Standard Specifications for Construction) typically used by the Wisconsin DOT. The Greenfield Avenue project site is located in Milwaukee, Wisconsin and consists of a buried sanitary sewer pipe beneath the roadway. The backfill in the sewer trench is a recycled concrete material to be compacted by jetting.

SECTION 2 - LITERATURE REVIEW

2.1 'BUMP AT THE END OF THE BRIDGE' PROBLEM

There is a wealth of literature investigating how to remediate poor compaction as part of a larger problem that is often called the “bump at the end of the bridge.” This moniker refers to the difference in settlement that occurs at the abutment-backfill interface. Because bridge abutments are commonly built into deep foundations and thus exhibit minimal settlement, any compression in the backfill supporting the approach pavement results in the bump (Schaefer et al., 2005). In this way, the compaction issues should be analyzed not as a stand-alone element but as part of a larger system with interrelated forces at work. Many authors have stressed a multidisciplinary approach to solve this problem incorporating improvements in geotechnical and structural design, as well as construction practices. Briaud et al. (1997) conducted a literature review and disseminated a questionnaire to 72 highway engineers from 48 states. The results of the review showed common causes for bumps; listed from highest to lowest importance they are (1) compression of fill material, (2) time dependent consolidation of the natural soil beneath the embankment, (3) poor construction practices, (4) high traffic loads, (5) poor drainage, (5) poor fill material, (6) loss of fill by erosion, (7) poor joints, and (8) temperature cycles.

In terms of this project, it is worthwhile to note that the most important and widespread cause of bumps near bridge abutments is compression of the fill material, often resulting from inadequate compaction. Furthermore, five of the eight primary causes of bumps listed above are related to geotechnical engineering aspects. Clearly, a specification system that addresses an improved drainage system, backfill type, foundation system, and/or compaction method in the confined space could aid greatly to eliminate the bump at the end of the bridge.

Related to this problem, White et al. (2005) developed a more in-depth focus on the geotechnical issues and performed research that led to simple recommendations to improve soil-structure interaction near bridges. The authors indicated that water management is critical,

both during and long after construction, for the proper long-term performance of backfill materials. During compaction, coarse-grained soil used in backfills may exhibit a phenomenon known as “bulking,” wherein the curved water-air interface is stressed in tension due to capillary effects, allowing the water to hold soil particles in place and resist compactive effort (Drnevich et al., 2007). The typical bulking water content is generally between 2-10% for coarse-grained backfill materials (6). To avoid this effect, the backfill should ideally be compacted at either oven dry, or completely saturated condition, as this results in the maximum dry density (Drnevich et al., 2007). However, this is not practical and it is acceptable to simply compact backfill outside the range of bulking moisture contents. If this objective is not achieved, the backfill could eventually collapse upon saturation, as the capillary tension is lost between water and solid particles (White et al., 2007). Please note that as matter of practice most materials are compacted within this bulking range which would lead to a decrease in stiffness if the material becomes saturated.

Other water management strategies are vital to prevent problems near the bridge approach, including the design of an effective subsurface drainage system and water-tight seals in any expansion joints in the pavement approach slab or bridge structure. Poor gradation design may lead to migration of fine particles into the 2.0 mm openings in a typical perforated subdrain tile, preventing water from draining away from the structure. The fine particle-clogged drain tile leads to pore water pressure buildup behind the structure, facilitating erosion of soils and loss of support beneath the pavement (White et al., 2007). The gradation limits, as prescribed by Briaud et al. (1997), of these finer, more erodible soils are shown in Figure 2.1. The figure also includes the minimum passing requirements set by WisDOT Specifications - Section 209 and the gradation of the material used in the compacted layers in the Highway 51 project.

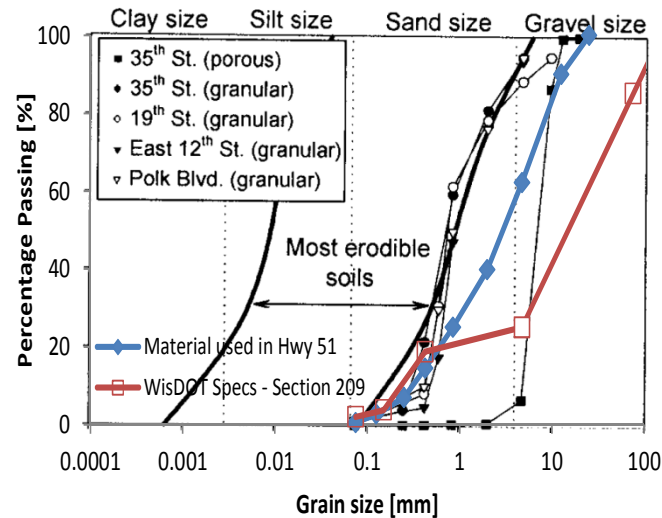


Figure 2.1. Most Erodible Soils. Note that coarse, gravel size backfill is preferred to increase drainage behind bridge abutments (modified after Briaud et al. 1997)

To remediate clogged drain tiles, it is recommended that an alternative gradation which limits materials passing the No. 8 sieve (2.4 mm – 0.1 in.) to less than about 60%, be implemented (White et al., 2007). It may even be possible to substitute pea gravel in place of sandy backfill. This more open-graded, coarser, porous backfill is less erodible, prevents plugging of the perforated subdrain, and increases the drainage capacity because it has higher hydraulic conductivity (White et al., 2007). This modification in gradation, from a well-graded material to a more uniformly graded material, would also enhance the effectiveness of the geosynthetic cover around the subdrain tile. On the other hand, simplifying expansion joint designs and sealing joints with premolded neoprene strip seals or field-molded polymer seals with asphalt plug joint systems represents a proactive method to limit the amount of water seeping beneath the approach pavements (White et al., 2007).

Besides implementing geotechnical strategies to reduce water infiltration, improve drainage, and reduce erosion, structural strategies have been proposed in the past to eliminate the bump at the end of the bridge. (WisDOT Specifications requires the specification of a drainage system in bridge abutments). The integral abutment bridge is an attractive design option because it has simple connections between the abutment and bridge deck. The system

performs as one single structure; however, when these bridges expand during the summer, the lateral pressure on the abutment from the backfill may actually approach the passive pressure limit. When the bridge contracts in the winter, a void develops between the abutment and the backfill, increasing in size with each passing year. The void naturally leads to severe erosion and loss of support beneath approach pavements.

To prevent these problems at integral abutment bridges, many states have incorporated a pavement approach slab that is connected with structural steel either to the bridge deck or the abutment, or simply left to rest on the paving notch in the bridge abutment (Greimann et al., 2008). Expansion joints are built in between the bridge deck and the pavement approach slab, between the pavement approach slab and the mainline pavement, or both. However, poor designs have led to issues with load concentrations, especially in the approach slab when the bridge expands, causing severe cracking of pavements (Greimann et al., 2008). Cai et al. (2005) proposed designing the approach slab-bridge deck connection to support traffic design loads as a free-standing simple beam, unsupported by underlying soils. This represents a conservative but costly design solution. For these reasons, it may be desirable to instead design improved expansion joints with good seals between the bridge, the bridge abutment, and the approach pavements with sound backfill materials beneath for structural support. But this goal in itself has proven difficult to achieve, leading to the prevalence of integral abutment bridges and/or pavement approach slabs in many different states.

2.2 COMPACTION AROUND UTILITIES AND MSE RETAINING WALLS

Now that the relevant geotechnical issues surrounding bridges have been outlined, it is logical to discuss geotechnical considerations specific to other important highway structures, specifically, utility trenches and mechanically stabilized earth (MSE) retaining walls. The design and construction practices surrounding these structures have many similarities in terms of compaction and, in addition to bridges, could indirectly influence experimental decisions for this

project. For example, it is worthwhile to know existing standards in compaction equipment, lift thickness, moisture control, gradation, soils plasticity, and/or construction methods for these unique structures. Then a tentative comparison can be made between potential differences or improvements that jetting or flooding would introduce to the practice.

Properly backfilling utility trenches represent a unique challenge because often the open trench is narrow, the compaction space is confined, and the structural integrity of the pipe must be protected. Good pipe installations are those which disturb the native soil the least, thereby ensuring continuous support of the pavement structure near the utility line (Moser et al., 2008). Backfills compacted with traditional methods should have lift thicknesses less than or equal to 30 cm (12 inches), although often lift thicknesses have been observed to be from 60 to 120 cm (2 to 4 feet) in the field (Schaefer et al., 2005), while WisDOT Specifications require lift thicknesses of 20 cm (8 in.) of loose materials. State Departments of Transportation commonly specify compaction should reach 90% to 95% of standard Proctor density for all backfill materials, depending on if the utility line is in the roadway (Schaefer et al., 2005). However, the relative density test has been shown to produce more reliable, reproducible results for maximum dry density, especially for uniformly graded coarse-grained materials (Drnevich et al., 2007).

Silt, silty clays, and clays should generally be eliminated as potential backfill material around utilities, especially if they are highly plastic with liquid limits greater than 50 percent, as these soils exhibit reduced strength and further settlement upon saturation (Moser et al., 2008). More suitable backfill includes materials classified as SM and GC; when these materials have less than 35% sand particles, they have been shown to achieve relative densities of dense to very dense without a significant amount of compaction (Schaefer et al., 2005). The gradation must be carefully designed however, because a well-graded coarse-grain material containing non-plastic fines has the potential to produce a high density in the field (Schaefer et al., 2005). The finer particles in a well-graded material reduce the volume of voids, leading to poor drainage and susceptibility to frost action and frost lense development (Monahan, 1994). Finally,

it has been suggested that achieving a relative density of 65% or greater after compaction represents an alternative standard to the more widely used standard Proctor method for trench backfill materials (Schaefer et al., 2005).

To complete the discussion of geotechnical considerations and compaction near highway structures, MSE retaining walls must be considered, because like bridge abutments, they too represent a confined area with unique challenges. It is recommended that a quality control program be implemented which requires a compaction method specification (Berg et al., 2009). For example, the actual number of passes made by the light, walk-behind vibratory plate or drum compactor, and the lift thicknesses, should be determined by construction of a separate test pad simulating field conditions. If compaction proves difficult to achieve, it may be more economical to place higher quality fill in contact with the wall face (Berg et al., 2009). Placing fill with high fines content at moisture contents wet of optimum makes it increasingly difficult to maintain an acceptable facing alignment due to increased horizontal earth pressures (Berg et al., 2009). Therefore, the backfill material should be placed and compacted in a nearly dry condition. Ultimately, without an adequate drainage system, flooding of the backfill to facilitate compaction should not be permitted.

2.3 TRADITIONAL COMPACTION METHODS

The following sections consider current field compaction methods for coarse-grained soils independently of whether they are used on highway projects. The science behind each method may lend further guidance towards experimental decisions for this project. The current methods can be summarized as dynamic, vibration in its various forms, and placement of hydraulic fills.

2.3.1 Rubber-tired Roller

The wheel dozer or rubber-tired roller for earthwork is a two-axle roller with 4 rubber tires. The rubber-tired roller has about 80% coverage with 700 kPa (100 psi) contact pressure comparing 100% coverage under the wheel with 380 kPa (55 psi) of the smooth-drum vibratory roller. This equipment is mainly used for filling in highway and earth dam constructions.

2.3.2 Dynamic Compaction

Dynamic compaction, also called impact densification or heavy tamping, entails systematically dropping large weights onto the ground surface to transfer energy to and compact the underlying ground (Mayne et al., 1984). The goal is to increase bearing capacity and decrease settlement over a large area and depth of improvement, with the advantage of treating the soil in situ, or in place. Typically steel or concrete blocks on the order of 4.54 to 18.14 metric tons (5 to 20 tons) are dropped from a height of up to 30.5 m (100 ft) using heavy crawler cranes in a process that affects soil compaction at depths up to about 30.5 m (100 ft) (Mayne et al., 1984). The large scale and potentially damaging ground vibrations likely make dynamic compaction unsuitable for use near highway structures. But the method has been proven to be effective in unsaturated coarse-grained soils as well as saturated fine-grained soils, as long as pore pressure is allowed to dissipate between passes (Mayne et al., 1984). The initial passes use high compactive energy on points spaced further apart, while the end passes use low energy on points spaced closely together (less than 1.5 m – 5 ft.) to densify the surficial layers. After each pass, the craters from the falling weight are usually backfilled with surrounding materials, and an elevation survey can be used to calculate subsidence over the desired area of influence.

2.3.3 Vibration Compaction

Vibration is widely recognized as the most efficient method to compact coarse-grained soils, and it can be separated into two forms – surficial vibration and deep vibration, with each form characterized by the use of a wide variety of equipment. Surficial vibration has been discussed in some detail above, as it is widely used for coarse-grained soils on highway projects. Generally the lift thickness should be limited to 60 cm (24 inches) for large smooth drum vibratory rollers, and only 7.5 to 15 cm (3 to 6 inches) for hand-operated equipment (Monahan, 1994). If the soil is saturated during compaction, the soil must be free-draining. Otherwise, fine particles will flow into place, but will subsequently settle only under buoyant weight; the effect is then essentially ponding of the soil (Moser et al., 2008). Additionally, if the soil is being over-vibrated, the fines will tend to settle toward the bottom of the layer, but if particle crushing occurs, the material at the top of the compacted lift will actually become much finer than the rest of the layer (Drnevich et al., 2007). This would result in a nonhomogeneous layer of fill, subsequently increasing the probability of differential settlement. Finally, it has been suggested that inserting concrete vibrators into a viscous, saturated water-soil mix could produce effective compaction near pipes (Moser et al., 2008).

This leads to the form of compaction known as deep vibration, characterized by the insertion of some type of probe to the desired depth of compaction of the soil layer. The typical equipment needed for deep vibration is shown in Figure 2.2. The probe should be inserted at a high frequency (greater than 30 Hz) such that minimal energy is transferred to the soil; in this way, ground vibrations are low and shaft resistance is dramatically decreased for easier insertion (Massarsch et al., 2005). During compaction, it is desired to achieve resonance between the probe and the soil (usually at 15 to 20 Hz) to efficiently transfer energy to the solid particles, allowing them to become mobilized and move into void spaces. Soils with higher shear wave velocity have increased stiffness and strength, and require a higher probe frequency to achieve resonance (Massarsch et al., 2005).

Although the displacement amplitude (S_0) is independent of the vibration frequency, it too is an important factor in effective deep compaction of coarse-grained soils. Defined as the difference between the ground vibration amplitude (S_G) and the probe vibration amplitude (S_P), it is the most important factor for soil compaction by vibration (Massarsch et al., 2005). When the displacement amplitude goes to zero, a different type of resonance is achieved and energy transfer is maximized between the probe and the soil. Probes have been designed with holes to not only increase contact with the soil, but also to reduce the dynamic mass, thereby allowing for greater flexibility in attaining small displacement amplitudes for a variety of soils (Massarsch et al., 2005). Additionally, the double Y-shaped probe has been proven to be the most efficient probe geometry because it has a rectangular influence area (Massarsch et al., 2005). While other probes have circular influence areas that dictate closer probe point spacing and overlapping influence areas, the double Y-shaped probe can be inserted into the soil layer in a simple rectangular array.

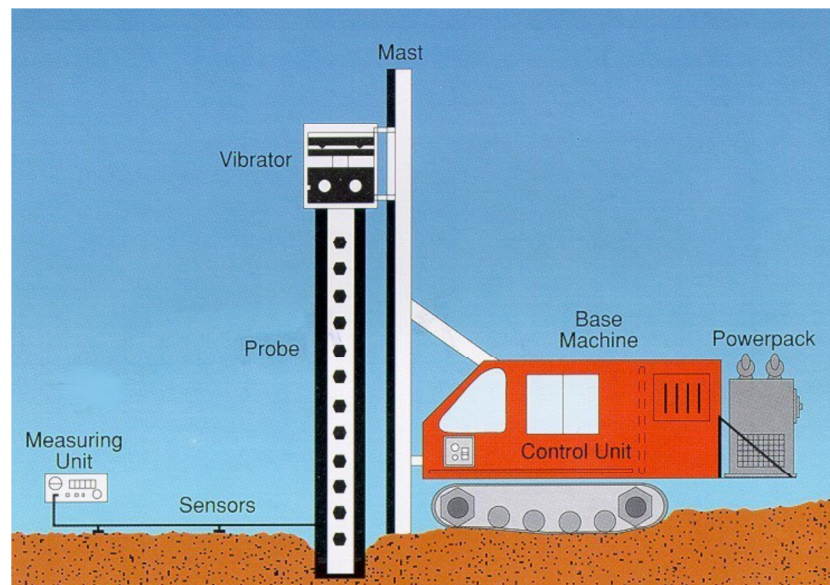


Figure 2.2. Equipment for Deep Vibratory Compaction (from Massarsch et al., 2005).

Another particularly interesting probe is that which is used to perform the vibroflotation method. During vibroflotation, large vibrating probes are inserted into the ground and vibrated within the hole while water is simultaneously injected or jetted (Zhou et al., 2008). The soil

“flows” toward the probe, creating a cone of depression much like water flowing toward a well during pumping. The soil gradation and angularity are important for this method to achieve maximum performance (Monahan, 1994).

In terms of construction practice and short- and long-term monitoring of deep vibration compaction, it is generally advantageous to perform compaction in two separate passes to achieve more homogeneous soil densification (Massarsch et al., 2005). The penetration speed of the probe during the second pass should be much lower than during the initial phase. This would indicate that the point spacing was chosen correctly, or possibly even closer than necessary (Massarsch et al., 2005). As expected, loose, water-saturated sands would have the tendency to liquefy during the first compaction pass due to buildup of pore pressures as the solid particles become mobilized. If pore pressures are allowed to dissipate, energy transfer is greatly improved, and liquefaction should be less likely to occur during the second pass (Massarsch et al., 2005). This indicates the soil layer has been densified and become more resistant to liquefaction. In the long-term, deep vibration causes a permanent overconsolidation effect due to changes in the stress state of the soil. The vertically oscillating probe actually creates horizontal vibrations due to friction between the probe and the soil, causing a significant increase in lateral earth pressure after horizontal stress pulses (Massarsch et al., 2005). It has been hypothesized that this increase in horizontal effective stress further improves soil parameters with time, as the rearrangement of soil particles would take place to adjust to a more isotropic stress field.

2.3.4 Hydraulic Fills

Hydraulic fills include those fills that are placed by the flow of water, or transported by the flow of water and then dumped into place (Sladen et al., 1989). This method of backfilling has often been used to create artificial islands in bodies of water across the world, and it is of particular interest to this project because hydraulic fills share similarities with specimens that are

flooded in preparation for compaction. One notable study by Hewitt et al. (1989) examined what they called the “overwhelming influence of method of placement on in situ density.” The authors summarized worldwide experience in the use of subaqueous hydraulically placed fills in the following points: (1) dense sand cannot be obtained by simple hydraulic placement, (2) average relative densities up to 60% can be achieved by hydraulic placement, but generally they will be less than 50%, (3) relative density within a given fill is highly variable, possibly from 10 to 70%, and (4) the factors affecting in situ density are little understood.

Hewitt et al. (1989) gathered details of the Canadian experience of hydraulically placed fills in the Beaufort Sea, and noted that liquefaction failures occurred at four separate islands. These failures occurred under both static loading and pulsating loading, and consisted of both large scale flow slides or liquefied sand that was restricted to the core of the island only. They cited a lack of confidence in the measurement of in situ void ratio of fills, despite using cone penetrometer testing. Nonetheless, a direct relationship was observed between the effective stress-corrected CPT results and a separation between liquefiable and nonliquefiable fills. Loose, fine sands with poor drainage and high void ratios proved to be the fills most susceptible to liquefaction (Sladen et al., 1989).

Finally, the authors made some “reasonable speculations” regarding the effect of method of placement on the in situ density of subaqueous hydraulic fills. Sand dumped from a hopper dredge has a greater initial bulk density than sand slurry in a pipeline, and therefore the sand from the hopper tends to fall as a slug rather than as individual particles. Additionally, the instantaneous dump limits the entrainment of “fresh” water into the slug that would reduce its fall velocity and expand its size. As a result, the increased fall energy of the discharge is dissipated through compaction of the berm. Also known as bottom-dumping, this method has proven to produce hydraulic fills with higher CPT resistances and improved compaction results (Sladen et al., 1989).

Meanwhile, pipeline placement can be differentiated by direction and location of discharge. When the discharge point is held close to the berm surface, there is a minimal opportunity for entrainment of “fresh” water into the flow, and a larger portion of the kinetic energy from the discharge velocity is absorbed by the berm. This effectively simulates a form of vibratory compaction in the berm (Sladen et al., 1989). However, if the discharge point is directed upward away from the berm surface, most of the vibratory compaction would be lost and an even looser in situ state would result. Directing the flow of fill upward would be implemented to create steeper slopes, but the result is a looser in situ state (Sladen et al., 1989). The loosest possible state would be expected if the discharge point were placed near the sea surface, allowing for the individual particles to become separated and fall in a cloud of sand arriving at the berm with low energy (Sladen et al., 1989).

2.4 RECOMMENDATIONS FOR JETTING AND FLOODING

Although there has been little academic research performed with respect to jetting or flooding of coarse-grained backfill materials, a number of metropolitan sewer districts and local municipalities have incorporated these methods into specification form with subtle differences. The Iowa Department of Transportation has recently drafted developmental specifications for backfilling and compaction of culverts by flooding. And a few textbook authors have offered their personal recommendations to responsibly practice jetting and flooding in compaction.

For example, Moser and Folkman (2008) offer guidelines on jetting and flooding backfill in trenches containing gravity flow pipes. During flooding, a lift of free draining soil is placed up to the mid-height of the pipe, and then completely saturated with water. Compaction is achieved when the soil is washed into voids and beneath the haunches of the pipe due to the downward seepage stress as the lift is drained. Care must be taken to hold the pipe in alignment, as most pipes will tend to float in saturated soil (Moser et al., 2008). While this is considered to be the least effective compaction method, it is often adequate for utility pipes outside roadways.

The authors also offer guidelines on jetting and indicate that dense soils can be achieved by jetting. The soil may be placed in large lifts, from 0.9 to 1.5 m (3 to 5 ft.) in thickness. A stinger pipe (2.54 cm – 1 in. - diameter and 1.52 to 1.83 m. – 5 to 6 ft. - long, attached to a water hose) is injected vertically down to the near bottom of the soil lift. A high-pressure water jet moves the soil into place to a dense state if the soil is free-draining and immediately dewatered (Moser et al., 2008). Jet injections are typically made on a grid every few feet, where 1.5 m (5 ft.) grids have been used successfully for 1.52 to 1.83 m (5 to 6 ft.) lifts of coarse-grained soil (Moser et al., 2008). In order to fill holes when the stingers are withdrawn, the stingers are simply vibrated upon removal. The jetting method is attractive for use around large buried structures where excavation is impractical or costly (Moser et al., 2008). Great care must be taken to ensure drainage of water out of the fill layer, especially in confined areas.

2.5 INDUSTRY SPECIFICATIONS

The following section presents an overview of specifications detailing how to perform jetting or flooding to achieve compaction on highway projects. Four agencies that use jetting or flooding have been identified, three of which are utility companies. The fourth agency is the Iowa Department of Transportation; they have published developmental specifications describing the application of flooding to compact controlled backfill around large culverts. However beyond the specifications shown below, the practice of jetting and flooding appears to be limited. It may be that agencies practice jetting and flooding informally and so have not published formal specifications on their practice. Common to each of the specifications below is the use of jetting and flooding in confined areas, especially in utility trenches, where large equipment cannot operate. Jetting and flooding is likely more practical and economical for these utility companies because only some kind of pipe with a nozzle attachment and a source of water are needed to perform the operation.

Agencies have specified some combination of acceptable backfill size and gradation, depth restrictions, lift thickness, timing of jetting, nozzle pressure, hose diameter, and drainage controls to perform jetting and flooding. The degree of specificity of each of these parameters depends on location relative to the roadway and the degree of compaction required for adequate backfill performance.

The Metropolitan Sewer Department of Greater Cincinnati has the most specific requirements for the application of jetting in the field. The scope of their jetting specifications includes compacting 'suitable soil or granular material free from rubbish, muck, or other unsuitable materials' around conduits and trenches. The specification goes on to state:

Stones and shale exceeding one-half (1/2) cubic feet in volume shall not be used in the backfill, and stones and shale that are used shall be separated by at least six (6) inches of earth. The backfill for Type "C" Conduit shall be finally consolidated by thoroughly jetting with water. Trenches over 14 feet in depth shall be consolidated by jetting in two (2) equal layers. For jetting other than granular material, a hose not smaller than 1 1/2 inches in diameter and nozzle not smaller than 1 inch in diameter and not shorter than 2/3 the depth of the trench carrying water at a minimum pressure of 40 pounds per square inch (psi) shall be inserted into the back fill in a uniform pattern in order to obtain maximum consolidation. After the final jetting of the trench, the backfill shall be left to settle and to permit drainage of the impounded water. Typical jetting procedure shall include a water removal system, either natural or mechanical, at intervals not to exceed 500 linear feet of trench. Settled trench surfaces then shall be brought to grade by filling with approved fill material and compacting to a density equal to that of adjacent ground.

From these specifications it is clear that large lift thicknesses may be implemented with jetting, as only trenches over 4.2 m (14 ft.) in depth need to be jetted in two layers. Furthermore, a large rigid pipe must be acquired to perform the operation, as the pipe will need to channel a large volume of water into these thick lifts. This Metropolitan Sewer Department of Greater Cincinnati has also included language highlighting the importance of removing the water from the system and waiting for the backfill to settle upon completion of the jetting. This would imply there is some residual compactive effect derived from water draining through the backfill, even

after jetting is complete. It may also be worthwhile during the course of this project to investigate the change in performance when water can and cannot effectively drain from the compacted lift. This could be evaluated in terms of materials with different hydraulic conductivity and different engineered backfill geometries and water removal systems.

The Mobile Area Water and Sewer System does not have the same degree of specificity in their jetting specifications, especially with regard to the actual application of jetting, as the Sewer Department of Cincinnati. However, this is likely because Mobile's sewer agency only allows flooding or jetting of sand in areas outside of 'state highways, county roads, or within City of Mobile streets and right-of-way.' The agency only allows the backfill of muck 'in fields and open country.' In this way jetting and flooding are implemented as an acceptable compromise to perform compaction where traditional methods are either unavailable or ineffective, and in areas where settlement is of low concern. The scope of the specification includes backfilling requirements for water mains, sanitary sewers, and sewage pumping stations:

Final Backfill: Flooding or jetting will not be permitted.

Backfill of Sand: Flooding or jetting will be permitted, unless specified otherwise, where the clay and silt content of the backfill material is low enough to permit this method of consolidation. When allowed, this method will be used from a point 2 feet above the top of pipe to the original ground line except under state highways, county roads or within City of Mobile streets and right-of-way.

Backfill of Muck: In fields and open country, flooding or jetting will be permitted or required where the clay and silt content or water content is so high as to make tamping ineffective. Flooding or jetting will be confined to that portion of the trench starting 2 feet above the top of pipe and ending 2 feet below the original ground surface. The last 2 feet shall be backfilled with selected earth and shall be mechanically rolled or tamped to the degree of compaction of the surrounding ground.

The City of Mountain View in California also allows for the application of jetting to compact backfill specifically in trench excavations. This agency once again does not go into the level of detail with regard to the actual jetting application as the Sewer Department of Cincinnati,

but they do have the most stringent quality control checks and the most detailed controls on suitable material for compaction by jetting. The scope of the specification includes work consisting of 'trench excavation, backfill, and resurfacing, all as required for the installation of underground utilities.' The city outlines the material acceptable for compaction by jetting:

Select backfill material shall be sand or granular material of the quality herein specified. Select backfill material shall have a size and gradation falling within the following limits:

Table 2.1. Gradation Limits of Select Backfill Material.

Sieve Size	Percentage Passing Sieve
1/2"	100
No. 4	50-100
No. 200	15 Maximum

The minus two hundred (200) portion of the material expressed as a percentage multiplied by the Plasticity Index shall not exceed one hundred (100). The material shall be compacted to a relative compaction of ninety percent (90%) as determined by Test Method No. California 216.

The stipulation regarding the plasticity of materials passing sieve No. 200 is a clever way of limiting both the amount and the plasticity of fine particles in the backfill. A material with greater fines with greater plasticity would have both lower hydraulic conductivity, and higher susceptibility to consolidation settlements over time. Both of these phenomena have been identified in the literature review to be detrimental to jetting performance. The specifications go on to state acceptable jetting methods with careful consideration of depth with respect to the finished roadway:

Initial Backfill. Select Backfill Material shall be used for initial backfill...steel dowel stakes (rebar), or other material approved by the Engineer, may be used to secure the pipes to the bottom of the trench to prevent the pipes from floating in the backfill. After the pipe has been properly laid and inspected, select backfill material shall be placed on both sides of the pipe to such a depth that after thorough consolidation by jetting or hand-tamping, the final depth of select backfill material shall be 12" above top of pipe.

Initial Backfill Compaction. Jetting may be allowed for compacting sand backfill when approved by the Engineer. When jetting, it is important

that proper precautions be taken to prevent floating of the pipe. The Contractor shall be wholly responsible for damage resulting from neglect of these precautions. After consolidation by jetting, the relative compaction of the initial backfill material shall be not less than ninety percent (90%) as determined by Test Method No. California 216.

Subsequent Backfill. Above the level of initial backfill, the trench shall be backfilled with select imported material. Subsequent imported backfill within 2-1/2' of the finished surface grade or 1-1/2' of the finished subgrade, whichever is lowest in elevation, shall be mechanically compacted by tamping or rolling to a relative compaction not less than 95% as determined by Test Method No. California 216. Subsequent imported backfill, below 2-1/2' of the finished surface grade or 1-1/2' of the finished subgrade, whichever is lowest in elevation, may be compacted by jetting or mechanical compaction to a relative compaction not less than 90% as determined by Test Method No. California 216.

If the Contractor elects to compact by jetting, the backfill material shall be placed in layers not exceeding 4' in loose depth, each layer being thoroughly and uniformly wetted by means of a jet pipe of sufficient length to reach the bottom of the layer being compacted. Subsequent backfill placed by jetting shall be free from stones or lumps exceeding three inches in greatest dimension, vegetable matter, or other unsatisfactory material.

The above specifications once again limit the proximity to the actual roadway where jetting may be performed, albeit in a manner different than the Mobile sewer agency. Where the Mobile sewer agency only allowed jetting to be performed outside the roadway, the City of Mountain View does allow jetting beneath the roadway, but only as long as it is performed at a depth greater than 63 mm (2.5 in.) of the finished surface grade or 38 mm (1.5 in.) of the finished subgrade. There is a theme developing in the specifications here where jetting is not expected to achieve the same degree of compaction as the more traditional method of vibration or tamping; instead it is used as a quick and efficient alternative in confined areas where a high degree of compaction is not necessary.

Finally the Iowa Department of Transportation has recently published developmental specifications for the backfilling and compaction of culverts by flooding. Of particular note in these specifications is the emphasis placed on maintaining a very coarse backfill material for compaction by flooding. In this regard the specifications read as follows:

Use floodable backfill material meeting the requirements of Section 4134 of the Standard Specifications. When required, use porous backfill material meeting the requirements of Section 4131 of the Standard Specifications.

The porous backfill material referred to in Section 4131 is actually gravel or crushed stone, free of any clay lumps, friable particles, and clay coatings. There are additional requirements on the abrasion and A Freeze parameters as well as the alumina and shale content of the aggregate. Meanwhile, the floodable backfill material referred to in Section 4134 is uncrushed natural sand and gravel or simply natural sand. The material must meet the requirements of at least one of the following gradations:

Table 2.2. Acceptable Gradation of Floodable Backfill Materials.

Gradation No. 35:	Gradation No. 36:
100% passing 11/2" sieve	100% passing No. 8 sieve
20-90% passing No. 8 sieve	0-2% passing No. 200 sieve
0-4% passing No. 200 sieve	

There is another continuing theme here where a coarse gradation free from highly plastic fine particles is the preferred material in the application of jetting and flooding. In terms of the Iowa specifications, the strict material recommendations are in accordance with the findings of White et al. (2007). The Iowa specifications go on to state acceptable flooding methods as well as contingency plans for the method of measurement and basis of payment of flooding:

CONSTRUCTION. When backfilling and compaction by flooding is required, backfill may be placed in lifts up to 2 feet (0.6 m) thick. Determine if culverts need to be restrained and take appropriate actions to prevent floating of culverts during backfilling, flooding, and compaction. Begin surface flooding for each lift at the inlet end of the culvert and progress to the outlet. To ensure uniform surface flooding and adequate compaction, fan-spray water in successive 6 to 8 foot (1.8 to 2.4 m) increments using a 2 inch (50 mm) diameter hose for three minutes within each increment. Run the hose fully, but with the water pressure low enough to avoid eroding cohesive soil plugs. After flooding, evaluate the effectiveness of the compaction with a vibratory pan compactor. If the pan compactor produces visible compaction, repeat the flooding process until the pan compactor produces no visible compaction.

METHOD OF MEASUREMENT. The quantity of Flooded Backfill, in cubic yards (cubic meters), will be the quantity shown in the contract documents regardless of the compaction method. The quantity measured for payment will not be adjusted unless the quantity of culvert installed is adjusted.

BASIS OF PAYMENT. The Contractor will be paid the contract unit price for Flooded Backfill per cubic yard (cubic meters). Backfill material, subdrains, restraining culverts against floating, and water required for flooding will not be measured separately for payment, but will be considered incidental to the contract unit price bid for Flooded Backfill.

Of note here is the specification of smaller lift thicknesses for the application of flooding compared to jetting. Where the Sewer Department of Cincinnati allowed for just two lifts within a total layer thickness of 4.2 m (14 ft.) or greater for jetting, the Iowa DOT has set a maximum lift thickness of just 0.6 m (2 ft.) for flooding. This may be explained in that flooding represents a lower energy application to the backfill compared to the more intensive process of jetting. Another continuing theme here is the importance of securing the pipe or culvert structure against floating; the experience of these agencies indicates the saturation of the system with water initiates enough of a buoyant force to cause misalignments and movement of the structure.

The quality control plan outlined in these specifications differs greatly from the specifications of the other three agencies. The compaction produced by flooding is actually checked after flooding is complete by the traditional method of applying the vibratory pan compactor. Furthermore, the method of measurement used to determine pay for the contractor does not change even if flooding must be performed more than once. This sort of contingency language shifts some of the risk to the contractor. This may be acceptable in light of the inexperience of state departments of transportation with the novel methods of jetting and flooding to date.

2.6 SUMMARY OF LITERATURE REVIEW

Current practices and problems in compaction on highway projects have been examined near structures such as bridges, MSE walls, and utility trenches. The science and methodology behind compaction methods for coarse-grained soils, including dynamic compaction, vibration, and hydraulic fill placement, have been outlined. The findings of studies focused on these traditional methods may prove useful in adapting and implementing specifications for jetting and flooding. The available literature and specifications on jetting and flooding have been presented in detail. The specifications regarding these methods are not particularly standardized, with each agency specifying various aspects of methods and materials. Common themes in the specifications have been identified, including

- (1) jetting is most often applied as a compaction method in utility trenches outside of the roadway where a high degree of compaction is not necessary,
- (2) jetting can compact material in large lift thicknesses,
- (3) coarser sands and gravels with limited fines are the preferred material for jetting and flooding,
- (4) care must be taken to prevent misalignment of pipes and other structures, and
- (5) drainage and dewatering of the system during and after jetting are critical to maximizing compaction and backfill performance.

Finally jetting and flooding have not been specified as methods to compact backfill behind MSE walls or bridge abutments. However, two of the most critical problems around these structures, poor drainage leading to erosion, and inadequate compaction due to confined spaces, may potentially be solved by jetting and flooding. This poses a completely novel design problem which will be addressed by the field work of this project. Each section of the literature review will help to guide experimental methods for this project.

SECTION 3 - CHARACTERIZATION OF TESTED MATERIALS AND FIELD METHODS

The materials tested in the lab are selected for both variety as well as expected effectiveness when subjected to flooding and jetting. Materials that are expected to perform well and are included in this study include a variety of poorly graded sands, a poorly graded gravel, and a few gap-graded sand-gravel mixtures; these materials are clean and have very few fine particles. Materials that are expected to perform poorly, due to their lower drainage capacity, and are also included in this study include finer, natural sands and a silty sand. In fact these natural sands constitute the backfills that are most commonly used by the Wisconsin DOT (Bareither et al., 2008). Clays are not tested due to their swell potential when hydrated and high resistance to flow. Other materials that are characterized include those found at the Highway 51 and Greenfield Avenue field sites, which served as application points for flooding and jetting, respectively. While lab tests of flooding and jetting and experiences at the field sites are detailed in subsequent sections, this section introduces all the materials in a way that allows for a basic understanding of the physics of jetting and flooding. The determination of particle size distribution, grain shape, and minimum and maximum density particle packing are critical to understanding the physics, and to developing and evaluating pre-existing and new hypotheses as the tests progress from the lab to the field.

3.1 PARTICLE SIZE DISTRIBUTION

Particle size distribution curves of the soils were determined according to ASTM D6913. The soils were placed in the oven until completely dry and carefully inspected to ensure that no solid particles were cemented together into larger aggregates. The particle size distribution curves for the clean sands, coarser materials, and materials present at the Highway 51 field site are shown in Figures 3.1, 3.2, and 3.3. Also included in the figures is the erodible boundary identified by White et al. (2007). Materials finer than this boundary are considered to be erodible

backfills due to their susceptibility to pore pressure buildup in confined spaces. When these finer materials are compacted to a dense condition, they have low hydraulic conductivity. This resistance to drainage, coupled with a long drainage path around confined structures as well as cyclic traffic loading, can cause the pore pressures to spike over time, finally causing the erodible soils to liquefy and washout.

Each of the materials shown in Figures 3.1 and 3.2 are tested in some capacity in the lab and are chosen to observe a variety of compaction behaviors. There are clean sands, gap-graded sand-gravel mixtures, well-graded sands, sands with gravel and fines, and a low plasticity silt with sand (henceforth known as silty sand for ease of identification). All of the materials shown in Figure 3.1 through 3.3 actually classify as poorly graded sands (SP) except for the patio/paver base, which classifies as poorly graded gravel with sand under the Unified Soil Classification System. The native soil and sandy backfill found at the project site, however, represent more natural materials with a broader distribution of particle sizes. The native soil and sandy backfill have 5% and 3% fines, respectively. Additionally the sandy backfill has a coefficient of curvature (C_c) of 0.4 and a coefficient of uniformity (C_u) of 4.7, making it close to being a well-graded sand. From the curves shown in Figure 3.3 it is also clear that the sandy backfill imported to the Highway 51 project site has a nearly identical gradation to the native soil already at the site. In this sense the performance of the 'controlled backfill' during flooding and jetting would likely be very similar to the native soil.

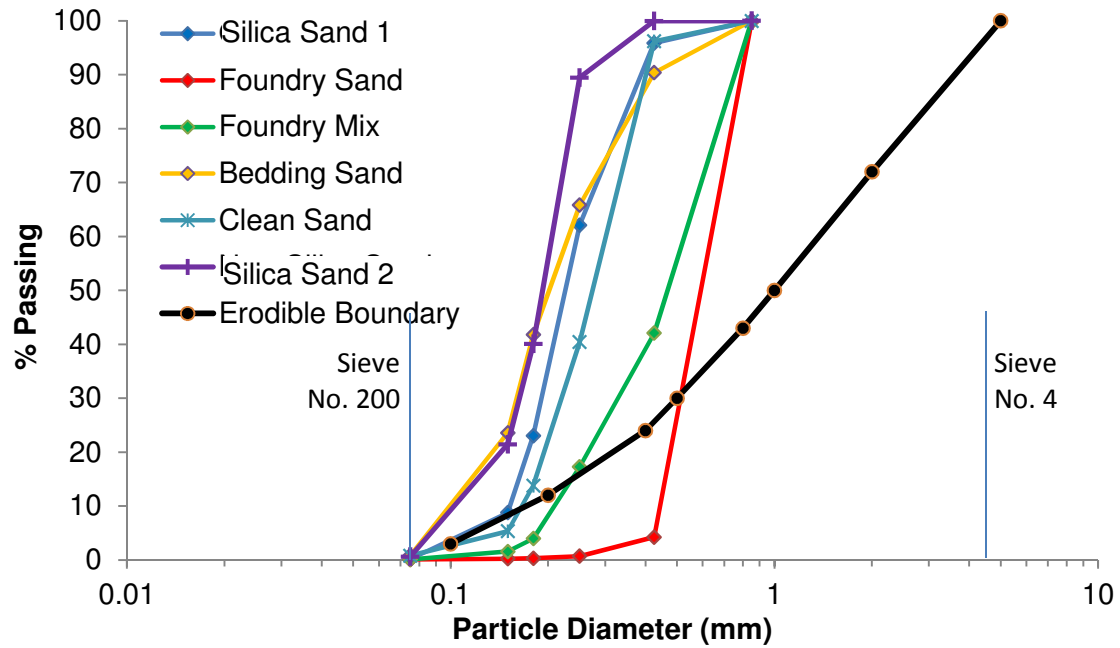


Figure 3.1. Particle Size Distribution Curves for Clean Sands.

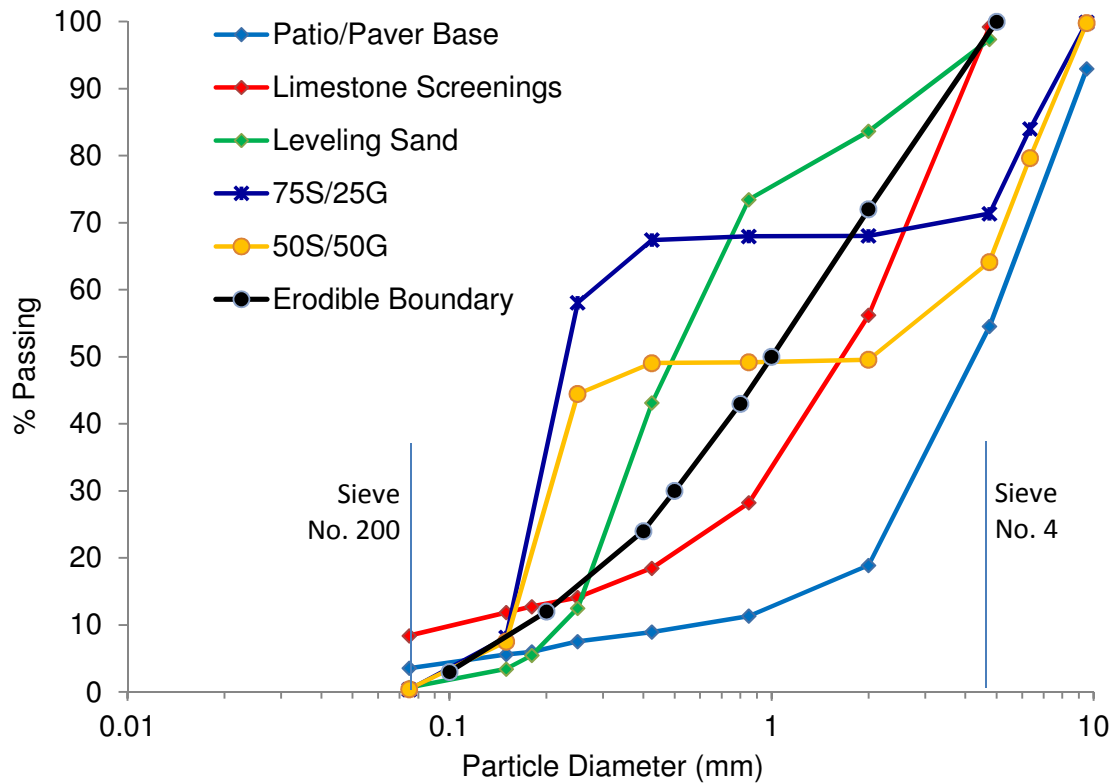


Figure 3.2. Particle Size Distribution Curves for Coarser Materials.

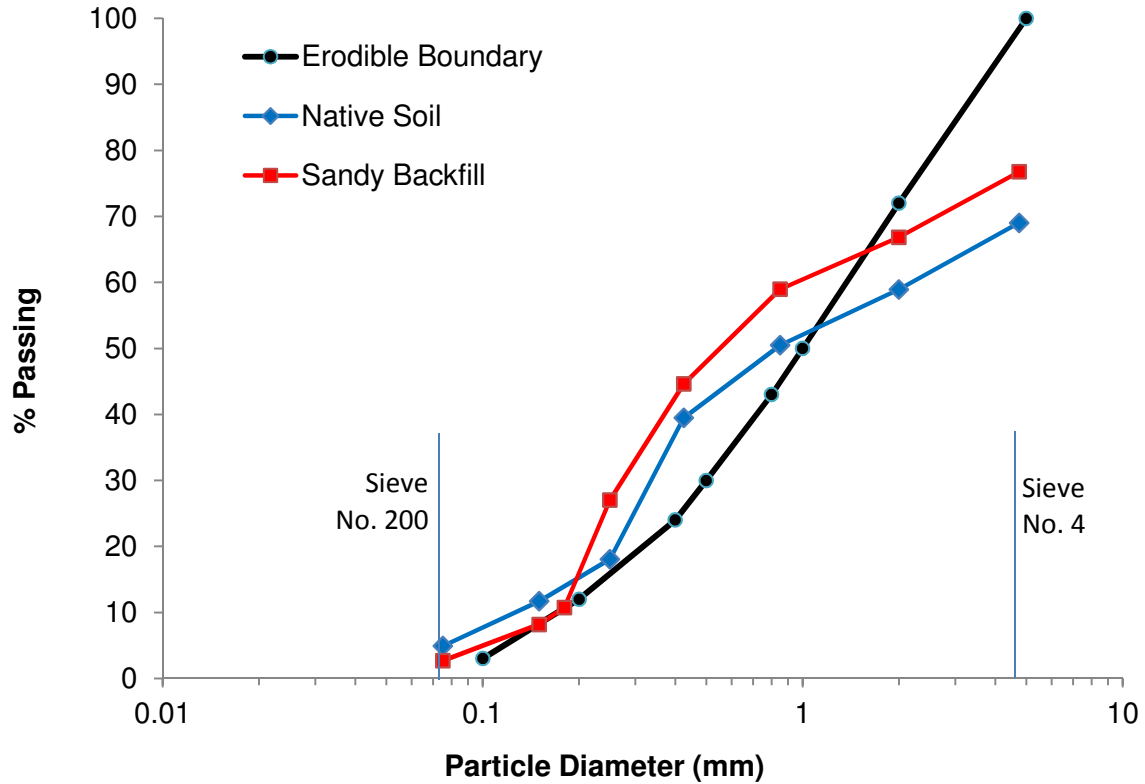


Figure 3.3. Particle Size Distribution Curves for Materials at Highway 51 Project Site.

3.2 SPECIFIC GRAVITY

The specific gravity test was performed according to ASTM D854 using the water pycnometer to evaluate the density of the solid particles in the various tested soils, and thereby to allow the determination of the porosity and void ratio of the soils. In this method the mass of a given volume of solid particles is compared to the mass of an equal volume of distilled water. Therefore the water pycnometer was placed under a vacuum to remove all the air bubbles before each specimen was weighed. Additionally, each of the soils was placed in the oven until completely dry before being weighed on the mass balance. The results of the specific gravity test are shown in Table 3.1 below. All values fall within the expected range of 2.6 and 2.8.

Table 3.1. Specific Gravity of Soils.

Soil Type	G_s
Silica Sand	2.662
Foundry Sand	2.645
Foundry Mix	2.633
Bedding Sand	2.638
Clean Sand	2.637
Leveling Sand	2.664
Pea Pebbles	2.702
Limestone Screenings	2.782
Patio/Paver Base	2.738
Sandy Backfill	2.716
Native Soil	2.720
Silty Sand	2.684

3.3 MAXIMUM AND MINIMUM VOID RATIO

The maximum void ratios of the soils were determined according to ASTM D4254. This method specifies the appropriate strategy to place the soils in the mold to achieve the minimum deposition energy. For the sands, a small funnel was used to slowly slide the soils into the mold in uniform layers. For the gravels, a scoop was used to produce a similar effect. All of the soils were oven dry before testing to allow the individual grains to gently slide into place. Meanwhile, an alternative round of tests to determine the maximum void ratio was conducted to examine the efficacy of the methodology described in ASTM D4254. During this round of tests, soils were placed dry into a long cylinder with approximately half the diameter of the standard mold. The cylinder was raised continuously and slowly to allow the grains to gently slide into place. After just one raising of the cylinder, the mold was leveled and the void ratio was determined.

The minimum void ratio of the soils was determined according to ASTM D4253 using the vibrating table. As the soils were placed into the 2832 cm³ (0.1 ft.³) standard mold, the

hammer was struck against the sides of the mold to facilitate the removal of entrapped air before commencement of the test. After the soil was leveled at the top of the mold with the yardstick, the surcharge plate was placed onto the soil. Finally the lead surcharge was positioned above the plate and locked against the guide sleeve. This assembly was vibrated at a frequency of 60 Hz for eight minutes. A Vernier caliper accurate to 0.02 mm ($7.9 \cdot 10^{-4}$ in.) was used to measure the final height of each specimen. All of the soils were oven dry during this first round of minimum void ratio index testing.

To further investigate the important index property of minimum void ratio, another round of tests was conducted by the wet, or saturated method of ASTM D4253. The “wet” method specifies that the soils be placed into the mold with enough added water to ensure saturation. This can be checked by vibrating the table as the soils are placed into the mold; if free water rises above the soil, then the soil is considered saturated. Once the mold is full, the vibrating table is used in a similar manner compared to the dry method to compact the soil and reach the minimum void ratio. The different results between the dry and wet method indicate the soil may be experiencing a bulking effect in the dry condition wherein capillary forces hold solid particles together. This may be the result of the “dry” soil absorbing moisture from the air before the start of the test. The results of these tests are shown in Table 3.2. The dry method and wet method of ASTM D4253 produced similar minimum void ratios, so the average minimum void ratio of these two tests was calculated and used in subsequent phase calculations. The raising cylinder method consistently produced greater maximum void ratios, and therefore these results were used in the phase calculations.

Table 3.2. Minimum and Maximum Index Void Ratios of Lab-Tested Materials.

	ASTM D4253		ASTM D4254	Alternative
	Dry Method	Wet Method	Small Funnel (Dry)	Raising Cylinder (Dry)
Soil Type	e_{min}	e_{min}	e_{max}	e_{max}
Silica Sand 1	0.539	0.551	0.793	0.800
Foundry Sand	0.401	0.450	0.584	0.650
Bedding Sand	0.496	0.472	0.746	0.784
Foundry Mix	0.448	0.491	0.640	0.674
Clean Sand	0.485	0.492	0.746	0.758
Leveling Sand	0.387	0.374	0.594	0.617
Limestone Screenings	0.468	0.529	0.822	0.814
Patio/Paver Base	0.369	0.298	0.662	0.649
Silica Sand 2	0.579	0.620	0.846	0.850
75S / 25G	0.389	0.426	0.572	0.609
50S / 50G	0.320	0.361	0.485	0.519

3.4 PARTICLE SHAPE

Microscope pictures were taken at 10x magnification to get a sense of the variety of particle shapes found in the lab-tested materials. The particle shapes were classified qualitatively based on the common Krumbein roundness chart, shown in Figure 3.4 below. The limestone screenings and paver base are angular, the silica sand and bedding sand are subangular, the leveling sand and clean sand are subrounded, and finally the foundry mix and foundry sand are rounded to well-rounded. Being cognizant of the grain shapes of each material will aid in forming and investigating hypotheses with regard to fundamental compaction mechanisms that occur during jetting and flooding. The microscope images of each of these soils are shown in order in Figures 3.5 to 3.12.

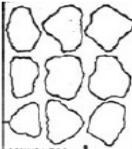
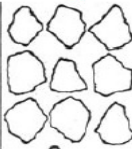
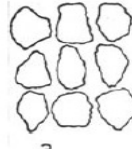




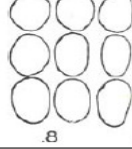
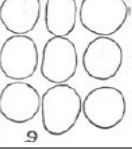
Roundness	Krumbein Image*	
Angular		
	ROUNDNESS = 1	2
Subangular		
	.3	.4
Subrounded		
	.5	
Rounded		
	.6	.7
Well-Rounded		
	.8	.9

Figure 3.4. Krumbein Roundness Chart for Visual Characterization of Particle Shape.

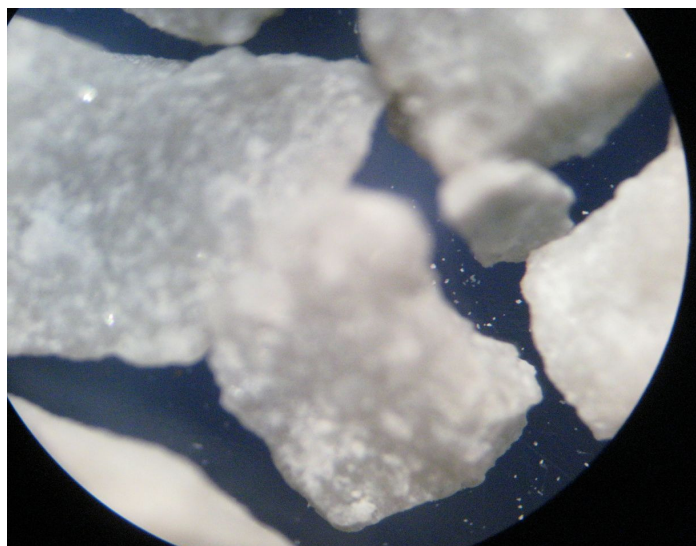


Figure 3.5. Microscope Image of Limestone Screenings.



Figure 3.6. Microscope Image of Patio/Paver Base.

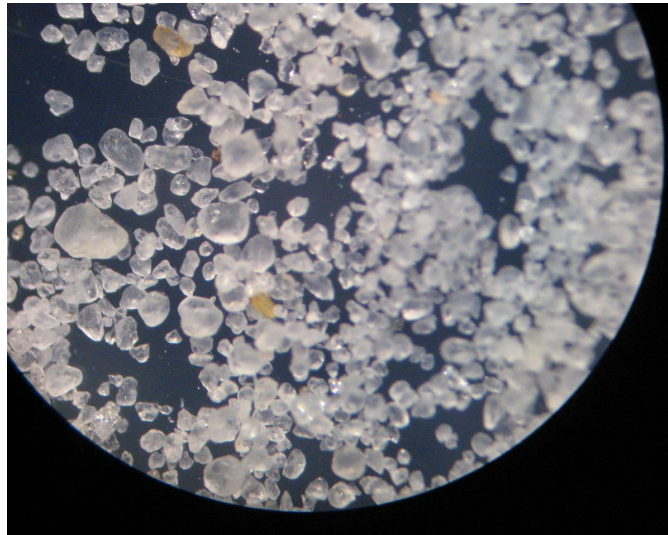


Figure 3.7. Microscope Image of Silica Sand.

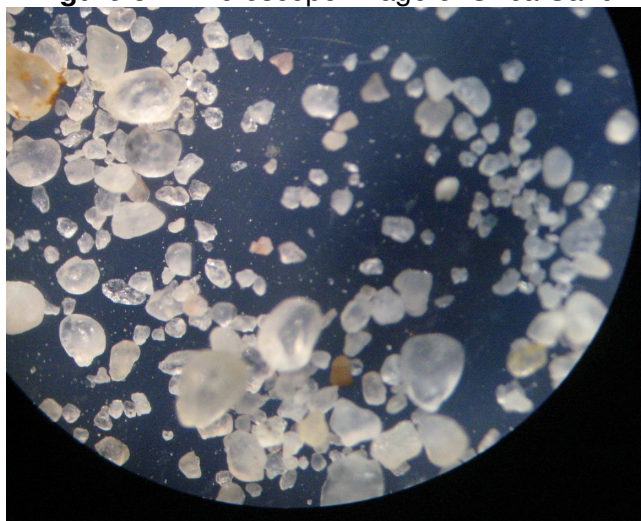


Figure 3.8. Microscope Image of Bedding Sand.

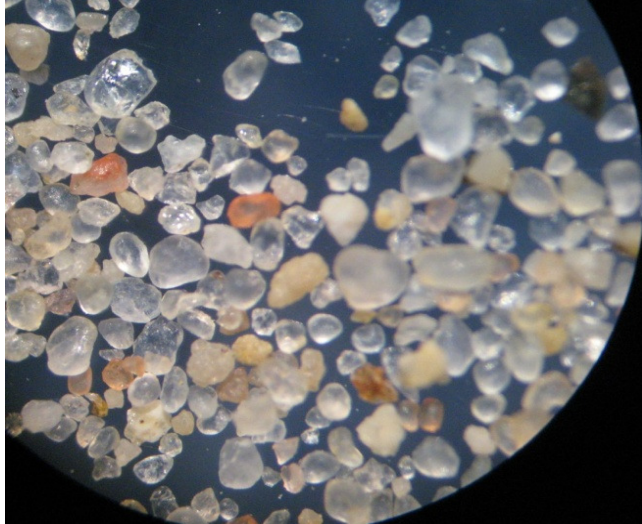


Figure 3.9. Microscope Image of Clean Sand.

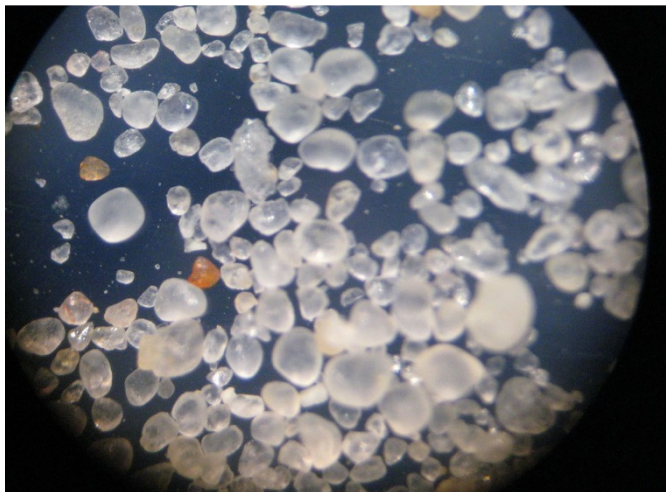


Figure 3.10. Microscope Image of Foundry Mix.

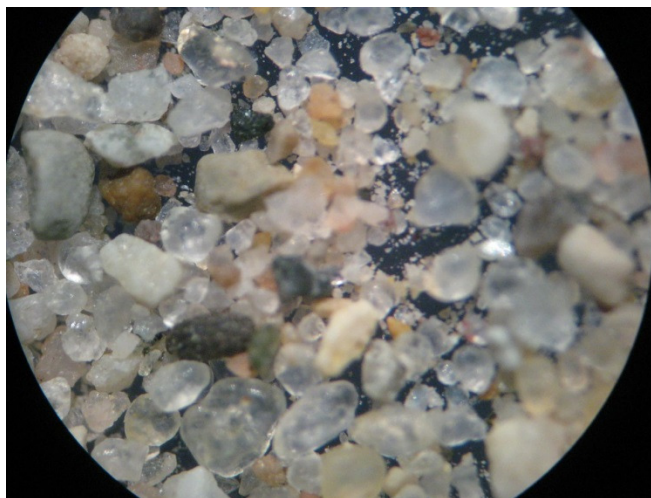


Figure 3.11. Microscope Image of Leveling Sand.

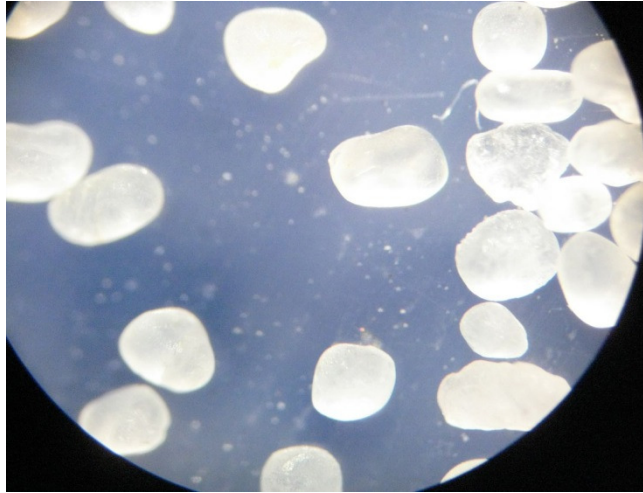


Figure 3.12. Microscope Image of Foundry Sand.

3.5 PROCTOR COMPACTION

Finally proctor compaction curves were created for the sandy backfill and silty sand materials, in lieu of the minimum and maximum void ratio index tests described above. The proctor compaction test was chosen for these materials because each material contains enough fines to produce a good compaction curve, and as a field material, the sandy backfill is subject to performance evaluation with respect to relative compaction, which requires the determination of maximum dry unit weight (γ_{dmax}) from the compaction curve. The Wisconsin Standard Specifications for Highway Construction call for backfill placed behind retaining walls and abutments to be compacted in 30 cm (1 foot) lifts to no less than 95% of γ_{dmax} . The standard energy proctor compaction test was carried out according to ASTM D698 for both the sandy backfill and silty sand materials. Meanwhile, an additional modified energy proctor compaction test was completed according to ASTM D1557 for the sandy backfill. These compaction curves are shown in Figures 3.13 and 3.14.

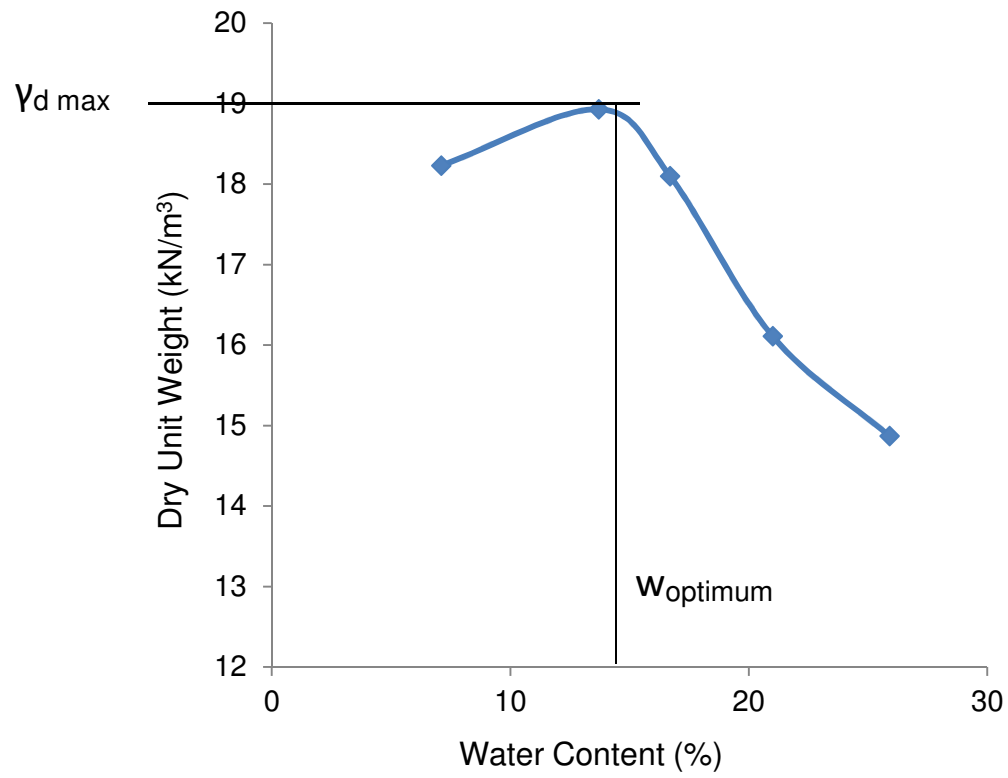


Figure 3.13. Standard proctor Compaction Curve for Silty Sand.

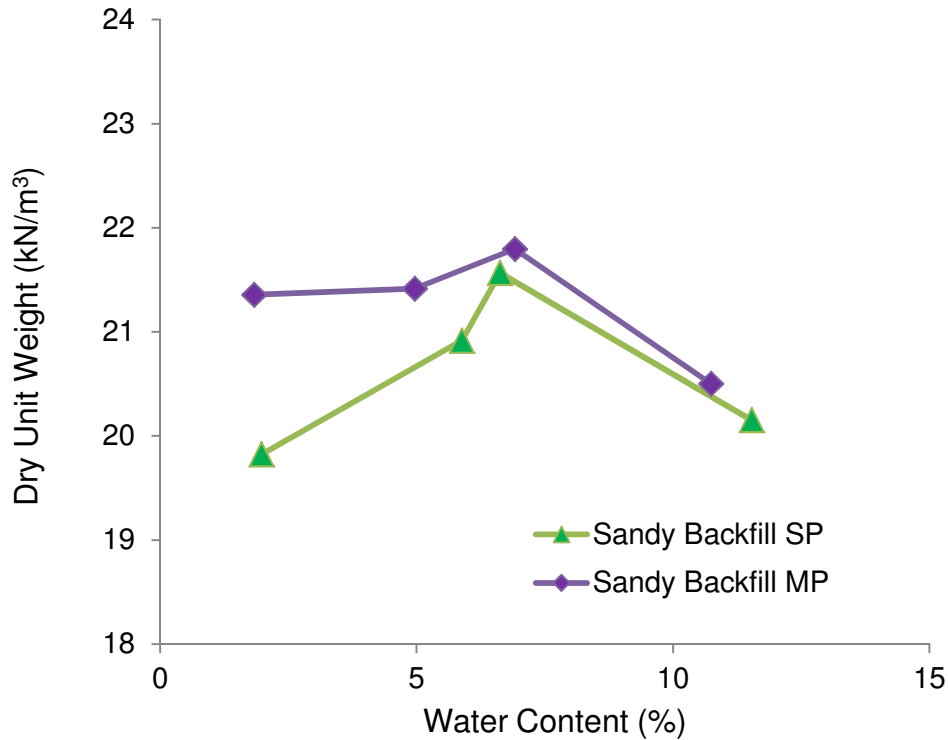


Figure 3.14. Compaction Curves for Sandy Backfill.

3.6 FIELD METHODS

The nuclear density gauge, soil stiffness gauge, and dynamic cone penetrometer are each used to assess the quality of compaction in the field. Each of these instruments are shown in Figure 3.15. The nuclear density gauge requires a guide hole to be hammered into the soil, after which the gauge can be placed and the probe lowered. The probe transmits fast neutrons directly through the soil to a receiver in the instrument. In this process, beryllium atoms eject the neutrons upon absorption of alpha particles from radioactive Americium-241. The number of neutrons counted by the receiver indicates both the dry density and water content of the soil medium (Office of Radiation Safety, UW-Madison).

The soil stiffness gauge uses an internal calibration derived from an elastic, half-space solution to measure stiffness. The gauge imparts a small cyclic force to the ground surface,

while measuring the resulting surface velocity. The cyclic force is applied over a range of frequencies and the results are averaged to yield the stiffness (ASTM D6758).

Finally the dynamic cone penetrometer measures the shear strength of the soil in the sense that a small cone is driven through the soil by a falling weight. The operator simply drops the weight from the standard drop height, and the blows per a given penetration distance are counted and recorded over the length of the guide rod, which is typically one meter long. To acquire a deeper profile of strength with the cone penetrometer, guide rod extensions may be connected to the instrument; however, it may be necessary to account for changes in skin friction at greater depth (ASTM D6951).

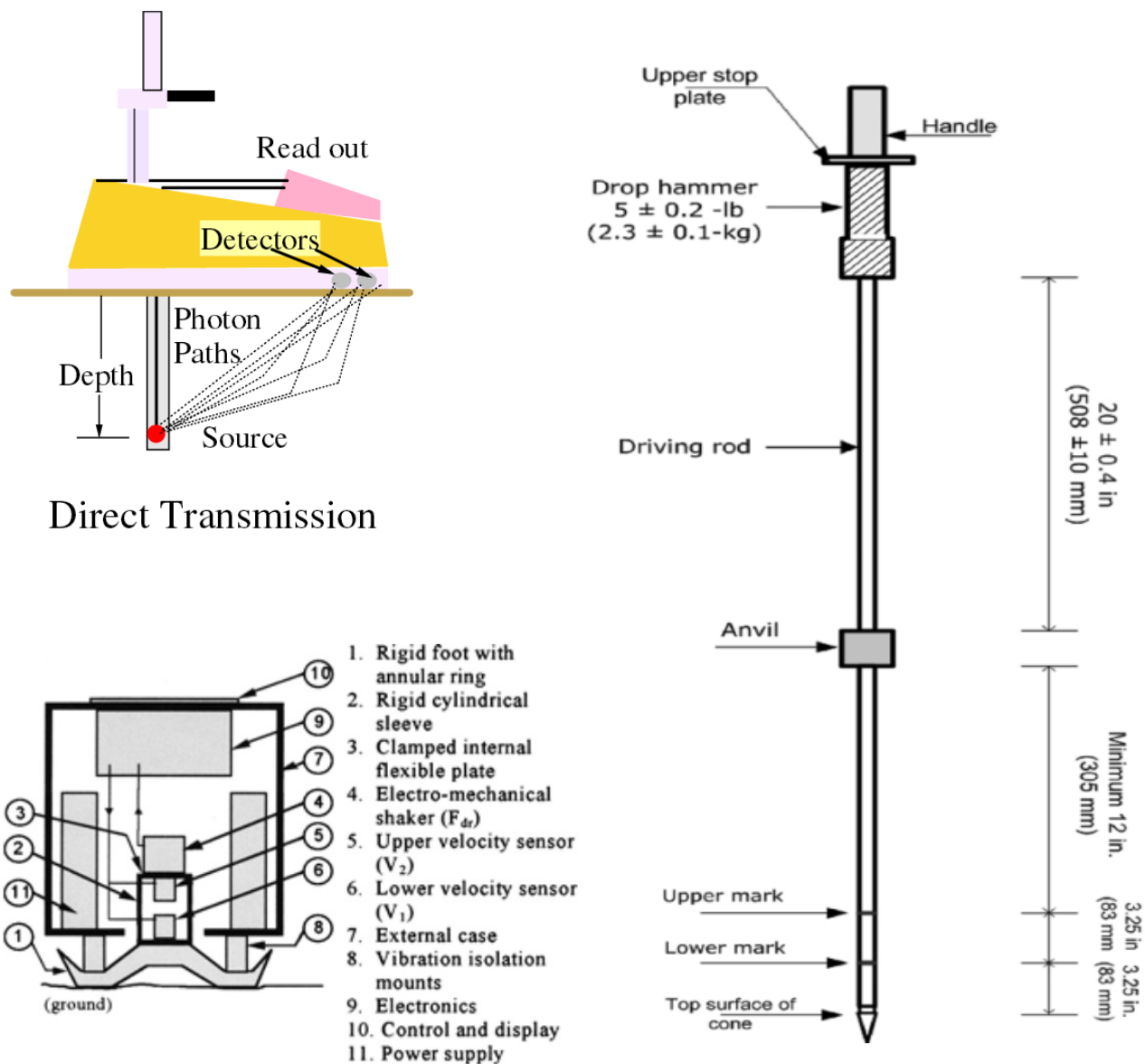


FIG. 1 Possible Apparatus Schematic

Figure 3.15. Nuclear Density Gauge (top left). Soil Stiffness Gauge (bottom left). Dynamic Cone Penetrometer (right). The schematics shown here point out the main features of each instrument.

SECTION 4 - LAB RESULTS AND DISCUSSION

The following sections detail the results from tests conducted in the lab to evaluate surface flooding, perhaps more accurately described as compaction by drainage, as well as jetting as methods to compact the various materials described above. Measurement methods and test setups are described in detail, and hypotheses and conclusions are made based upon the knowledge gained during index testing and the observed test results.

4.1 LABORATORY TESTING DESCRIPTION

Initial tests of jetting and flooding were conducted on a smaller scale in the liquefaction tank. To further characterize the materials and gain a better sense of the sensitivity of the soil structure to compaction by drainage, laboratory tests were conducted in a rigid wall permeameter, which allowed for the determination of falling head hydraulic conductivity of the materials. Larger scale lab tests were also completed in plastic storage containers with actual drain tile and geotextile filters to better simulate drainage conditions in the field. An important thought to keep in mind when reading and interpreting the following sections is that compaction in the most fundamental sense requires a failure of the soil: the existing particle contacts must be broken, and there must be a relative displacement between grains so the soil can reach a more compact arrangement. In this regard the lab tests will seek to evaluate this failure, or compaction, under a variety of scenarios. The test controls include deposition method, which will produce varying in situ densities, as well as material type. The varied particle sizes and shapes of each material will produce different interparticle contacts and different levels of friction between the grains. The first round of tests in the liquefaction tank is introduced below.

4.2 COMPACTION BY DRAINAGE IN THE LIQUEFACTION TANK

4.2.1 Flooded Deposition

The liquefaction tank used in this experiment is 20 cm in diameter and 60 cm in height. Flooded deposition is achieved by first treating the soils to oven dry condition before placing them into a column of water in the liquefaction tank. The soil enters the tank through a funnel situated on the rim of the tank to facilitate an even deposition around the middle of the water column. With this setup, the soil is deposited by individual grains falling through the water with low energy. A schematic of flooded deposition in the tank is shown in Figure 4.1.

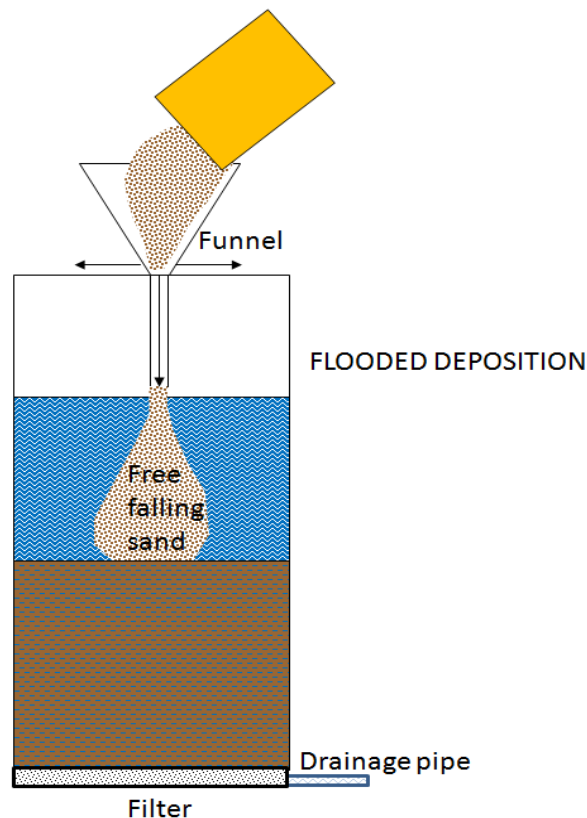


Figure 4.2. Flooded Deposition in the Tank. Individual sand grains fall through a column of water before they are deposited in the soil column. The funnel prevents the grains from caking onto the side of the tank. After the soil is deposited, the valves on the drainage pipe are opened, and the water column above the soil is allowed to drain.

This low energy method of deposition actually produced some of the higher in situ densities prior to compaction by drainage. As each individual grain falls through the column of

water, it is completely mobilized, free to fall into any void space in the soil column. In this sense the soil column that builds up as the grains fall into the tank is instantaneously saturated. With minimal capillary forces acting at the curved grain-water interface to bulk the sand into clumps, the grains are able to fill the void spaces more fully and achieve greater relative density. After the soil column has been fully deposited, the outflow valves are opened, and the soil is allowed to drain. It is hypothesized that the seepage force from the flowing water as well as the suction developed as the soil becomes unsaturated after drainage (matric suction increases) serve to compact the grains into a denser state.

During the first round of flooded deposition testing, the results were evaluated by determining the mass of solids before placement in the tank. Then the void ratio before and after drainage could be calculated by simply measuring the total volume of the soil column before and after drainage:

$$e_{in\ situ} = \frac{V_{total\ in\ situ} - V_{solids}}{V_{solids}} \quad (4.1)$$

$$e_{final} = \frac{V_{total\ final} - V_{solids}}{V_{solids}} \quad (4.2)$$

where $e_{in\ situ}$ equals the void ratio upon deposition and before drainage, e_{final} equals the void ratio after compaction by drainage, and V_{total} and V_{solids} equal the total volume of the soil column and the volume of solids in the column, respectively.

The final total volume seen in the Equation 4.2 was measured immediately after the water drained out of the soil column. As such, this measurement method likely did not allow for the full suction potential to develop within the soil column. Additionally, the water content of the soil was not measured after drainage. The water content may be used not only to determine the final void ratio, but also to determine the suction potential of the soil. In this sense a soil with higher water content post drainage would likely have not experienced the same suction as a soil with a lower water content. If the water is held in place in the soil even after drainage, the

increase in the effective stress felt by the solid matrix would be minimal at best. This may limit the effectiveness of compaction by drainage.

For the above concerns, a second round of compaction by drainage tests for flooded deposition was conducted with a few key improvements. First, the final total volume and total weight of the soil was measured 24 hours after completion of the initial drainage when most of the water left the soil column. The time period of 24 hours was selected as this would be a reasonable amount of time to allow a backfill to drain in the field before a construction crew would need to perform further work at the site. Additionally, the water content of the soil was measured at the 24 hour mark to get a better sense of the full suction potential of each soil. With these changes in place, the calculations for the second round were:

$$V_{total} = \frac{\pi}{4} d_{tank}^2 \bar{h}_{tank} \quad (4.3)$$

$$w = \frac{m_w}{m_s} \quad (4.4)$$

$$m_{solids} = \frac{m_{total}}{1 + w} \quad (4.5)$$

$$V_{solids} = \frac{m_s}{G_s} \quad (4.6)$$

$$V_{voids} = V_{total} - V_{solids} \quad (4.7)$$

$$e = \frac{V_{voids}}{V_{solids}} \quad (4.8)$$

$$D_R = \frac{e_{max} - e}{e_{max} - e_{min}} \quad (4.9)$$

where, V_{total} equals total volume of soil, d_{tank} equals diameter of tank, e equals void ratio, D_R equals relative density, \bar{h}_{soil} equals average height of soil, derived from five height equispaced measurements around the outside of the tank, and w equals water content. The water content was determined by dumping the entirety of the soil column into an empty bucket after 24 hours, thoroughly mixing, then taking three samples for the oven according to ASTM D2216.

This measurement methodology was followed for all subsequent tests in the liquefaction tank to improve the accuracy of the results. See below for a sensitivity analysis of void ratio and relative density to the measurement of water content and total volume of the soil in the tank.

The results for both the first and second round of flooded deposition tests are summarized in Tables 4.1 and 4.2. The most striking result is the increase in the measured relative density between the two rounds of testing. The silica sand, foundry sand, bedding sand, and foundry mix exhibited increases in relative density of 18%, 38.4%, 34%, and 55%, respectively. Some portion of the large increases in observed relative densities for these soils may be due to measurement error during the first round of tests, but it also highlights the importance of allowing the soils to drain for some time after the initial drainage is complete. During the second round of tests the soils were allowed to drain for a much longer period of time; this allows for the full compactive effect derived from suction to develop in the soil.

Table 4.1. First Round of Tests for Flooded Deposition in the Liquefaction Tank.

Soil Type	e	Δe	D_R (%)
Silica Sand	0.771	-0.011	11.4
Foundry Sand	0.598	-0.008	23.2
Bedding Sand	0.696	-0.009	29.3
Foundry Mix	0.628	0.000	22.5
Leveling Sand	0.521	-0.003	40.7
Limestone Screenings	0.587	-0.080	72.8
Paver Base	0.520	-0.012	43.3

Table 4.2. Second Round of Tests for Flooded Deposition in the Liquefaction Tank.

Soil Type	e	Δe	w (%)	D_R (%)
Silica Sand	0.724	-0.006	25.2	29.8
Foundry Sand	0.512	-0.004	5.3	61.6
Bedding Sand	0.593	-0.007	14.0	63.7

Foundry Mix	<i>0.515</i>	<i>-0.006</i>	<i>8.2</i>	<i>77.9</i>
Leveling Sand	<i>0.461</i>	<i>-0.015</i>	<i>7.6</i>	<i>66.1</i>
Limestone Screenings	<i>0.733</i>	<i>-0.066</i>	<i>22.7</i>	<i>27.6</i>
Clean Sand	<i>0.593</i>	<i>-0.009</i>	<i>18.6</i>	<i>61.3</i>

The relative density increases significantly between the two rounds of testing for all soils except the limestone screenings and the paver base. During the first round of testing, the large amount of fine particles in the limestone screenings and paver base migrated through the geotextile and out of the soil column. Due to the crude measurements made during the first round of testing, this decrease in the volume of solids present in the column was not accounted for, likely resulting in inaccurate measurements of void ratio. In fact, the limestone screenings was the poorest performing soil during the second trials, achieving a relative density of only 28%. The limestone screenings had the highest percentage of fines of all the materials at 8.4%. During deposition, these fines fell more slowly through the column of water according to Stokes' Law, forming a cap that significantly reduced both the conductivity of the soil and the energy with which water flowed through the soil.

Upon examination of Table 4.2, it is clear that high relative densities may be achieved by flooded deposition followed by compaction by drainage. The highest performing soils are the foundry mix, bedding sand, and foundry sand. These soils achieved the first, second, and fourth highest relative densities of all the soils tested at 78%, 64%, and 62%, respectively. The uniformity in grain size of these materials allows water to flow with greater compactive energy through the soil column.

On the other hand, the leveling sand, a much more well-graded material, also performed well during these tests. The leveling sand achieved the second highest relative density of all the soils tested at 66%. The high performance of this material is derived from the ability of all the different grain sizes to fill the void spaces as they fall freely through the column of water. This advantage is particularly relevant for a well-graded material like the leveling sand, a material

that is susceptible to bulking of particles due to capillary forces. Additionally, the smaller particles present in the leveling sand are more easily moved into the void spaces by the energy of the water flowing through the column during drainage.

Earlier it was hypothesized that a material with a higher water content post drainage would likely not perform as well due to a reduction in the effect of suction, an effect which increases the effective stress. The strongest proof of this hypothesis is seen in the poor performance of the silica sand. The silica sand is very similar in particle size distribution to the bedding sand, yet it had the highest water content post drainage at 25%, and the third lowest relative density at only 30%. Meanwhile, three of the higher performing materials, the foundry sand, leveling sand, and foundry mix had the lowest water contents at 5%, 7%, and 8%, respectively. Checking the water content of a backfill post drainage could be a quick and easy way to evaluate both the suitability of the material for this method as well as the effectiveness of the compaction.

Another important theme seen in both Tables 4.1 and 4.2 is the modest decrease in void ratio produced by compaction by drainage. Of all the materials in each round of testing, the leveling sand achieved the greatest void ratio reduction before and after drainage of only 0.015. This reduction was achieved in the second round of testing when the soils were allowed to drain for 24 hours. Clearly the fairly high relative densities seen in the second round of testing are due primarily to the highly effective flooded deposition method. Unfortunately flooded deposition is extremely difficult to recreate in the field. To perform flooded deposition at a bridge abutment for example, some kind of water-tight structure would need to be erected adjacent to the abutment, and filled with a large amount of water prior to deposition. This would create large lateral stresses on the wall from the hydrostatic force of the water. What has been observed in the lab is essentially individual grains falling into a column of soil with high in situ density, after which their compactness is very modestly improved by drainage. It will be important to monitor the change in void ratio caused by drainage for the other deposition methods.

Of particular note going forward is the impact of fine particles on the performance of compaction by drainage for a flooded soil. The cap of fines seen in the limestone screenings and the paver base is reason for concern for both practicality and performance. If the conductivity is too low, it will take too long for the backfill to drain, causing delays in the construction process. Furthermore, if the conductivity is too low, the downward energy of the water flowing through the soil will be reduced, resulting in less effective compaction.

4.2.2 Wet Deposition

Wet deposition was performed by dumping wet soils into the tank with a large scoop. The soils were dropped from the top of the tank such that they fall in slugs with a high amount of energy. After the soil was placed, a small amount of water was added from the top of the soil column to saturate the soil before initiating drainage. A schematic of flooded deposition in the tank is shown in Figure 4.2.

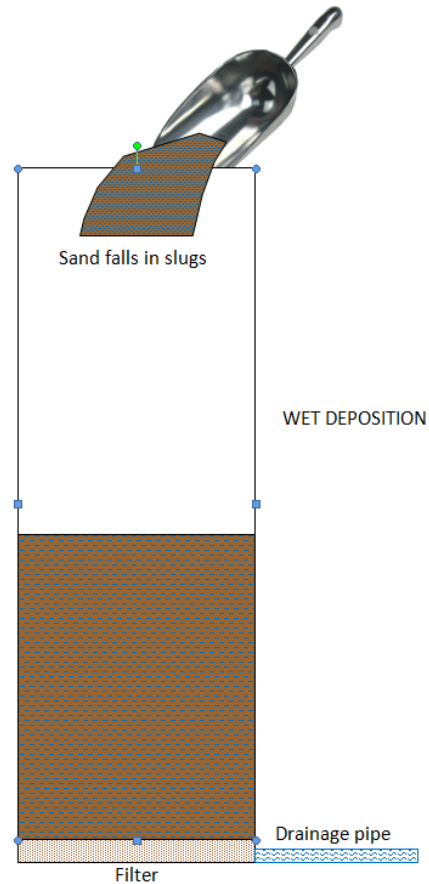


Figure 4.2. Wet Deposition in the Tank. Individual sand grains fall through a column of water before they are deposited in the soil column. After the soil is deposited, the valves on the drainage pipe are opened, and the water column above the soil is allowed to drain.

Similar to flooded deposition testing, two rounds of wet deposition tests were conducted. The primary reason for conducting two rounds of wet deposition tests was to investigate in a qualitative sense the difference in final relative density of a soil deposited slightly wet and very wet. Despite the high amount of energy with which the soil slugs were placed, during the first round of testing, it was common to observe large air voids against the side of the tank. These voids developed because the slugs in the slightly wet condition were in the range of bulking water contents, where grains are held together by capillary forces. During the second round of tests, the soil was treated to a very wet condition such that the slugs easily slid into place and filled the void spaces against the side of the tank.

It was hypothesized that it would be worthwhile to investigate the difference between the slightly wet and very wet conditions in the laboratory, because in the field, large air voids against an abutment wall would greatly accelerate erosional processes. With large pockets of air to travel through, flow paths could transport large quantities of fill away from the wall, causing loss of support beneath the pavement structures. At the same time, it was hypothesized that while a soil in the very wet condition may not leave behind large air voids against a confining structure, the grains would be pushed apart by the greater amount of water between them, resulting in lower final relative density.

The results for both the first and second round of wet deposition testing are shown in Tables 4.3 and 4.4. From Table 4.3, it is clear that compaction by drainage offers little improvement over the in situ structure of the soil upon wet deposition. The energy of the water flowing through the soil is simply not great enough to move the grains into a denser arrangement. This is a continuing theme from the results of flooded deposition testing. The silica sand experienced the greatest decrease in void ratio after drainage at only 0.006. Essentially the results of the wet deposition testing indicate the density achieved by either slightly wet or very wet deposition.

Table 4.3. First Round of Tests for Wet Deposition in the Liquefaction Tank.

Soil Type	<i>e</i>	Δe	<i>w</i> (%)	D_R (%)
Silica Sand	<i>0.641</i>	<i>-0.006</i>	<i>23.0</i>	<i>62.4</i>
Foundry Sand	<i>0.436</i>	<i>-0.003</i>	<i>3.0</i>	<i>95.5</i>
Bedding Sand	<i>0.555</i>	<i>0.000</i>	<i>22.0</i>	<i>76.3</i>
Foundry Mix	<i>0.553</i>	<i>-0.004</i>	<i>17.0</i>	<i>59.3</i>
Leveling Sand	<i>0.443</i>	<i>-0.002</i>	<i>8.4</i>	<i>73.7</i>
Limestone Screenings	<i>0.663</i>	<i>-0.004</i>	<i>13.9</i>	<i>49.2</i>
Clean Sand*	<i>0.846</i>	<i>-0.003</i>	<i>15.0</i>	<i>-32.7</i>
Paver Base	<i>0.599</i>	<i>-0.002</i>	<i>10.5</i>	<i>19.2</i>

*sand slugs left large air voids against the side of the tank

Table 4.4. Second Round of Tests for Wet Deposition in the Liquefaction Tank.

Soil Type	E	w (%)	D_R (%)
Silica Sand	<i>0.603</i>	<i>20.5</i>	<i>77.3</i>
Foundry Sand	<i>0.554</i>	<i>8.0</i>	<i>42.9</i>
Bedding Sand	<i>0.569</i>	<i>20.7</i>	<i>71.7</i>
Foundry Mix	<i>0.499</i>	<i>18.5</i>	<i>85.8</i>
Leveling Sand	<i>0.605</i>	<i>12.3</i>	<i>5.1</i>
Clean Sand	<i>0.660</i>	<i>12.1</i>	<i>36.4</i>

Along this line of thinking, the relative densities achieved by wet deposition can be quite high. Tests from both rounds of tests, the foundry sand, foundry mix, and silica sand achieved the highest relative densities at 96%, 86%, and 77%, respectively. These materials are very uniform and more fine in grain size, well within the erodible zone denoted by White et al. (2007). Of note is the close relationship between the foundry sand and the silica sand. Silica sand is often used in steel foundries to cast various parts under high temperatures and pressure. When the silica sand reaches the end of its life cycle in the foundry, it becomes the recycled material foundry sand. Where silica sand is finer and more angular, the spent foundry sand is coarser and very well rounded. It is hypothesized that rounded grains are much more easily moved into a more compact arrangement by the low compactive energy imparted by Compaction by drainage. The rounded grains do not tend to interlock in the way that angular grains do (Cho et al., 2006). From all the results, it is clear that the energy with which the slugs fall into the tank is great enough to create a dense volume of soil before any compaction by drainage occurs.

Table 4.5. Changes to Water Content and Relative Density between Rounds 1 and 2. Positive ΔD_R indicates that relative density increased in round 2.

Soil Type	Δw (%)	ΔD_R (%)
Silica Sand	<i>-2.5</i>	<i>+14.9</i>
Foundry Sand	<i>+5.0</i>	<i>-52.6</i>

Bedding Sand	-1.3	-4.6
Foundry Mix	+1.5	+26.5
Leveling Sand	+3.9	-68.6
Clean Sand	-2.9	+69.1

The next most striking result seen in Tables 4.3 and 4.4 is the great and seemingly inconsistent differences in relative density between the two rounds of testing. These differences are highlighted in Table 4.5. In fact, these results indicate that there is some optimum water content where the soil will fall as a slug with enough energy to fill the voids against the walls of the tank, but where there is also not too much water pushing the grains apart as the soil is deposited. The soils that exhibited the greatest change in water content after drainage also showed the greatest change in relative density. As the water content of the leveling sand increased by 3.9%, its relative density decreased from 74% to only 5%. Another soil that exhibited this type of sensitivity was the foundry mix; when its water content increased by 1.5%, its relative density increased from 59% to 86%. Further examination of the other soils tested indicates a similar type of sensitivity to the degree of saturation of the soils as they are wet deposited into the tank.

Similar to the flooded deposition, wet deposition is capable of producing high relative densities for these clean sands. Most of the compactness of the soil results from their in situ placement; the drainage experienced by the soils after placement offers a very modest improvement in compactness. Another continuing theme seen here is the high performance of soils with lower water content post drainage. Four of the six soils tested in both rounds, including the silica sand, foundry sand, leveling sand, and the clean sand, all experienced an increase in relative density as their post drainage water content decreased between rounds. Soils with a lower water content post drainage may not only have experienced more suction

during drainage, but they may also have been placed at a higher in situ density, with less water in the void space pushing the grains apart during deposition.

4.2.3 Dry Deposition at Low and High Energy

Dry deposition at low energy was performed in two separate rounds of testing. During the first round, the soils were first treated to oven dry condition, then gently placed into the tank with a ladle. This process is shown in Figure 4.3. During the second round of testing, the soils were oven dried, then placed into a long cylinder in the tank. This process is shown in Figure 4.4 below. The diameter of the cylinder is 10 cm, about half the diameter of the tank. This cylinder was raised slowly and the grains slid gently into place in a manner similar to that described in the maximum void ratio test. It was hypothesized that applying two low energy methods to all the soils may produce varying in situ densities and different soil structures. These differences allow for a more thorough evaluation of compaction by drainage for loose soils. Meanwhile, dry deposition at high energy was performed by again oven drying, then dumping the soil all at once into the tank just above the rim of the tank. This process is shown in Figure 4.5.

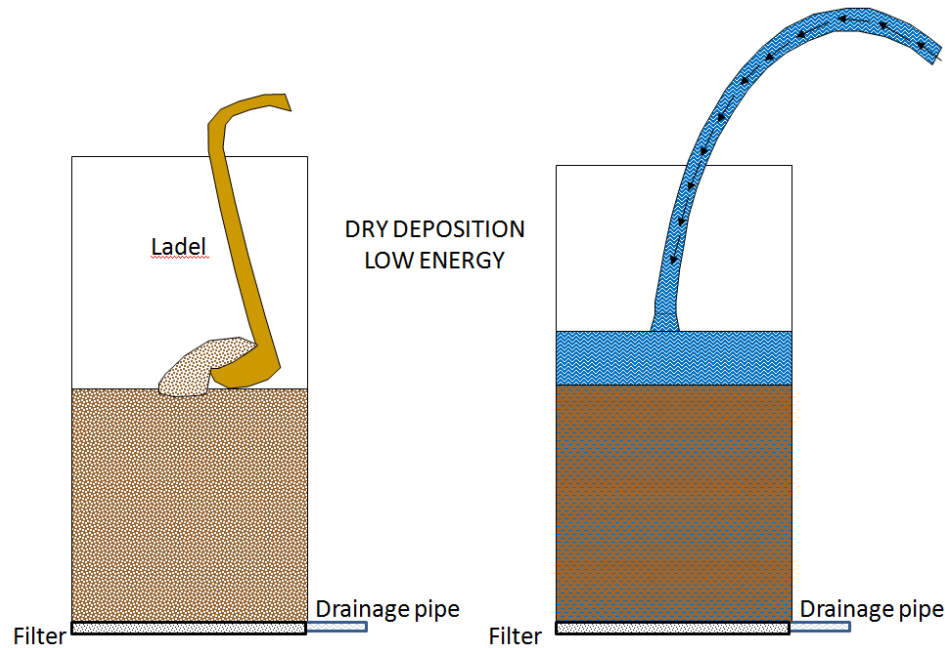


Figure 4.3. Low Energy, Dry Deposition in the Tank during Round 1. The soil grains are deposited gently with the ladel into the tank. The column is fan-sprayed on the surface to initiate Compaction by drainage.

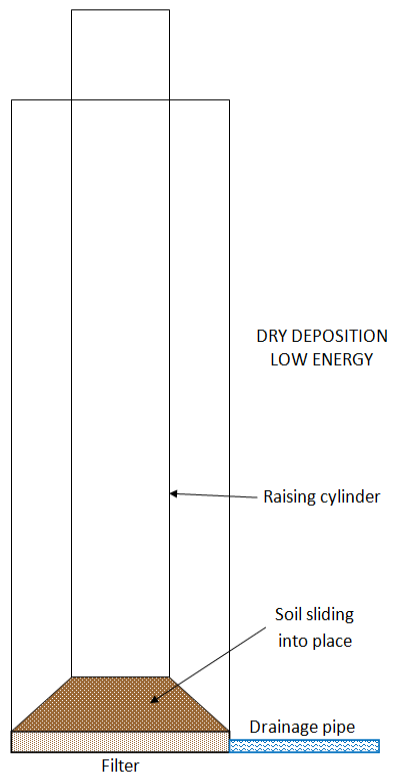


Figure 4.4. Low Energy, Dry Deposition in the Tank during Round 2. The soil grains slide into place as the cylinder is raised.

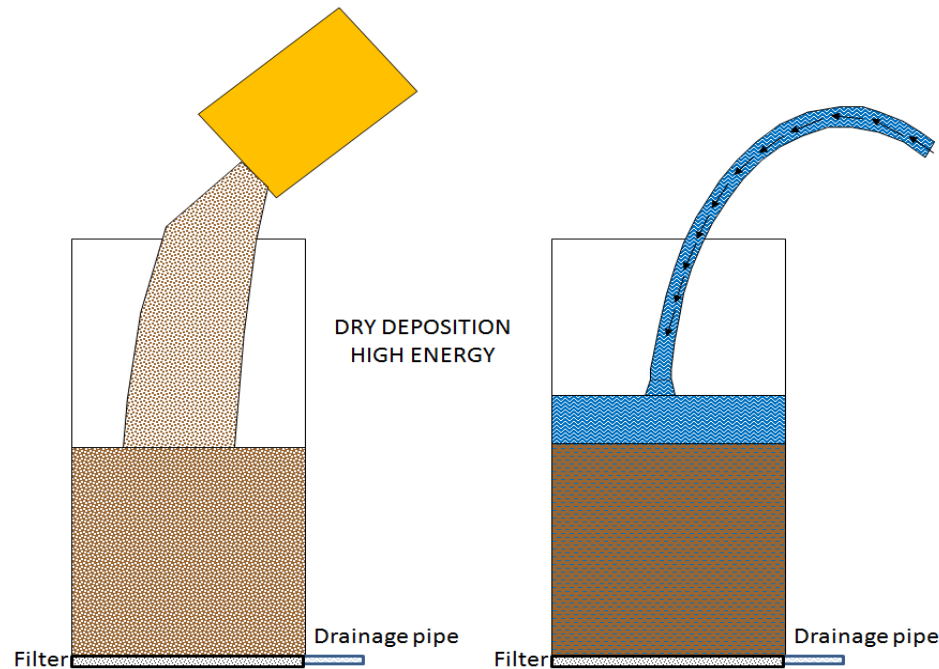


Figure 4.5. High Energy, Dry Deposition in the Tank. The soil grains fall from an elevation just above the top of the tank. The column is fan-sprayed on the surface and compacted by drainage.

After each soil was placed, water was gently fan-sprayed onto the surface and allowed to drain through the column to initiate compaction by drainage. For these dry deposition methods, it was difficult to ensure that the soil became fully saturated. The water often followed preferential flow paths through the column, leaving dry pockets of soil behind. These dry pockets often could be saturated eventually as water was fan-sprayed for a longer period of time, but nonetheless the pockets could reduce the potential for the suction mechanism to compact the soil.

The results for both the first and second round of dry deposition at low energy testing are shown in Tables 4.6 and 4.7. Even for these loose soils, the change in void ratio before and after drainage is minimal. The limestone screenings experienced the greatest decrease in void ratio at only 0.013. As noted during flooded deposition testing, the limestone screenings have the highest percentage of fines of all the soils at 8.4%. These small particles can be mobilized

into the void space by the low energy of water seeping through the soil. The modest improvement in soil compactness due to drainage observed here continues a theme seen in both flooded and wet deposited soils.

Table 4.6. First Round of Tests for Dry Deposition at Low Energy in the Liquefaction Tank.

Soil Type	E	Δe	w (%)	D_R (%)
Silica Sand	0.790	-0.004	29.4	3.9
Foundry Sand	0.544	-0.004	7.2	47.3
Bedding Sand	0.645	-0.005	22.4	46.3
Foundry Mix	0.567	-0.002	19.6	52.5
Leveling Sand	0.564	-0.006	18.1	22.5
Limestone Screenings	0.644	-0.013	11.2	55.1
Clean Sand	0.661	-0.003	13.4	36.1
Paver Base	0.655	-0.006	10.5	2.1

Table 4.7. Second Round of Tests for Dry Deposition at Low Energy in the Liquefaction Tank.

Soil Type	E	w (%)	D_R (%)
Silica Sand	0.685	20.3	45.1
Foundry Sand	0.619	11.9	13.8
Bedding Sand	0.631	23.6	51.0
Foundry Mix	0.572	14.7	50.0
Leveling Sand	0.518	9.1	41.9
Clean Sand	0.676	17.4	30.5

The ladle method implemented in the first round of testing produced greater final relative densities for the foundry sand, foundry mix, and the clean sand. These three soils exhibited a decrease in relative density of 32.5%, 2.5%, and 5.6% in round 2. This indicates that the raising cylinder method produces looser states for very uniform, coarser sand size particles like those found in these three soils. However, the raising cylinder method produced greater final relative densities for the silica sand, bedding sand, and the leveling sand. These three soils exhibited

increases in relative density of 41.2%, 4.7%, and 19.4% in round 2. Overall loose deposition produced low relative densities as expected. The greatest relative density achieved by any of the soils for both methods was the limestone screenings in round 1 at 55.1%. Of the 14 total tests conducted, four soils achieved relative density between 40-50%, three soils achieved relative density between 20-40%, and three soils achieved relative density between 0-20%.

As expected, dry deposition at high energy produced soils with greater relative density than those soils subjected to dry deposition at low energy. The results for both rounds of dry deposition at high energy testing are shown in Tables 4.8 and 4.9. The foundry mix, foundry sand, and bedding sand achieved the highest relative densities of all the soils at 84%, 65%, and 58%, respectively. These relative densities are within the acceptable range for a construction application if the backfill were placed outside the roadway.

Table 4.8. First Round of Tests for Dry Deposition at High Energy in the Liquefaction Tank.

Soil Type	e	Δe	w (%)	D_R (%)
Silica Sand	0.749	-0.005	25.1	20.0
Foundry Sand	0.504	-0.002	8.9	65.2
Bedding Sand	0.626	-0.002	22.8	52.7
Foundry Mix	0.502	-0.007	13.5	84.3
Leveling Sand	0.504	-0.003	9.2	47.9
Limestone Screenings	0.634	-0.014	7.8	58.2
Clean Sand	0.723	-0.004	24.3	13.0
Paver Base	0.602	-0.002	10.6	18.3

Table 4.9. Second Round of Tests for Dry Deposition at High Energy in the Liquefaction Tank.

Soil Type	e	w (%)	D_R (%)
Silica Sand	0.752	27.2	18.8
Foundry Sand	0.518	3.4	58.9
Bedding Sand	0.609	22.9	58.3
Foundry Mix	0.508	12.2	81.4
Leveling Sand	0.571	13.6	19.5
Clean Sand	0.694	19.4	23.8

While dry deposition most closely simulates deposition that occurs in the field, where backfill falls out of a dump truck at air dry condition, it also produced the most variable in situ relative densities. This is concerning because greater uncertainty with respect to the in situ density of backfills necessitates more thorough compaction to ensure adequate performance. The variable relative densities for dry deposition are particularly visible in Figure 4.6, which shows the summary of results for compaction by drainage in the liquefaction tank by deposition method. The relative densities for dry deposition at low energy and high energy range from 4% to 55%, and 20% to 84%, respectively. Furthermore, angular materials perform poorly in dry deposition due to the interlocking of particles and creation of void spaces upon deposition. The silica sand and clean sand, each material with subangular Krumbein roundness, were the worst performers during dry deposition. Figure 4.6 also shows how these angular materials do not follow the same trend as the more rounded materials in the group. The top half of the graph features materials with a predictable increase in relative density from the dry deposition methods to wet deposition methods. These materials include the foundry sand, foundry mix, and leveling sand, all materials that are subrounded to well-rounded. With the exception of one outlier, the relative densities for flooded and wet deposition for these materials range from 62% to 78%, and 74% to 96%, respectively. All of these findings are particularly relevant considering the Wisconsin DOT's use of more angular, natural sands deposited at air dry condition as backfill. The results of lab tests indicate in fact that wet deposition methods with more rounded and uniform materials produce much greater and more predictable in situ relative densities.

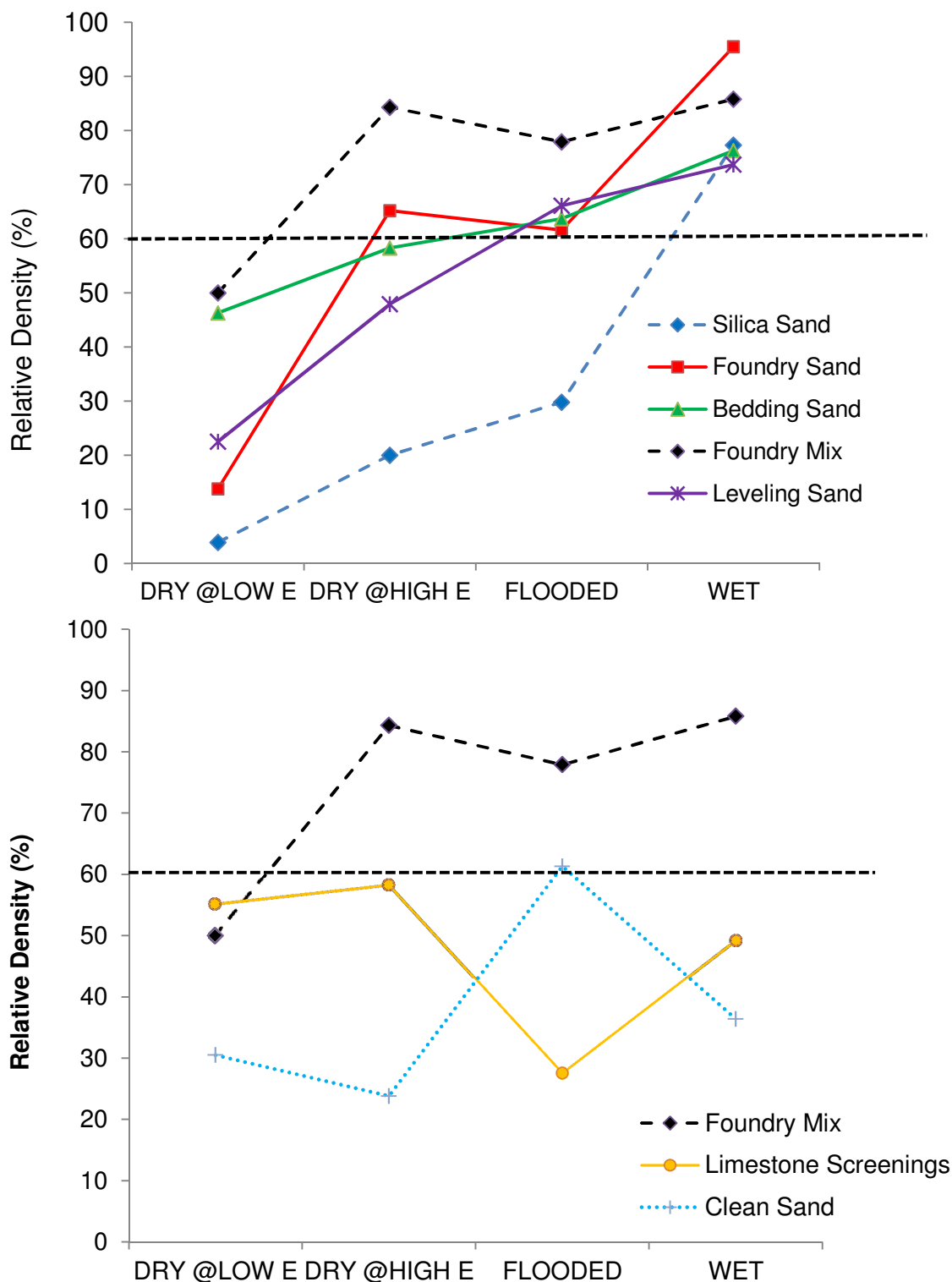


Figure 4.6. Summary of Compaction by Drainage in the Liquefaction Tank. Results are shown from lowest D_R in dry deposition at low energy trials, highest D_R in wet deposition and dry deposition at high energy trials, and Round 2 of flooded deposition, when measurement methods were improved. The dashed line at $D_R = 60\%$ shows an alternative compaction standard to the more commonly used relative compaction = 90% or greater.

4.2.4 Sensitivity Analysis

At this point it is prudent to examine both the reproducibility of tests conducted in the liquefaction tank and the sensitivity of the void ratio and relative density to changes in the measurement of water content and total volume. Where the dry deposition at low energy testing focused on comparing different loose deposition strategies, the two rounds of dry deposition at high energy testing were conducted in exactly the same manner. To help examine reproducibility, the change in water content and relative density between each round for six of the soils tested is shown in Table 4.10.

Table 4.10. Changes to Water Content and Relative Density Between the Identical Round 1 and Round 2 of Testing for Dry Deposition at High Energy. Positive ΔD_R indicates that relative density increased in round 2.

Soil Type	Δw (%)	ΔD_R (%)
Silica Sand	+2.1	-1.2
Foundry Sand	-5.5	-6.3
Bedding Sand	+0.1	+5.6
Foundry Mix	-1.3	-2.9
Leveling Sand	+4.4	-28.4
Clean Sand	-4.9	+10.8

The results between the two rounds are fairly consistent; five of the six soils exhibited changes in relative density of 10% or less, and all of the soils exhibited changes in post drainage water content of 5.5% or less. This inspires some confidence in the measurement methods implemented for the liquefaction tank as detailed in the flooded deposition section above. However, the leveling sand exhibited a decrease in measured relative density of 28% and an increase in measured water content of 4.4 % between the two trials. This discrepancy warrants a kind of sensitivity analysis. For example, if the measured post drainage water content of the leveling sand was the same as that measured in round 1 at 9.2%, the calculated

void ratio and relative density would be 0.510 and 45%, respectively. These estimates are very close to the void ratio and relative density of 0.504 and 48% that were actually measured in trial 1. Along a similar line of thinking, if the measured average height of the leveling sand was 1 cm less in round 2, the calculated void ratio and relative density would be 0.518 and 42%, respectively. Being inaccurate to 1 cm of height difference for a soil column that is 30 cm high and sloping and dipping on the surface is not out of the question, and the 42% relative density calculated in the sensitivity analysis is not far from the 48% that was actually measured in trial 1. The question to ask is, 'Is the structure and packing of the grains actually different between trial 1 and trial 2? Or is the difference in calculated relative density due to measurement errors?' Furthermore, a soil with a narrow range of e_{min} and e_{max} would be more prone to large differences in calculated relative density. In light of the sensitivity analysis, relative density is reliable as a general indicator of the performance of each material when subjected to compaction by drainage. However, other measurement techniques involving strength and stiffness may be more sensitive than relative density to changes in soil structure, and therefore could be more effective in evaluating compaction methods.

4.2.5 Compaction by Drainage Conclusions

With relative density and water content as good general indicators of performance, a number of themes and key results have been identified in the preliminary investigations of compaction by drainage in the liquefaction tank. First, soils should be allowed to drain for some time (24 hours is recommended) to allow for the maximum suction potential to develop in the soil. In theory this suction will increase the strength of the soil, although further tests are needed to evaluate this phenomenon. Second, fine particles tend to form an impermeable cap during flooded deposition which limits the practicality of compaction by drainage. Third, compaction by drainage has been observed in the lab to produce very modest increases in compactness of soils regardless of the deposition method. Fourth, calculated relative density has some

sensitivity to measurements of water content and total volume of soils in the liquefaction tank. Additional tests with less sensitivity to these kinds of measurements would be beneficial to further evaluating compaction by drainage. Fifth, in situ relative densities up to 60-80% can be achieved by flooded deposition and wet deposition for rounded and uniform materials, or materials that have high drainage capacity. However, flooded deposition would be particularly difficult to perform in the field because temporary water containment structures would need to be constructed. Finally more angular materials such as the clean sand and limestone screenings are prone to particle interlocking and reduced mobility of grains during compaction by drainage, leading to unexpected and often lower in situ relative densities.

4.3 COMPACTION BY JETTING IN THE TANK

4.3.1 Test Setup

Upon completion of compaction by drainage testing, a new program to evaluate compaction by hydraulic jetting was implemented. Once again, tests were conducted in the 20 cm (8 in.) diameter by 60 cm (24 in.) high liquefaction tank. A 0.64 cm (0.25 in.) outer diameter SharkBite pipe was hooked up to the sink and used as the jetting instrument. To perform the jetting, the pipe was inserted and removed from the soil column in a continuous fashion with the outflow valves open throughout the process. Meanwhile the soil columns were at least 30 cm high before jetting for each of the tests.

4.3.2 Initial Observations and Hypotheses

Where the fundamental phenomena involved in compaction by drainage could be simulated accurately in the liquefaction tank, the physical processes involved in jetting posed some challenges and limitations in the laboratory environment. The most important limitation is derived from the small size of the tank. During jetting, the water reflects off the walls and up from the bottom of the confined tank; in this manner the water tended to push the solid particles

apart instead of compacting them together. In a field application, the jet of water would flow predominantly downward, mobilizing the grains into a denser arrangement. Additionally the erratic flow of water in the tank produced greater noise in the results than the more controlled process of compaction by drainage. In a sense it was difficult to jet the soil columns exactly the same way twice to isolate the effect of soil material characteristics on final relative density.

Due to these limitations, the focus of jetting tests shifted from deposition methods and material characteristics, which were investigated in the compaction by drainage tests, to the energy with which water drains from the soil column. It was hypothesized that the deposition method will have little to no effect on the final compactness of a jetted soil because jetting greatly disturbs the soil solid matrix. During each test, the soils were observed to liquefy in localized areas around the jetting instrument. In this way the final compactness of the soil would depend not on the in situ density upon deposition, but on the energy with which water drains out of the column while the grains are liquefied and free to move into a new arrangement. If water drains through the column with low energy or not at all, the grains will be pushed apart, unable to move into a denser arrangement. However, water draining with a high amount of energy tends to carry the liquefied, mobilized grains into a denser arrangement, producing stronger interparticle contacts and reduced compressibility.

4.3.3 Comparison of Deposition Method and Material Type

The results for all the jetting tests are summarized in Tables 4.11 to 4.15. A comparison of the results for jetting selected materials deposited dry at high energy and those deposited wet illustrates the noise in the results identified above. All of the soils subjected to both rounds of tests experience changes in relative density greater than 15%. The silica sand, foundry mix, and leveling sand experienced increases in relative density during wet deposition of 29%, 15%, and 28%, respectively. These results seem to indicate that wet deposition produces better results than dry deposition for soils subjected to jetting. However, each of these materials are different

in shape and gradation. Where the leveling sand is well-graded, the silica sand and foundry sand are very uniform. Where the silica sand is angular and finer, the foundry sand is very well rounded and consists of much coarser sand particles. Also of note is how dissimilar the performance of the foundry mix is against that of the foundry sand; while the foundry mix increased in relative density from dry to wet deposition, the foundry sand decreased by 16%. These two materials are similar in shape and gradation; the only difference is that the foundry mix is slightly finer than the foundry sand, with a D_{10} grain size of 0.2 mm, compared to 0.4 mm for the foundry sand. Both rounds of testing produced negative relative densities for the leveling sand, which by definition means the leveling sand was in a looser state than that produced by the maximum void ratio index tests. This is likely the result of the energy of the water being reflected back up off the bottom of the confined tank. Combined with the concerns over the erratic flow of water in the tank during jetting, it is difficult to infer the effect of material characteristics on jetting performance from tests conducted in the tank.

Table 4.11. Jetting Selected Materials Deposited Dry at High Energy in the Liquefaction Tank.

Soil Type	<i>e</i>	<i>w</i> (%)	D_R (%)
Silica Sand	<i>0.630</i>	<i>14.3</i>	<i>66.7</i>
Foundry Sand	<i>0.580</i>	<i>8.8</i>	<i>31.3</i>
Foundry Mix	<i>0.650</i>	<i>16.1</i>	<i>11.8</i>
Leveling Sand	<i>0.708</i>	<i>16.7</i>	<i>-38.6</i>
Clean Sand	<i>0.641</i>	<i>13.7</i>	<i>43.5</i>

Table 4.12. Jetting Selected Materials Deposited Wet in the Liquefaction Tank.

Soil Type	<i>e</i>	<i>w</i> (%)	D_R (%)
Silica Sand	<i>0.704</i>	<i>13.9</i>	<i>37.6</i>
Foundry Sand	<i>0.615</i>	<i>5.7</i>	<i>15.6</i>
Foundry Mix	<i>0.620</i>	<i>15.5</i>	<i>26.5</i>
Leveling Sand	<i>0.641</i>	<i>11.1</i>	<i>-10.2</i>

Table 4.13. Third Round of Tests: Jetting Selected Materials Under Greater Hydraulic Gradient. Two outflow hoses were lowered to the floor during this round of testing.

Soil Type	<i>e</i>	<i>w</i> (%)	<i>D_R</i> (%)
Silica Sand	<i>0.727</i>	<i>17.7</i>	<i>28.6</i>
Foundry Sand	<i>0.522</i>	<i>4.7</i>	<i>57.1</i>
Foundry Mix	<i>0.626</i>	<i>14.6</i>	<i>23.5</i>
Leveling Sand	<i>0.589</i>	<i>8.4</i>	<i>11.9</i>
Clean Sand	<i>0.653</i>	<i>11.9</i>	<i>39.0</i>

Table 4.14. Fourth Round of Tests: Jetting Selected Materials Under Vacuum of Approximately -20 kPa Gauge Pressure.

Soil Type	<i>e</i>	<i>w</i> (%)	<i>D_R</i> (%)
Silica Sand	<i>0.638</i>	<i>8.5</i>	<i>63.5</i>
Foundry Sand	<i>0.519</i>	<i>2.9</i>	<i>58.5</i>
Leveling Sand	<i>0.491</i>	<i>5.6</i>	<i>53.4</i>
Clean Sand	<i>0.686</i>	<i>11.6</i>	<i>26.8</i>

Table 4.15. Fifth Round of Tests: Jetting Selected Materials Under Vacuum of Approximately -20 kPa Gauge Pressure.

Soil Type	<i>e</i>	<i>w</i> (%)	<i>D_R</i> (%)
Silica Sand	<i>0.664</i>	<i>9.1</i>	<i>53.3</i>
Foundry Sand	<i>0.545</i>	<i>4.2</i>	<i>46.9</i>
Leveling Sand	<i>0.523</i>	<i>5.5</i>	<i>39.8</i>
Clean Sand	<i>0.622</i>	<i>8.4</i>	<i>50.6</i>

4.3.4 Comparison of Drainage Energy

These concerns and limitations aside, further tests were conducted to evaluate the impact of drainage energy on jetting performance. Upon completion of the first two rounds of tests, the outflow hoses were lowered by approximately 75 cm, thereby increasing the hydraulic gradient across the soil columns and the energy with which water drained through the soils. The results of this third round of testing are shown in Table 4.13. The foundry sand and leveling

sand achieved greater relative density during the third round than either of the first two rounds at 57% and 12%, respectively. Meanwhile, the expected increase in suction potential in the soils under the increased hydraulic gradient is confirmed in the post drainage water contents. Four of the five soils tested in each of the three rounds exhibited lower post drainage water content during the third round than either of the first two rounds. Once again the results support the use of post drainage water content as an indicator of the compactness of soils when subjected to drainage and jetting. Finally each of the other three soils achieved relative densities close to the maximum relative density observed in the first two rounds of tests. The foundry mix and clean sand came within 3% and 4.5% of the maximum relative density observed in the first two rounds, within the level of measurement error identified in the compaction by drainage sensitivity analysis.

Upon observing modest improvements to the compactness of soils subjected to jetting under a greater hydraulic gradient, the system was altered significantly to be able to increase the gradient to a much greater degree. During the fourth and fifth round of tests, the outflow hoses were routed into an intermediate drainage tank measuring 30 cm (12 in.) in diameter and 100 cm (39.4 in.) in height. This intermediate tank was then subjected to a vacuum via a Venturi style aspirator. A picture and schematic of this setup are shown in Figure 4.7. In this way it was possible to apply a vacuum to the outflow end of the soil with no danger of soil particles clogging up the vacuum. The setup was capable of applying vacuum gauge pressures up to -40 kPa to the intermediate tank. The intermediate tank was also large enough to drain a large amount of water from the soil without interrupting the flow of air out of the tank, a condition necessary to maintain the vacuum pressure. To alleviate some of the concerns with regard to the suitability of the liquefaction tank as an apparatus to investigate jetting, and to examine the reproducibility of the results, the fourth and fifth round of tests were identical. During all of the tests for both rounds, a vacuum gauge pressure of approximately -20 kPa was maintained in the intermediate tank throughout the jetting process.

The results of the fourth and fifth round of jetting tests are shown in Tables 4.14 and 4.15 as well as Figure 8. The most striking trend seen in the results is the increase in relative density observed for the silica sand, foundry sand, and leveling sand, shown in Table 4.16. In this table, the relative densities from the identical fourth and fifth rounds of testing were averaged, and then the differences between this average and the relative densities observed in the first three rounds were calculated. A positive difference indicates a higher relative density was achieved under the vacuum. The well-graded leveling sand experienced the greatest improvement in compactness under the vacuum. This observation is expected as a well-graded material tends to have less drainage capacity and a lower minimum void ratio. Each of these barriers to performance of the material when subjected to compaction by jetting are overcome by the greatly increased energy with which water drains through the leveling sand. Drainage capacity of the material is not as significant of an issue, and a wider range of grain sizes are mobilized into place. Meanwhile, the silica sand and the foundry sand showed increases in relative density ranging between 21% to 37% from the various tests performed during the first three rounds.

Table 4.16. Comparison of Relative Density of Soils Subjected to Varying Drainage Energies Across the Five rounds of tests.

Soil Type	Average D_R from Round 4 & 5 (%)	ΔD_R from Round 1 (%)	ΔD_R from Round 2 (%)	ΔD_R from Round 3 (%)
Silica Sand	58.4	-8.3	+20.8	+29.8
Foundry Sand	52.7	+21.4	+37.1	-4.4
Leveling Sand	46.6	+85.2	+56.8	+34.7
Clean Sand	38.7	-4.8	--	-0.3

The only material that did not exhibit a consistent increase in relative density under the vacuum was the clean sand. In fact, this material behaved consistently across the range of drainage energies applied in all the rounds of testing. The range of relative density across all the

rounds for the clean sand was only 24%, from a minimum of 27% to a maximum of 51%. Even more perplexing is that the minimum and maximum relative densities were observed in the fourth and fifth rounds of testing. These two rounds were conducted using the exact same procedure. It is difficult to isolate the cause of these unexpected results. The clean sand is most similar in gradation to the silica sand yet is not nearly as responsive to changes in testing procedure. Further analysis and/or testing would need to be implemented to determine why only the clean sand behaves independently of drainage energy. Further tests could be directed at isolating the effects of surface roughness, or unique capillary or osmotic effects based on grain shape or mineralogy, on the performance of this material when subjected to jetting.

4.3.5 Jetting Conclusions

A number of themes and key results have been identified in the preliminary investigations of compaction by hydraulic jetting in the liquefaction tank including (1) the small size of the tank imposes the undesirable effect of water energy reflecting off the walls of the tank during jetting, (2) wet deposition produced higher relative densities than dry deposition, although this may be due to the difficulty of jetting in the same manner twice, (3) drainage energy appears to be the most important factor for effective jetting, as jetting under the vacuum produced the greatest relative densities, (4) most relative densities produced under the vacuum ranged from 50 to 60%, a level of compactness acceptable for fills outside the roadway, and (5) lower post drainage water contents continue to be directly related to higher observed relative densities, likely due to the increased suction in the pore water.

Going forward, tests in the laboratory should focus on increasing the scale of compaction procedures, especially for compaction by jetting. The tank was simply too small to evaluate important parameters such as spacing of jetting events and effective compaction radius, flow rate out of the instrument, layer thickness, drainage capacity of the system, and duration of jetting or rate of insertion and removal of the instrument. All of these parameters

influence not only the performance of the soils subjected to jetting but also the practicality and efficiency of the operation. These important jetting parameters will be investigated and evaluated with larger scale lab testing, flow modeling, and full-scale field applications.

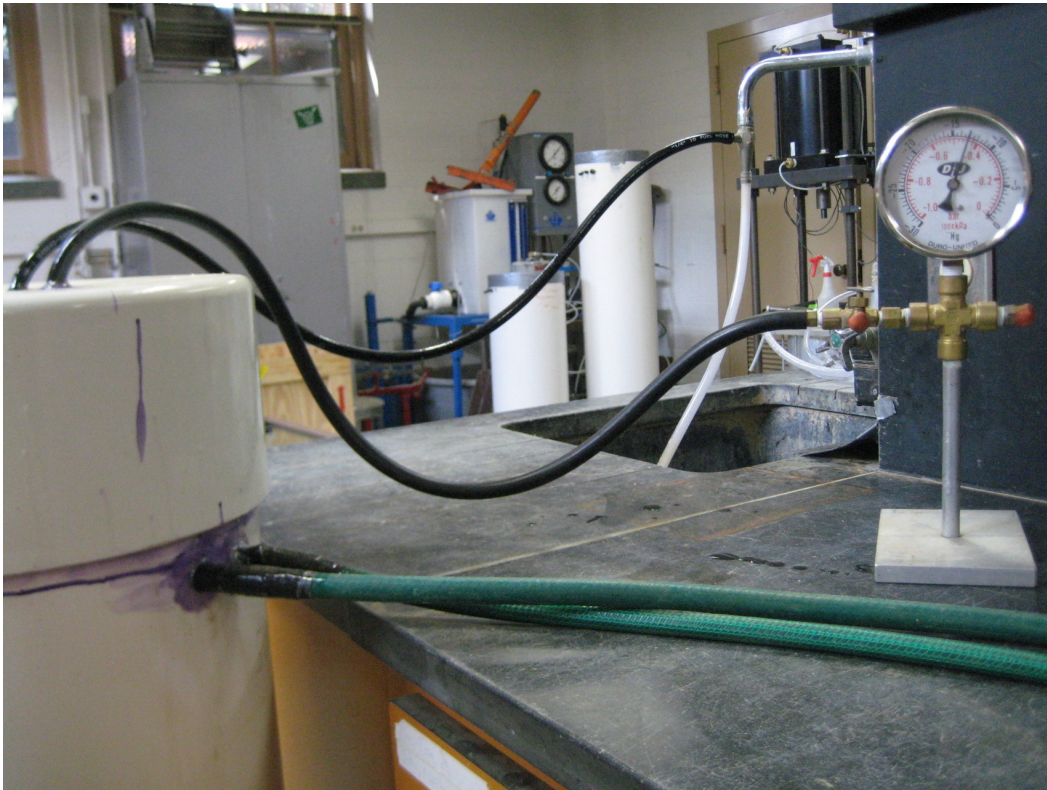


Figure 4.7. Hydraulic Jetting in the Tank. Also shown here is the intermediate drainage tank as subjected to the vacuum in the fourth and fifth rounds of testing.

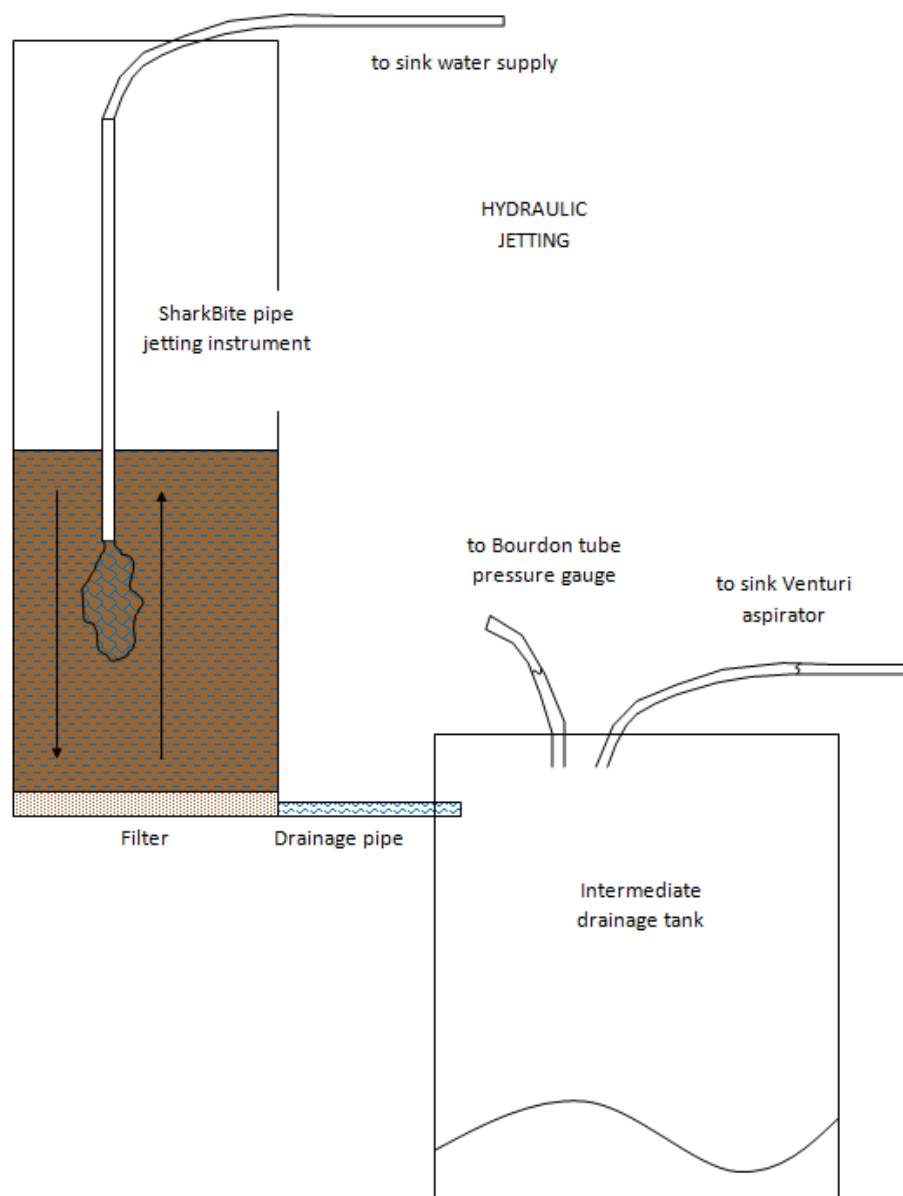


Figure 4.7. Hydraulic Jetting in the Tank. Also shown here is the intermediate drainage tank as subjected to the vacuum in the fourth and fifth rounds of testing.

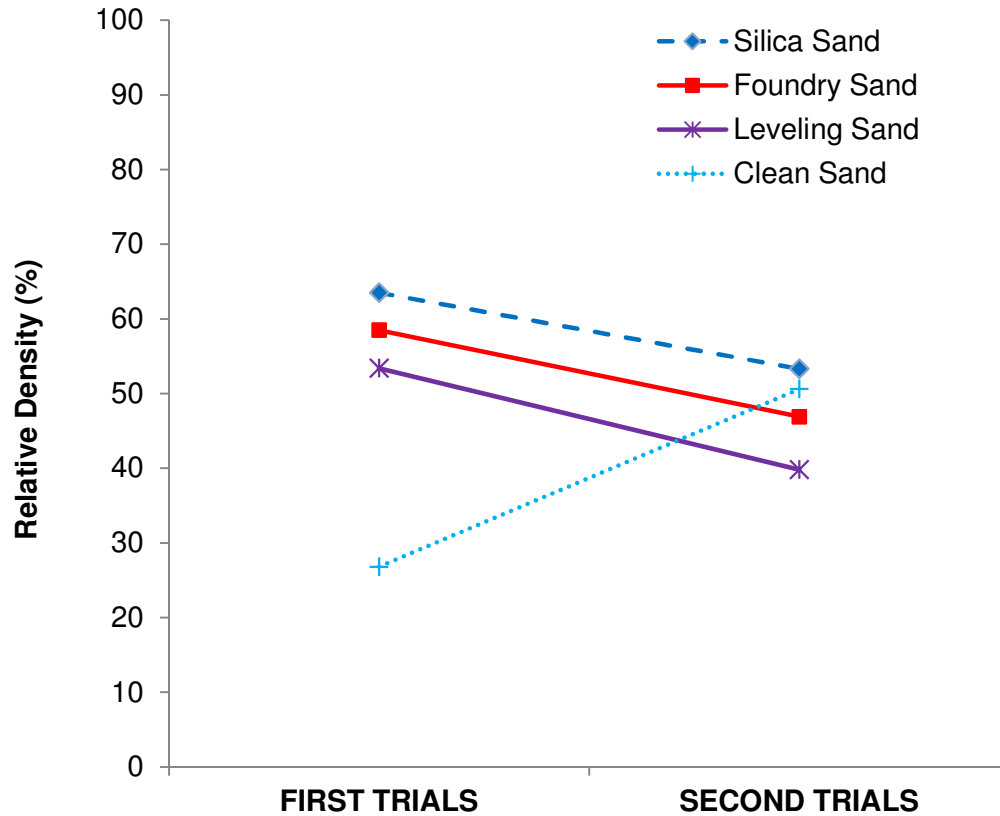


Figure 4.8. Results From the Identical Round 4 and Round 5 of Jetting Tests Under the Vacuum in the Liquefaction Tank.

4.4 RIGID WALL-FALLING HEAD CONDUCTIVITY TESTING

Hydraulic conductivity tests have been performed on the materials used both in the liquefaction tank and the plastic container setups. These tests were performed to compare the suitability of each material for compaction by drainage or jetting. It was hypothesized that increased drainage capacity of the backfill material is directly related to improved performance of these compaction methods. If drainage capacity is inadequate, water will back up in the system, push the solid grains apart, and reduce the effectiveness of the compaction.

The conductivity tests serve not only as an index of the suitability of each material for these alternative compaction methods, but also as a convenient analog for compaction by drainage. In the liquefaction tank, each material was fan sprayed on the surface for a time until

water began to pond in a column above the soil. The gentle spray of water was then turned off, and water was allowed to flow through the soil. The working processes in the conductivity tests are actually very similar to this process in the liquefaction tank. During each conductivity test, water is filled in a standpipe high above the soil, and then allowed to flow through to the outflow end. In this way the conductivity tests mimic the seepage force and potential suction that are the fundamental mechanisms of compaction by drainage. Most important to this analog though, is the ability to evaluate the compaction with the result of the conductivity test itself. A lower measured hydraulic conductivity indicates the solid particles in the soil have rearranged into a denser state. This small-scale phenomenon was actually quite difficult to observe in the liquefaction tank. In the tank, the change in void ratio was calculated by measuring the change in height of a soil column that was not nearly uniform. The soil surface sloped and dipped in a way such that it was difficult to measure the exact total volume of the soil with the five measuring sticks taped around the outside of the tank. In light of the sensitivity analysis performed earlier for results obtained from the liquefaction tank, conductivity measurements before and after drainage may be more sensitive to changes in soil structure.

Each of the conductivity tests were performed with the rigid wall permeameter under a falling head setup according to ASTM D 5084. The only material that was not tested in this manner was the silty sand due to its high fines content; the silty sand conductivity test was conducted in a compaction mold permeameter under a constant head setup. The rigid wall permeameter measures 10.1 cm in diameter, while the heights of all the soil columns in the permeameter were between 18 and 20 cm. The inflow standpipe was raised up above the soil such that the hydraulic gradient across the soil at the start of each test ranged between 5.5 and 6. When possible, each material was subjected to four separate trials to determine the conductivity at a range of void ratios and to take advantage of the compaction by drainage analog. The trials were implemented as follows:

- *Trial 1:* Dry soil is compacted into the mold in five lifts with a hand tamper. The soil is gently saturated from the inflow side, and its conductivity is measured in this condition.
- *Trial 2:* Conductivity is measured again, now that the soil has been subjected to compaction by drainage in the Trial 1 test.
- *Trial 3:* Outflow tube is hooked up to the sink to allow water to flow up through the soil, creating a loose state. Conductivity is measured in this loose condition.
- *Trial 4:* Conductivity is measured again, now that the soil has been subjected to compaction by drainage in the Trial 3 test.

The conductivity-void ratio relationships produced by these tests are shown in Figures 4.9 and 4.10. The most striking feature of the two graphs is that the conductivities of all the materials across a wide range of void ratios are within the same order of magnitude at 10^{-2} cm/s. This is likely due to the fact that all the soils tested are coarse-grain soils, where the D_{10} grain size is expected to control the hydraulic conductivity to a greater degree than the void ratio. The bedding sand has the smallest D_{10} grain size at 0.06 mm, and the foundry sand has the largest D_{10} grain size at 0.4 mm, a difference of only 0.34mm. Additionally, the soil with the highest fines content among all the materials in Figures 4.9 and 4.10 is the bedding sand at only 0.83%. All of the sands are clean, and all the sands have similar hydraulic conductivity.

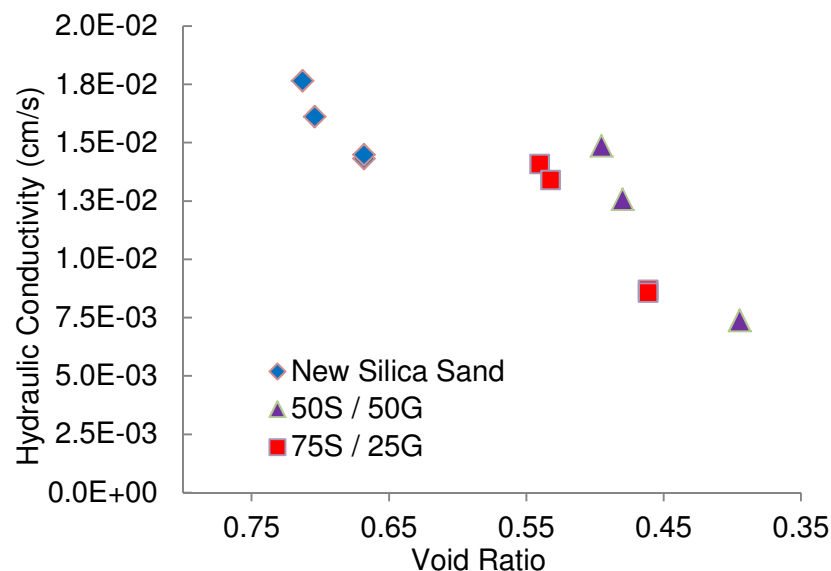


Figure 4.9. Conductivity versus Void Ratio Relationships for Plastic Container materials.

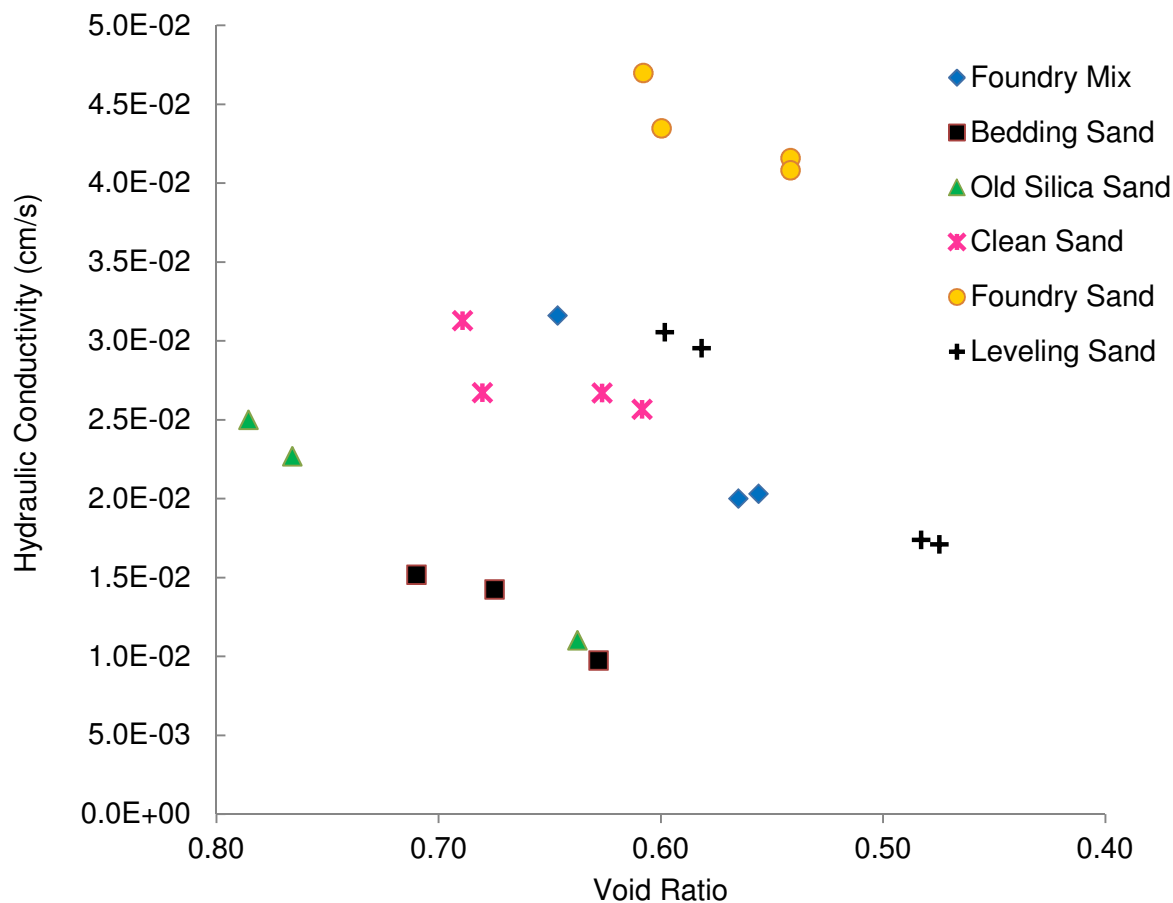


Figure 4.10. Conductivity versus Void Ratio Relationships for Liquefaction Tank materials.

Additional conductivity results for the materials at the Highway 51 project site as well as the silty sand are shown in Table 4.17. The sandy backfill is a well-graded sand, and as such, when it is compacted to a dense condition it has a relatively low conductivity. This makes the backfill specified at Highway 51 a less than ideal candidate for compaction by drainage or jetting. With regard to lab testing, both the native soil as well as the sandy backfill at the site have greater fines contents which necessitated modifications to the four trial processes described above or the use of a different setup altogether. The native soil and the sandy backfill have fines contents of 4.9% and 2.7%, respectively. When each of these soils were treated to a

loose state as detailed in Trial 3, the fines washed up to the top of the soil and formed a cap. This cap of fines reduced the conductivity of each soil to the point where a relationship between conductivity in void ratio could not be reasonably developed due to the acute heterogeneity in the soil. Additionally, the conductivity of both the native soil and sandy backfill measured during Trial 1 and Trial 2, or before and after compaction by drainage, was for all intents and purposes equal. This indicates that the compactive effect caused by drainage is effectively negated for a soil with higher fines content. The flow slows down to the point where the seepage force is simply ineffective in compacting the soil. However, the results shown in Table 4.18 were particularly useful in implementing a working finite difference model of the system (see Section 6) to analyze the directional flow of water through the abutment-backfill-native soil system during the jetting process. Finally the results from Trial 1 are shown in Table 4.19.

As mentioned earlier, the nature of the liquefaction tank-permeameter analog allows for an evaluation of the effectiveness of compaction by drainage for each material. The conductivity measurements, especially between Trial 3 and Trial 4, are sensitive to changes in soil structure in a way the volume measurements made in the liquefaction tank simply are not. The decrease in void ratio seen between Trial 3, when the soil is in an extremely loose state, and Trial 4, after the soil has drained, should give a sense of the maximum compactive potential of the drainage method. The results used to make the evaluation of this method, including the void ratio, conductivity, and relative density before and after drainage, are shown in Table 4.17. From this table it is immediately clear that the void ratio of every material decreases after drainage. However, the improvement is minimal at best; the energy imparted onto the soil through compaction by drainage is simply not enough to reach recommended relative densities near 0.7 or greater for adequate compaction. The bedding sand achieved the greatest decrease in void ratio at 4% as well as the greatest increase in relative density, moving from 25% to 38%.

Table 4.17. Comparison of conductivity and void ratio results between Trial 3 and Trial 4.

	Trial 3: Loose		TRIAL 4: After Compaction by Drainage		
Soil Type	Conductivity (cm/s)	D _R (%)	Δe	% Conductivity Decrease	D _R (%)
Bedding Sand	1.52E-02	25	-0.04	7	38
Clean Sand	3.13E-02	25	-0.01	15	29
Foundry Sand	4.70E-02	18	-0.01	7	22
Leveling Sand	3.06E-02	7	-0.02	4	16
Silica Sand 1	2.50E-02	4	-0.02	9	12
Silica Sand 2	1.76E-02	56	-0.01	9	60
75S / 25G	1.41E-02	34	-0.01	5	39
50S / 50G	1.49E-02	11	-0.02	15	22

While many of the materials started in a very loose condition during Trial 3, the new batch of silica sand started at the highest relative density before drainage at 56%. This batch of silica sand, which is finer than the old batch of silica sand, performed moderately well during compaction by drainage. During Trial 4, the relative density increased to 60%, and the conductivity decreased by nearly 9%, the third greatest decrease among all the materials tested. These results indicate that compaction by drainage is most effective in finer sands with uniform gradation and high drainage capacity (i.e., high hydraulic conductivity). The low energy of the water flowing through the soil is able to move the smaller grains into a denser arrangement. Of note however, is the potential for erosion of this finer, uniform material. The new batch of silica sand is well within the erodible zone, as seen on the particle size distribution curve in Figure 3.1. The high performance of two other materials, the clean sand and the 50% sand and 50% gravel mixture, is consistent with the high performance seen in the new batch of silica sand. Both materials are coarse, and where the clean sand is highly uniform, the 50% sand and 50% gravel mixture is gap-graded uniform. The 50% sand and 50% gravel mixture and the clean sand saw the greatest decrease in conductivity at 15.4% and 14.7%, respectively.

Finally the leveling sand performed the poorest of all the materials when subjected to compaction by drainage. The decrease in conductivity was the lowest of all the materials at 3.6%, and the relative density increased from a very loose 7% in Trial 3 to only 16% after drainage. The leveling sand is one of the more well-graded sands of all the materials. The nature of the flow paths and pore suction for this well-graded material reduce the effectiveness of compaction by drainage.

Table 4.18. Additional Conductivity Results for Finer Soils seen at Highway 51 Project Site.

Soil Type	Void Ratio	Conductivity (cm/s)	Test Method
Native Soil	0.68	4.60E-04	1
Sandy Backfill	0.38	2.84E-04	1
Silty Sand	0.50	1.01E-02	2
1=Rigid Wall-Falling Head test. apparatus did not allow for development of conductivity-void ratio relationship			
2=Constant Head test in Compaction Mold Permeameter			

Table 4.19. Void Ratio and Conductivity for Trial 1. These are the void ratios achieved by hand compacting with the tamper in five lifts.

Soil Type	Void Ratio	Conductivity (cm/s)
Bedding Sand	0.63	9.74E-03
Clean Sand	0.63	2.67E-02
Foundry Sand	0.54	4.08E-02
Foundry Mix	0.56	2.03E-02
Leveling Sand	0.48	1.74E-02
Silica Sand 2	0.67	1.43E-02
Silica Sand 1	0.64	1.10E-02
75% sand and 25% gravel	0.46	8.57E-03
50% sand and 50% gravel	0.39	7.37E-03

The conductivity tests have provided an added element of sensitivity to better interpret compaction by drainage. Compaction by drainage is best suited for modestly improving the relative density of materials that are placed in a fairly dense in situ condition before compaction.

This low energy method may be best suited to achieving relative densities required of fills in confined spaces outside of the roadway.

4.5 COMPACTION BY JETTING IN THE PLASTIC CONTAINERS

Jetting tests at low and high pressure have been conducted in rectangular plastic containers with dimensions 45.7 cm x 61.0 cm x 61.0 cm. A few pictures of the setup are shown in Figure 4.11. The tests were conducted on four different materials including 100% silica sand, 75% silica sand and 25% gravel, 50% silica sand and 50% gravel, and silty sand mixtures. The percent composition of the sand-gravel mixtures refers to their proportion by weight. During low pressure jetting, water flowed out of a 1.9 cm (0.75 in.) rigid cast iron pipe at a rate of 0.35 m³/hr (92 gal./hr). During high pressure jetting, water flowed out of the same cast iron pipe, but with a simple nozzle attachment concentrating the water into a narrow stream, at a rate of 0.30 m³/hr (79.3 gal./hr). In both cases the pipe was inserted into each soil in a fairly regular rectangular grid with spacing between points of about 5 cm (2 in.).

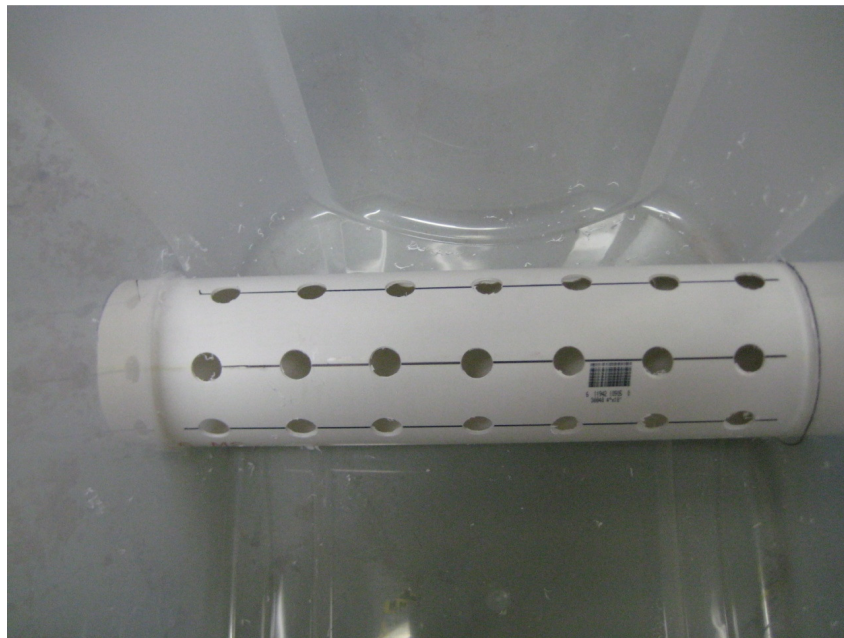


Figure 4.11. Drain Tile Constructed from PVC Pipe (top).



Figure 4.11. Setup with Central Drainage Column (bottom). The PVC pipes were angled downward into the central drainage column; water flowed into the column and out of additional hoses connected to the base of the column. The tubs shown in the bottom image were filled to the top with the soils and jetted.

However, upon inserting the pipe in this regular grid, large voids were left behind; this effect can be seen in Figure 4.12. The soil did not immediately flow into place around the probe in some circular influence area as expected. Instead, to achieve the full compactive effect of jetting, the pipe had to be further inserted and removed from the layer until the soil coalesced into a more uniform viscous mixture. The jetting operation should be terminated at this critical time, before adding too much water, thereby pushing the particles apart, but after adding enough water to eliminate the large voids in the grid.



Figure 4.12. Voids Left Over After Jetting a Regular Grid. 100% silica sand soil is shown here.

The nuclear density gauge, soil stiffness gauge, and dynamic cone penetrometer were used to assess the compaction results both immediately after and 24 hours after the completion of each jetting application. The results from the nuclear density gauge and the soil stiffness gauge can be seen in Figures 4.13 and 4.14. At first glance, it is clear that a number of the measured dry unit weights by the nuclear density gauge are actually greater than the maximum dry unit weights determined by the ASTM D4253 index test, yielding relative compactions over 100%. This is likely due to edge effects caused by placing the gauge in the confined box. During operation of the gauge, the neutron source was lowered to a depth in the middle of the layer; then density was measured by the direct transmission of neutrons from the probe to the receiver of the gauge on the surface of the soil. However, it is possible that the walls of the plastic tubs absorbed a portion of the neutrons, causing a higher dry density measurement. Another plausible explanation for the high dry unit weight readings revolves around the probe compacting the soil in a localized area as it was inserted to make the measurement. If the probe slid along the guide hole the friction between the soil and the probe could certainly cause the soil to slide into a more compact state. Nonetheless, the depth of the probe and the placement of the gauge with respect to the tubs was performed the same way after each jetting application,

and for this reason, the results shown in Figure 4.13 may still be reasonably applied to assess the performance of each material relative to one another.

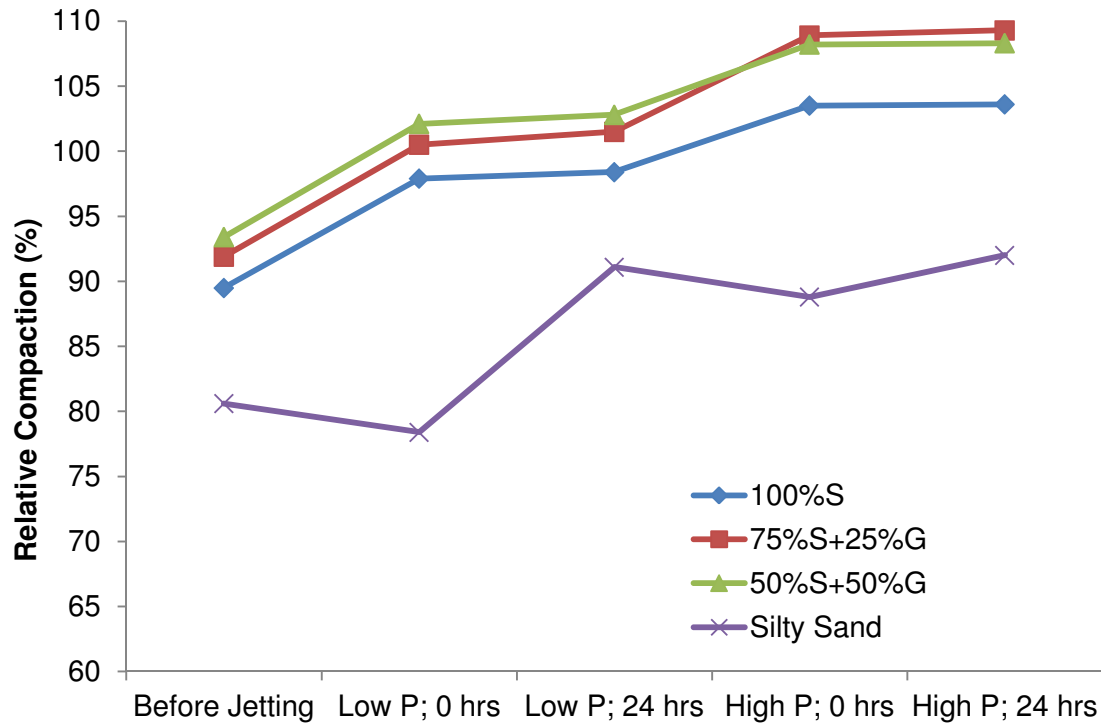


Figure 4.13. Soil Relative Compaction with respect to Jetting Application as measured with the Nuclear Density Gauge.

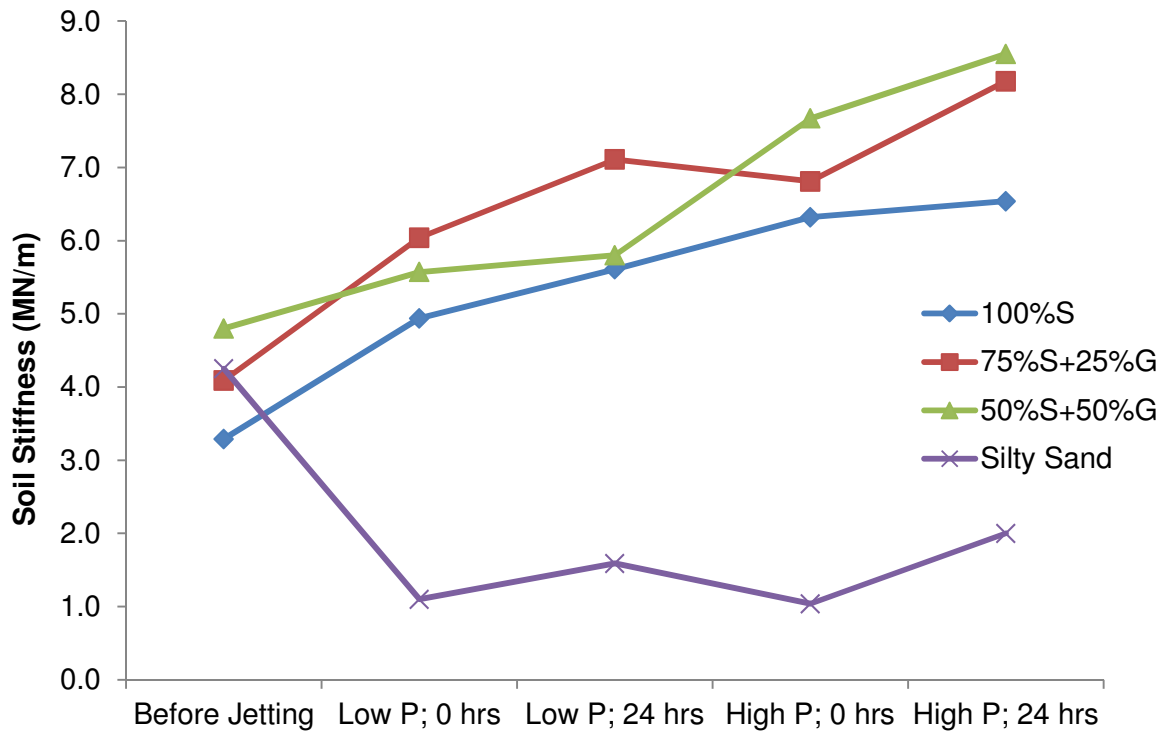


Figure 4.14. Soil Stiffness with respect to Jetting Application.

The most striking result from these tests is the difference in performance between the silty sand and each of the other three clean materials. The silty sand performed the worst of all the soils, and this is likely due to its inability to drain water. Upon completion of jetting, the silty sand was observed to be very loose and muddy. It began to flow as a viscous fluid upon the application of any sort of load. These observations are confirmed by the low strength readings from the stiffness gauge and the dynamic cone penetrometer (Figure 4.14). In each of the tests on the silty sand, the dynamic cone penetrometer sank to the bottom of the box under its own self weight. Additionally the stiffness readings of the silty sand were the lowest of all the soils, ranging between 1.04 and 2.00 MN/m. The 24 hour reading showed only a slight increase in residual strength. The condition of the silty sand after jetting in the box is shown in Figure 4.15 below.



Figure 4.15. Silty Sand in Viscous State Upon Completion of Jetting.

It is clear from Figure 4.13 that regardless of the proportion of sand to gravel, as long as the material is clean and free draining, adequate compaction can be achieved by jetting. The silica sand and two sand-gravel mixtures were placed at a similar initial void ratio, and then follow a strikingly similar trend upon the application of first low pressure jetting, and then high pressure jetting. While there is virtually no residual change to the structure 24 hours after both low and high pressure jetting, there is a clear improvement to the compactness of these materials after performing high pressure jetting. It is hypothesized that the greater energy in the jet of water shifts the balance where more particles are being mobilized into the void spaces instead of being pushed apart by the water which is itself occupying the void space. The results indicate that it would be worthwhile to first perform low pressure jetting, followed by high pressure jetting to achieve a more compact soil structure.

Meanwhile, each of the four soils were deposited into the plastic containers in a nearly dry condition with a high amount of energy, similar to the dry, high energy condition implemented in earlier testing in the liquefaction tank. The measurements in the 'Before Jetting' data series in Figure 4.13 and Figure 4.14 correspond to this in situ condition. After deposition, all of the soils except the silty sand showed an increase in dry unit weight and stiffness upon the application of low pressure jetting. The 50% sand and 50% gravel mixture experienced the greatest increase in dry unit weight at 1.68 kN/m^3 , corresponding to an 8.7% increase in relative compaction. This increment was observed immediately after the application of the low pressure jetting.

Where each of the three free draining (i.e., high hydraulic conductivity) materials performed similarly in terms of relative compaction, they exhibited differences in stiffness with respect to both timing after jetting as well as jetting pressure. Each of the three materials became stiffer 24 hours after jetting due to the increase in matric suction. The 75% sand and 25% gravel mixture exhibited the greatest increase in stiffness at 1.1 MN/m , 24 hours after high pressure jetting. It is important to note that this increase in stiffness would in all likelihood be temporary, as it was previously noted that the soil structure remained the same 24 hours after jetting. Meanwhile, high pressure jetting improved the stiffness of the 50% sand and 50% gravel mixture much more than the two other mixtures containing less gravels. Where the pure silica sand and 75% and 25% gravel mixture exhibited increases in stiffness between low and high pressure jetting of 1.3 and 0.7 MN/m , respectively, the 50% sand and 50% gravel mixture exhibited an increase of 2.1 MN/m . These results indicate that a coarser material has the potential to reach high stiffness after effective compaction, especially when a simple increase in water pressure during jetting is applied.

Finally the dynamic cone penetrometer (DCP) appears to be particularly useful in evaluating the quality of the material after jetting as it is highly sensitive to changes in soil fabric and especially water content in its indication of soil shear strength. Although the soils achieved

relatively high dry unit weights and fair soil stiffness, the penetrometer results reveal that all of the soils are weak after jetting. In the field, penetrometer measurements of backfill compacted in the traditional manner, with the large vibratory roller, indicate that even right next to the wall where the roller cannot operate, it takes 15 to 20 blows to reach the a penetration depth of 40 cm (16 in.). It took anywhere from 0 to 6 blows for all the jetting tests for the penetrometer to reach the bottom of the box, or a depth of 40 cm (16 in).

4.6 TESTS OF WISDOT BACKFILL MATERIALS

A final lab testing program utilizing the liquefaction tank has been completed to investigate the effectiveness of hydraulic methods to compact sandy backfills typically used by the Wisconsin DOT. Previous tests on the lab were conducted on very clean sands. The materials chosen for this program are P3-S7, P3-S2, and P2-S3, materials that contain 0.6%, 5.7%, and 12.6% fine particles, respectively. Seven of the nine data series on the abscissa in Figure 4.16 are identical to the previous testing program in the tank for the very clean sands.

The first new compaction technique implemented in this program is flooded deposited materials. In this technique, materials are subjected to a vacuum immediately after falling into place and during the compaction by drainage phase. The second compaction technique implemented is exactly the same as the first technique, but with the application of vibration energy to the soil column during the vacuum drainage phase. This vibration energy is produced by rapping the side of the tank with a large rubber mallet.

These two new techniques are implemented in light of the observations of the jetting application performed at Greenfield Avenue (see Section 5), which is hypothesized to mirror very closely flooded deposition in the lab. While flooded deposition works well by itself for the cleaner sands, it is particularly ineffective for the P2-S3, which contained the most fines. The fines were observed to entrain a large amount of water as they fell into the column of water. This water pushes the small particles apart and produces a relative density of only 8%. When

this soil was excavated from the tank, it had the consistency of sludge, very similar to a clay at its liquid limit.

Where the P2-S3 material improved in performance upon increasing the energy through first the vacuum, and again through the vacuum with the vibration energy, the P3-S7 and P3-S2 materials both decreased in performance during the vacuum drainage only trial. This is best explained by the phenomenon where, during flooded deposition by itself, the individual grains have more time to settle into all the void spaces in the column as they fall gently through the water. Vacuum drainage actually interferes with this process for the coarser materials as more water is sucked into the voids than otherwise would be during flooded deposition alone.

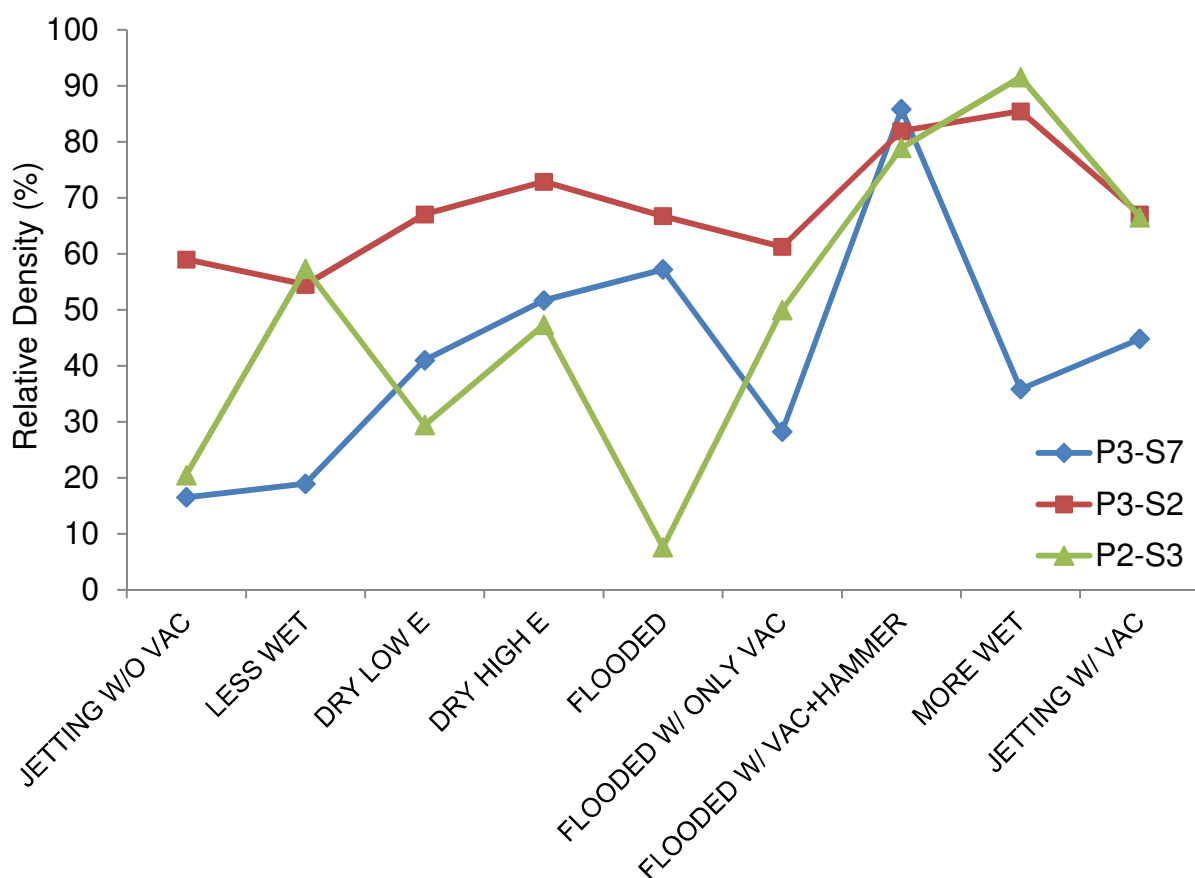


Figure 4.16. Comparison of Deposition Techniques and Drainage Conditions for Wisconsin DOT Backfills Subjected to Both Jetting and Compaction by drainage in the Tank in the Lab.

Most fascinating among the flooded deposition results is the great increase in the performance seen in all three materials during the highest energy trials, which include the application of vibration energy. Although the 'more wet' trials produced greater relative densities for the P2-S3 and P3-S2 materials, flooded deposition with vibration energy is much easier to reproduce on a consistent basis. Wet deposition is highly subjective, and the backfill must be treated to an optimum water content where there is not too much water pushing the particles apart, but also enough water to lubricate the particles as they fall into the tank in slugs with a high amount of energy. The results of the 'more wet' trials in Figure 4.16 are more a chance coincidence than an indication that wet deposition followed by drainage is the most effective compaction method.

With evidence that applying vibration energy during flooded deposition produces a very dense soil structure, it would be enlightening to see the effect of vibration energy applied in the field during a jetting application like the one at Greenfield Ave. (see Section 5). Because the pipes are typically further beneath the surface, it would be safe to operate a vibratory roller above the utility trench during jetting, potentially greatly increasing the effectiveness of jetting compaction.

SECTION 5 - FIELD RESULTS AND DISCUSSION

This section details the work performed and results gathered at the Highway 51 and Greenfield Avenue project sites. Flooding, or compaction by drainage, specifications were introduced as a special provision into the Highway 51 project documentation. The work was performed by a contractor inexperienced with this type of operation. Meanwhile, observations were made of an experienced contractor performing jetting around a buried utility pipe at the Greenfield Avenue site. Valuable information regarding best practices in jetting, obtained from an impromptu interview with the contractor, is chronicled in this section as well.

5.1 COMPACTION BY DRAINAGE AT HIGHWAY 51 SITE

Upon completion of lab tests, compaction by drainage was performed in the field at a bridge abutment wall along Highway 51 and Bear Tree Parkway in DeForest, Wisconsin. The abutment wall was constructed with cast-in-place concrete and stands at 2.32 meters (7.6 ft) high. There is a 1.43 m (4.7 ft.) parapet wall on top of the abutment that was poured after placement of the initial 2.32 m (7.6 ft.) of backfill. The wing walls extend nearly perpendicular to the abutment face and can be seen in Figure 5.1. Additionally the native soil was excavated behind the abutment face at a slope of approximately 1.5H:1V. The backfill brought to the site was initially characterized based on visual inspection to be a well-graded sandy material containing a small portion of gravels and a fair amount of silty finer materials. Upon wetting the material became muddy and viscous as would be expected of a sand with silty particles. According to the special provisions in the project plans, the backfill was placed in a single layer approximately 2.3 m. (7.6 ft.) in height, or the full height of the abutment wall. The backfill was placed at air-dry condition and pushed into place by a front end loader up against the abutment face and wing walls. A 20 cm (8") diameter drain tile pipe had been placed along the base of the abutment to provide drainage for the system.

After the backfill was placed in the single, continuous layer it was flooded from the surface. During the process, one worker from the contractor team simply fan-sprayed the surface with water supplied by the water truck used for dust control at the site. This process can be seen in Figure 5.2. Initially the water appeared to drain through the backfill well, with minimal ponding on the surface. The flow rate chosen to avoid eroding the backfill was initially low enough so as to avoid overtaxing the drainage capacity of the system. However, after 15 minutes of flooding the backfill some ponding was observed on the surface. At 30 minutes, more extensive ponding was observed and the water began to push the solid particles apart, turning the backfill into more of a viscous muck. This ponding is shown in Figure 5.3. It became clear that during the first 15 minutes, the water was simply filling the air voids in the backfill. After this time, the hydraulic conductivity of the backfill was too low to be able to reach any kind of steady state flow regime necessary for compaction by drainage. In fact the flow of water was impeded to such a degree that no water was observed to leave the layer through the drain tile at the base of the wall throughout the duration of the flooding process.

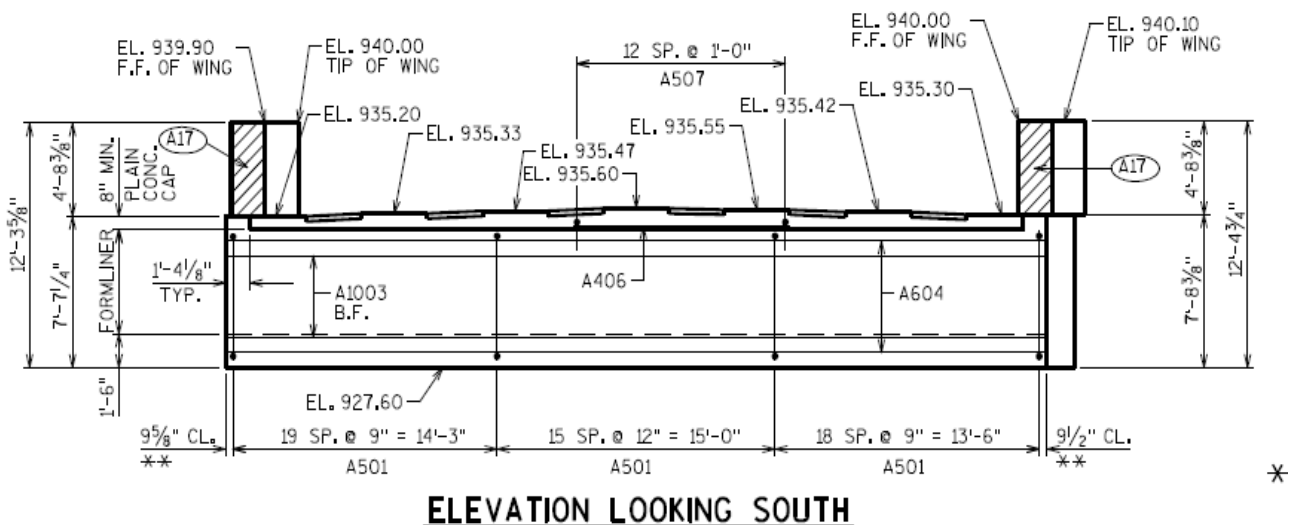


Figure 5.1. Bridge plans from Highway 51 at Bear Tree Parkway (top). Shown here in the beam seat plans is the elevation of the abutment face with the parapet wall.

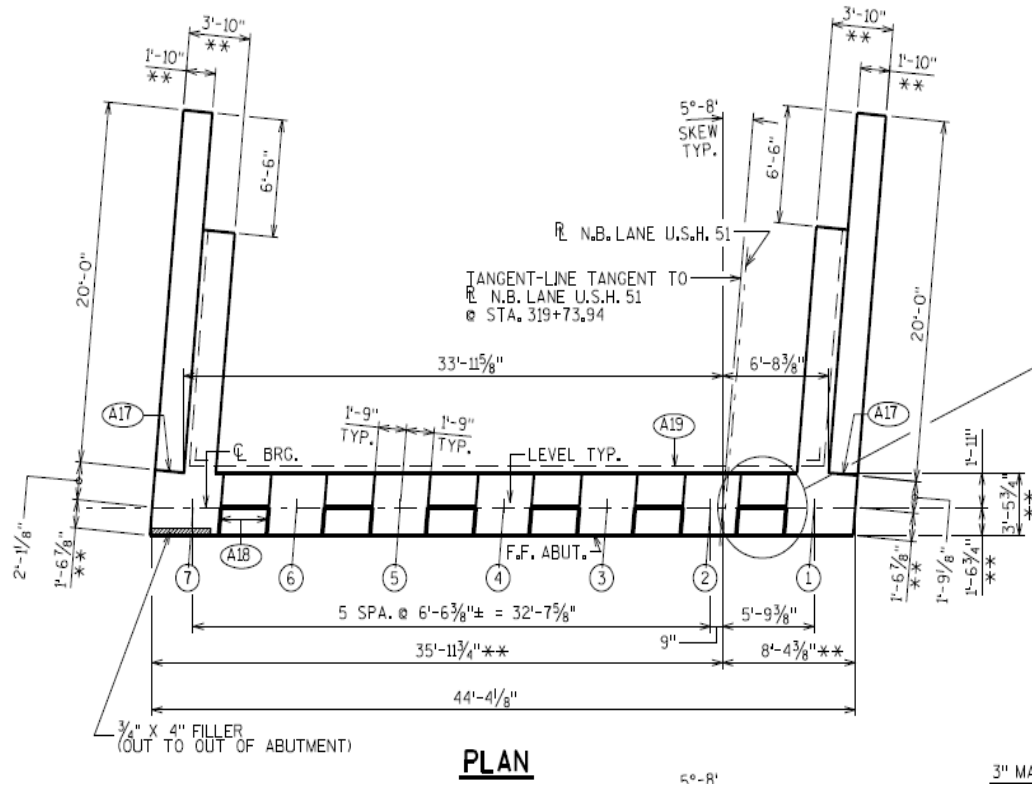


Figure 5.1. Bridge plans from Highway 51 at Bear Tree Parkway (bottom). Shown here in the beam seat plans is the orientation of the wing walls.



Figure 5.2. Flooding the Backfill to Initiate Compaction by Drainage. Just one water truck and one member from the contractor team was needed for the operation.



Figure 5.3. Ponding Observed on the Backfill Surface During Flooding. The picture here was taken 30 minutes after the water was turned on.

Further tests in the lab conducted on samples of the backfill after the field work, and detailed in the above sections, confirmed the observations made at the site. The well-graded sandy backfill is able to be compacted to a high maximum dry unit weight ($21.6 \text{ kN/m}^3 - 134.8 \text{ lbs/ft}^3$), or equivalently, a relatively low minimum void ratio (0.204), such that in a reasonably compact state the material has very low hydraulic conductivity. The hydraulic conductivity of the sandy backfill measured in a rigid permeameter with the falling head setup was measured to be fully two orders of magnitude less than the cleaner sands tested in the lab at $2.84 \cdot 10^{-4} \text{ cm/s}$ ($1.1 \cdot 10^{-4} \text{ in/s}$). In many ways this makes the sandy backfill a poor candidate for compaction by drainage. Any water in the pores tends to push the solid particles apart, decreasing the strength. Additionally, a very high suction is needed to drain the pores and increase the effective stress felt by the solid skeleton to the point where the grains slide past each other, producing compaction in the soil.

Nonetheless measurements of the backfill's compactness, stiffness, and strength near the surface were made with the nuclear density gauge (NDG), soil stiffness gauge (SSG), and dynamic cone penetrometer (DCP), respectively. The final measurements of these soil properties were made after a second application of jetting, performed a few hours after the first application, and these measurements are shown in Figure 5.4. Also included in the figure are similar measurements made at the control abutment. This control abutment was essentially identical to the flooded abutment, located directly on the other side of the overpass at Bear Tree Parkway. The backfill at this abutment was placed air dry in one foot lifts and compacted by a large steel drum roller up to about 0.5 m (1.64 ft.) from the abutment face itself. Although typically compacted with a walk-behind vibratory plate, this last 0.5 m (1.64 ft.) of fill next to the face was not compacted in any way as the steel drum roller could not safely reach this confined area. The inability of the steel drum roller to reach the confined space is evident in the results. Where the dry unit weight of the fill at the control abutment 1.2 m (4 ft.) away from the wall is 20.1 kN/m³ (125.5 lbs/ft³), yielding relative compaction of 93%, the dry unit weight of the fill at the wall is only 18.0 kN/m³ (112.4 lbs/ft³), yielding relative compaction well out of specification at only 83%. Furthermore the strength of the fill at the control abutment near the wall is greatly reduced. Where 25 blows were needed to achieve 25 cm (10 in.) of penetration with the DCP 1.2 m (4 ft.) away from the wall, only 8 and 9 blows were needed adjacent to the middle of the abutment face and at the intersection of the face and the wind wall, respectively. Overall the compaction at the control abutment was completed hastily with no inspection presence at the site and it shows in the decreased compactness of the backfill near the abutment structure.

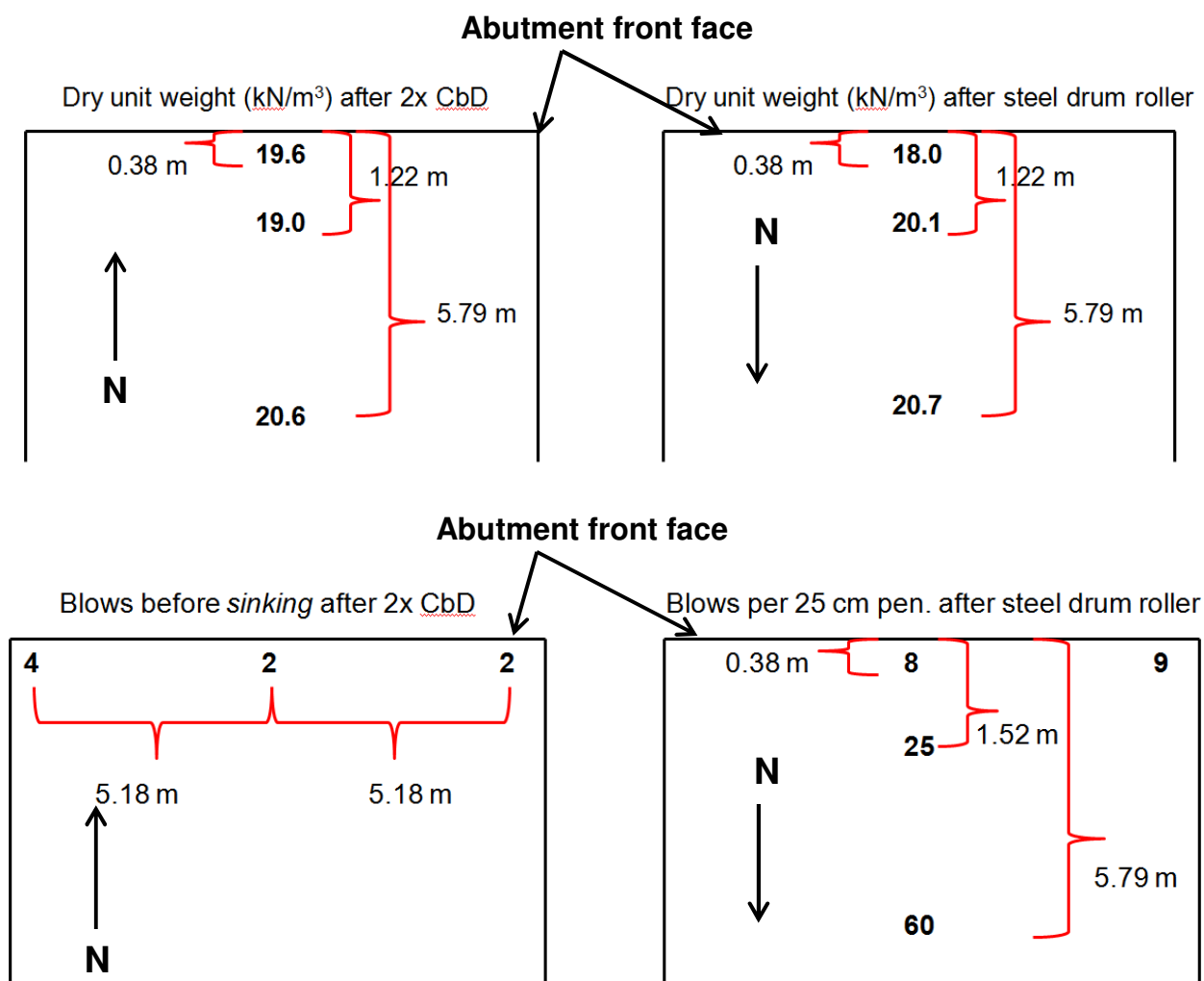


Figure 5.4. Compaction Results at the Highway 51 Site. The top half of the figure shows the dry unit weights on the surface of the layer at the flooded wall and the control wall. The bottom half of the figure shows the dynamic cone penetrometer results similarly at each of the walls.

Beyond the control abutment results, however, the flooding application was not particularly effective given the sandy backfill material, especially in terms of strength. A review of the Nuclear Density Gauge results indicates the backfill actually reached a fairly dense state following flooding, as the relative compaction ranges from 85% to 90% within the area surveyed. These results are supported by an observation made over the course of the day; after initial placement of the air dry backfill, a line was traced along the surface of the fill on the abutment face. At the end of the second flooding application, the fill had been compacted and reduced in

height by about 3 cm (1.2 in.) below the initial trace. A sense of this effect can be seen in Figure 5.5 (below, bottom right) where the backfill actually began to fissure around the corner of the structure where the suction was particularly high. The state of compactness aside, the fabric of the backfill post-flooding was such that the layer had unacceptably low shear strength. Placing the DCP upright above the fill resulted in the instrument literally sinking into the backfill as if it were quick sand. Where two blows could be achieved before the instrument completely sunk into the fill after the second flooding application, four blows could be achieved before sinking the following day after flooding. These results indicate there was a noticeable, yet minimal effect of the increased suction, as water was allowed to drain for a longer time, on the increased effective stress felt by the soil.



Figure 5.5. DCP in Action (left). Close-up of Fissured Flooded-Compacted Backfill (right).



Figure 5.5. Perspective of Fissured Flooded-Compacted Backfill (right). Drain Tile at the Base of the Abutment Wing Wall (left).



The first field test of compaction by drainage has shown promise, but was not adequate in this particular application. The strength of the backfill was too low to be left in place, and the backfill had to be dug out and recompact by the contractor. Factors contributing to the less than adequate performance include the low conductivity and low minimum void ratio of the well-graded backfill, layer thickness too great at 2.3 m (7.5 ft.), and an inadequate drainage system with only one drain tile at the base of the abutment. One perplexing aspect of this case is the similarity of the sandy backfill brought to the site by the DOT and the native soil already in place. An examination of Figure 3.3 in Section 3.1 indicates the gradation of these materials is nearly identical. Additionally the two materials have similar fines content at 3% and 5% for the backfill and native soil, respectively. Considering the D_{10} grain size and fines content control hydraulic conductivity of coarse-grain materials, it is not surprising that the flow of water exited through the native soil rather than the drain tile; the two materials have such similar behavior in a drainage application.

5.2 COMPACTION BY SLURRY FLOODING AT HIGHWAY 51 SITE

On October 2013 a final set of tests was run on a new bridge being constructed along the south bound lane on Highway 51 and Bear Tree Road, just south of Deforest, WI (Figure 5.6). In this test, the contractor used a slurry against the abutment of the bridge. The technique was designed to fill the backfill using just gravity and the flowability properties of the slurry without the assistance of mechanical equipment. Then the draining properties of the flown material would allow draining the water while the solid skeleton would increase the unit weight and gain shear strength. The properties of the slurry as presented by the contractor in the field are presented in Figure 5.7: Sand 39.2%, Stone 1 21.6%, Stone 2 32%, and Water 7.2% by weight. The slurry was mixed in a concrete mixer and flown in the back of the abutment as shown in Figure 5.8. Figure 5.9 presents the complete fill after the flooding. In this last picture, it can be easily seen the stones on the surface of the materials as the water begins to drain out of the slurry. Note that the slurry must be contained (at least with temporary forms), due to the fluid nature of the backfill.

To assess the quality of this compaction technique, we designed a field experimental study that included the assessment of both the slurry flooding compaction and a control backfill. Measurement instruments included the nuclear density gauge, Geogauge and dynamic cone penetrometer. The general distribution of the measurement locations is presented in Figure 5.10 and includes four measurement points in the new slurry flooding compaction backfill and four measurement points in the opposing backfill. The opposing backfill was compacted with traditional compaction equipment shown in Figure 5.11. This opposing controlled backfill was the controlled area.



Figure 5.6: Geographic location of the Highway 51 and Bear Tree Rd. Bridge for the slurry flooding compaction field test (Map source: Google Maps).

Ticket: 1757
 Customer Name:
 Delivery Address:
 Job Description:
 Instructions:
 Formula: 555
 Pur Order#
 Load Size: 9.00 yards
 Daily Qty 0.00 Ord Qty 0
 Driver: Tom Wheeler
 Truck: 67

10/15/2013 12:37:58 PM
 Job Name:
 SLURRY
 Project #
 Resold Amt 0.00
 Del Qty 0.00
 Slump: 0.00
 Mix Time: 0
 Quantity: 0
 Water to Cement Ratio: 76.80

Product Name	Target	Actual		Error	%MC
Sand	12,860	12,840	lbs	-0.2%	5.5
#2 stone	10,400	10,460	lbs	0.6%	0.5
#1 Stone	7,010	7,060	lbs	0.7%	0.5
COLD WATER	283	283	gallons	0.0%	

Trim Water: 1 gallons Total Water: 3151 sack Water to Add: 0 gallons
 Production Total: 50.00 yards

Batch Weight: 32717.39 lbs
 Batch Time: 41 Wait Time: 20 Tolerance Table: T1800-1
 Dsch Time: 140 Total Time: 20

B1 AGG ST: 0 B1 AGG ET: 20 B1 CEM ST: 0 B1 CEM ET: 0

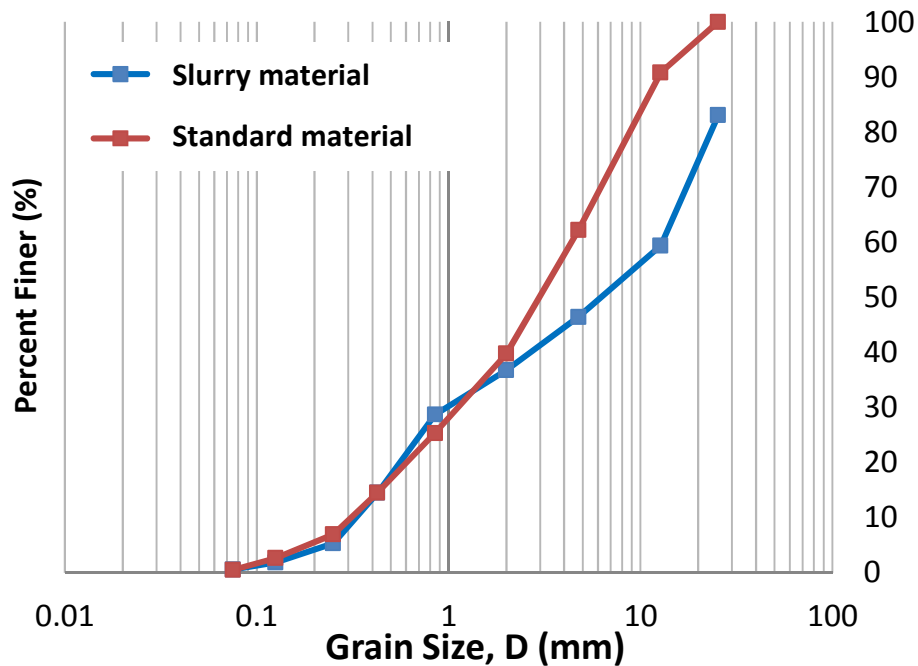


Figure 5.7: Properties of the slurry as presented by the contractor in the field and tested by the research group.



Figure 5.8: Construction of the backfill using slurry flooding compaction technique.



Figure 5.9. Complete flooding of the backfill. Please note that the stone are now visible soon after the completion indicating the drainage characteristics of the solid material in the slurry.

South Abutment – Slurry compaction North Abutment – Control compaction

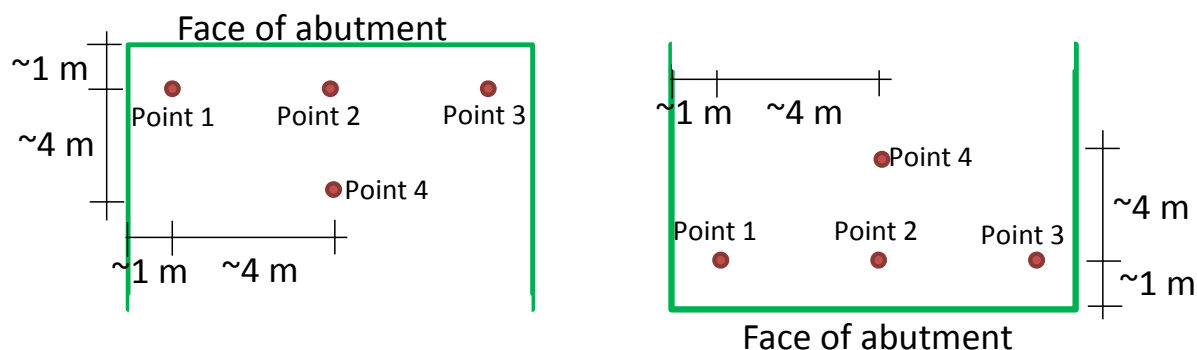


Figure 5.10: Approximate location (red dots) of the nuclear density gauge, Geogauge, and dynamic cone penetration testing in both slurry and control compaction.



Figure 5.11: Compaction equipment used on the controlled backfill.

The monitoring testing was performed as follow: for each of the testing points, density and water content were measured at 15 cm (6 in.) and 28 cm (11 in.) depth, stiffness measurements were determined with the GeoGauge device, and the strength of the compacted soils was estimated using the dynamic cone penetrometer. All these measurements were performed once on the control backfill and three times on the one slurry flooding compaction. As the slurry flooding compaction increases strength with time (i.e., decrease in saturation and increase in matric suction), we measured the physical and mechanical properties as the flown material drained the water. The first test was performed on a lift that was placed by the

contractor in days previous to testing. This lift is considered that have completely drained and already had densified and gained shear strength do to the increase in matrix suction. The other two tests were performed in a new lift of slurry: 45 minutes and two hours after flooding. Please note that testing point 4 in the slurry flooding section also serves as a control test point. This testing point was located in an area of transition between traditional compaction and slurry flooding. The next sets of figures summarize the results.

Figures 5.12 through 5.15 summarize the shear strength of all testing points both in the control and in the slurry flooding compaction areas. The three first testing points in Figure 5.12 document the shear strength of the compacted soil next to the abutment. In these testing points, the large compacted equipment cannot deliver all its compaction effort. Throughout the lifts the results range between 0.4 and 1.1 blows/cm while point 4 that is about 5 m from the wall the strength measurements reaches about 4 blows/cm. This point could be considered the full strength of a proper compacted soil.

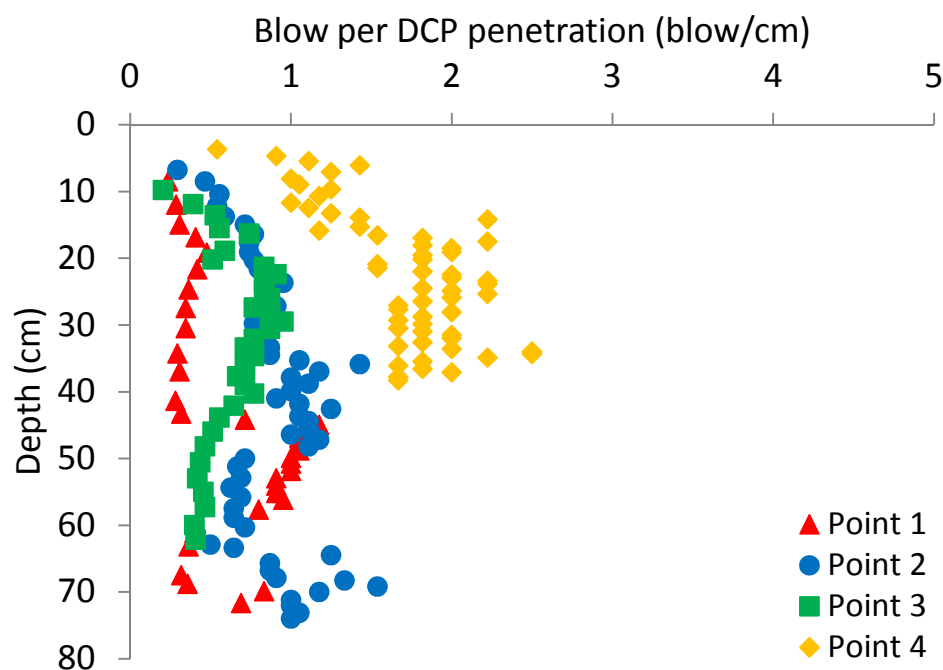


Figure 5.12. Dynamic cone penetration results on the control back fill the plot shows an equivalent measurement of shear strength as measured as blow per cm of DPC penetration. Points 1, 2 and 3 are 1 m (3.3 ft) from the abutment while Point 4 is 5 m away.

Figures 5.13 through 5.15 document how the strength of the slurry increases as the water drains from the lift. After 45 minutes, the shear strength along the depth of the lift does not reach 0.5 blows/cm. However after 2 hours the strength reaches 0.6 to 0.7 blows/cm while a day after the initial flooding, the compacted slurry reaches values of about 1.3 blows/cm. While this value is much smaller than the value of 2 blows/cm reached on the control system away from the abutment (Point 4 – Figure 5.12), it is much higher than the value of strength obtained by the traditional compaction next to the abutment wall. Furthermore, note how uniform the values of strength are in the slurry flooding compaction in comparison to the traditional compaction.

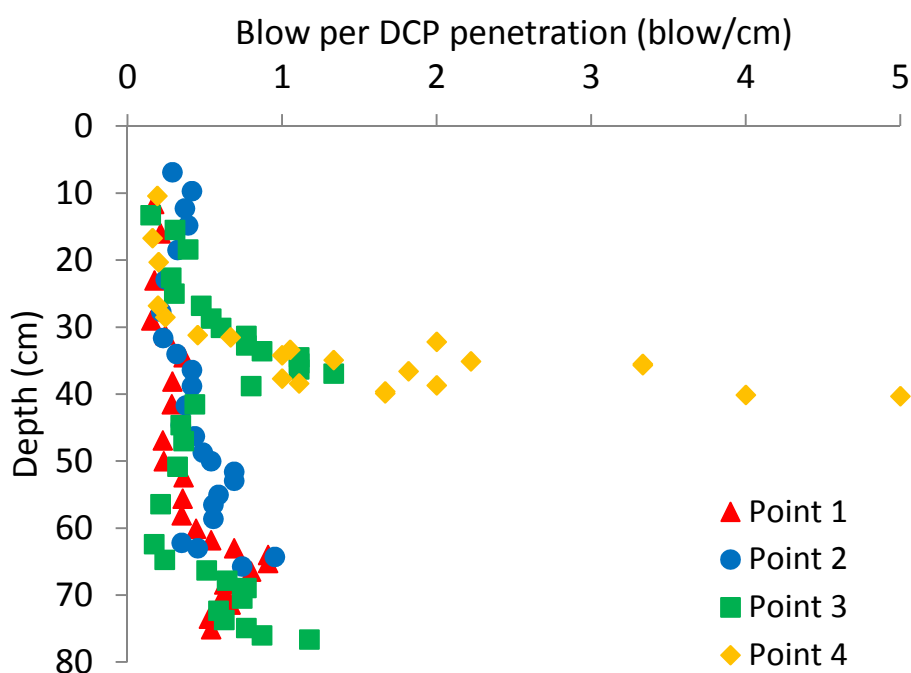


Figure 5.13. Dynamic cone penetration results on the slurry flooding compaction 45 minutes after flooding: the plot shows an equivalent measurement of shear strength as measured as blow per cm of DPC penetration.

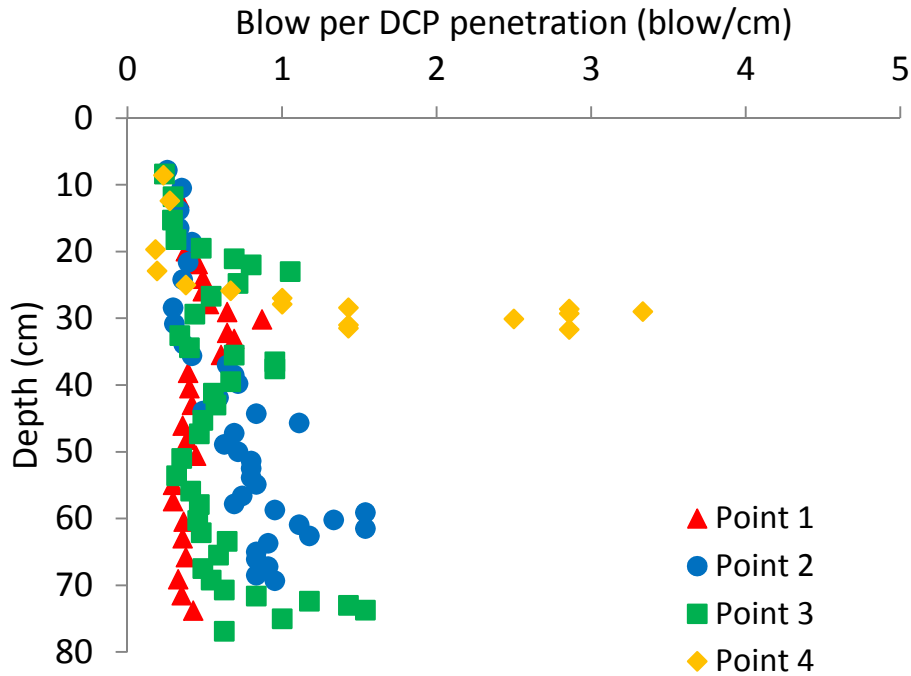


Figure 5.14. Dynamic cone penetration results on the slurry flooding compaction two hours after placement: the plot shows an equivalent measurement of shear strength as measured as blow per cm of DPC penetration.

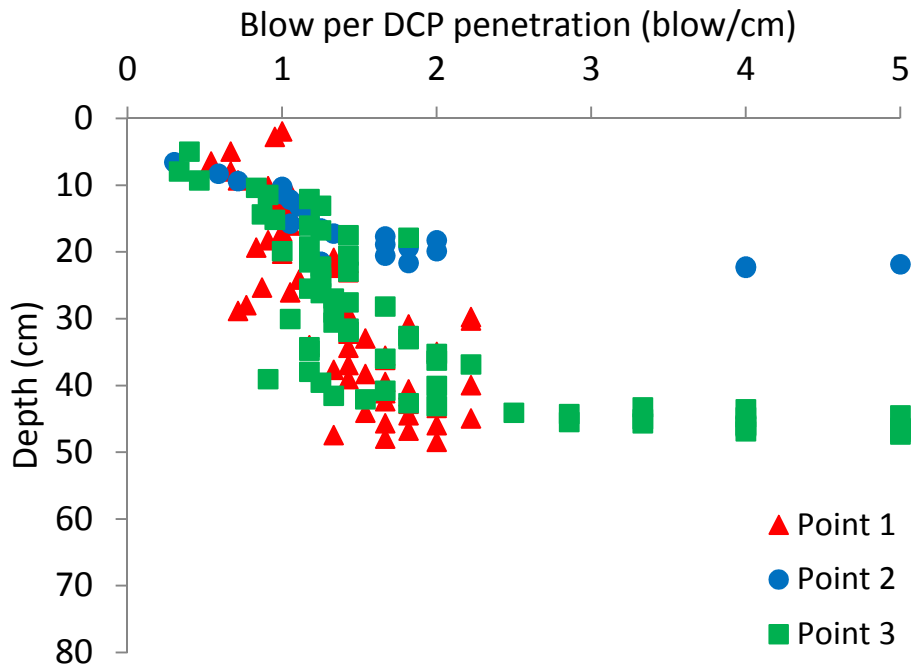


Figure 5.15. Dynamic cone penetration results on the slurry flooding compaction one day after placement: the plot shows an equivalent measurement of shear strength as measured as blow per cm of DPC penetration.

Tables 5.1 through 5.4 summarize both the nuclear density and GeoGauge testing results. While these data are not as compelling as the dynamic cone penetration results, there are several pieces of information that are very relevant. The dry density is much greater in the case of the slurry than in the case of the compacted soil with the tradition compaction equipment. That is an indication that the materials used in the two abutments are significantly different. One must consider both the grain size distribution to evaluate the maximum achievable compaction level and the angularity of the particles to assess the shear strength. It appears that the material used in the slurry is both well distributed and spherical in such a way it yields both higher dry densities yet comparable shear strength results. In light of these results, it appears that slurry flooding compaction is an excellent alternative for the compaction of back fills: it is simple, provides a uniform compaction system and yield much better shear strength that tradition compaction equipment next to abutments. However, contractors should be careful to provide materials that would yield excellent drainage properties to allow for the reduction of matric suction and the increase of shear strength.

Table 5.1. Summarizes the nuclear density gauge results on the control compaction

Dry Unit Weight (kN/m³) at 15 cm (6 in.) below the surface				
	Point 1	Point 2	Point 3	Point 4
Control	15.34	16.17	16.02	17.36
Water Content (%) at 15 cm (6 in.) below the surface				
	Point 1	Point 2	Point 3	Point 4
Control	13.22	12.17	12.13	11.89

Dry Unit Weight (kN/m³) at 28 cm (11 in.) below the surface				
	Point 1	Point 2	Point 3	Point 4
Control	17.10	17.99	18.08	18.88
Water Content (%) at 28 cm (11 in.) below the surface				
	Point 1	Point 2	Point 3	Point 4
Control	11.81	11.32	10.97	11.89

Table 5.2. Summarizes the nuclear density gauge results on the slurry flooding compaction

Dry Unit Weight (kN/m³) at 15 cm (6 in.) below the surface				
	Point 1	Point 2	Point 3	Point 4
45 min after flooding	20.11	19.16	20.09	20.77
2 hours after flooding	20.78	20.56	20.96	20.19
Days after flooding	20.85	20.17	20.24	N/A
Water Content (%) at 15 cm (6 in.) below the surface				
	Point 1	Point 2	Point 3	Point 4
45 min after flooding	4.48	5.33	5.60	7.71
2 hours after flooding	6.11	7.32	7.0	8.4
Days after flooding	4.75	5.41	4.88	N/A

Dry Unit Weight (kN/m³) at 28 cm (11 in.) below the surface				
	Point 1	Point 2	Point 3	Point 4
45 min after flooding	22.58	23.88	22.26	23.88
2 hours after flooding	22.87	22.69	21.99	22.50
Days after flooding	22.76	22.76	23.16	N/A
Water Content (%) at 15 cm (6 in.) below the surface				
	Point 1	Point 2	Point 3	Point 4
45 min after flooding	3.99	4.39	5.28	6.27
2 hours after flooding	5.45	6.34	6.3	8.04
Days after flooding	4.55	4.62	4.45	N/A

Table 5.3. Summarizes the GeoGauge results on the control compaction

Geogauge Stiffness (MPa)				
	Point 1	Point 2	Point 3	Point 4
Control	6.07	7.42	6.17	6.61

Table 5.4. Summarizes the GeoGauge results on the slurry flooding compaction

Dry Unit Weight (kN/m³) at 15 cm (6 in.) below the surface				
	Point 1	Point 2	Point 3	Point 4
45 min after flooding	5.44	5.8	N/A	N/A
Days after flooding	7.32	8.13	7.88	N/A

5.3 COMPACTION BY JETTING AT GREENFIELD AVENUE

To supplement the results gathered at Highway 51, further field observations were made at a second project site at Greenfield Avenue in Milwaukee. At this site, a contractor experienced with jetting (UPI) compacted the backfill around a city sanitary sewer by jetting. The sanitary sewer consisted of a 30 cm (12 in.) diameter PVC pipe. The pipe was placed onto a bed of 1.9 cm (0.75 in.) open-graded crushed stone, which was additionally filled halfway up

around the pipe to provide further structural support. Although a sandy backfill had been brought to the site, the contractor opted to backfill the top half of the pipe with the recycled concrete present in abundance at the site, as the passing sieve No. 200 fraction of the sandy backfill was out of specifications. The UPI employer indicated this recycled concrete backfill was placed loosely around the pipe to a thickness where large compaction equipment could begin operating above the pipe safely.

Upon reaching the subgrade level, the jetting was performed. The cross-section of the sewer trench at this time consisted of 15 cm (6 in.) of recycled concrete at the surface, as shown in Figure 5.16. The recycled concrete layer rested on top of a 25 cm (10 in.) thick layer of large crushed concrete rocks of about 20 cm (8 in.). Below the large crushed stone there is more recycled concrete down to the sanitary sewer. The pipe lies at an elevation of 2.4 m (8 ft.) beneath the subgrade level.

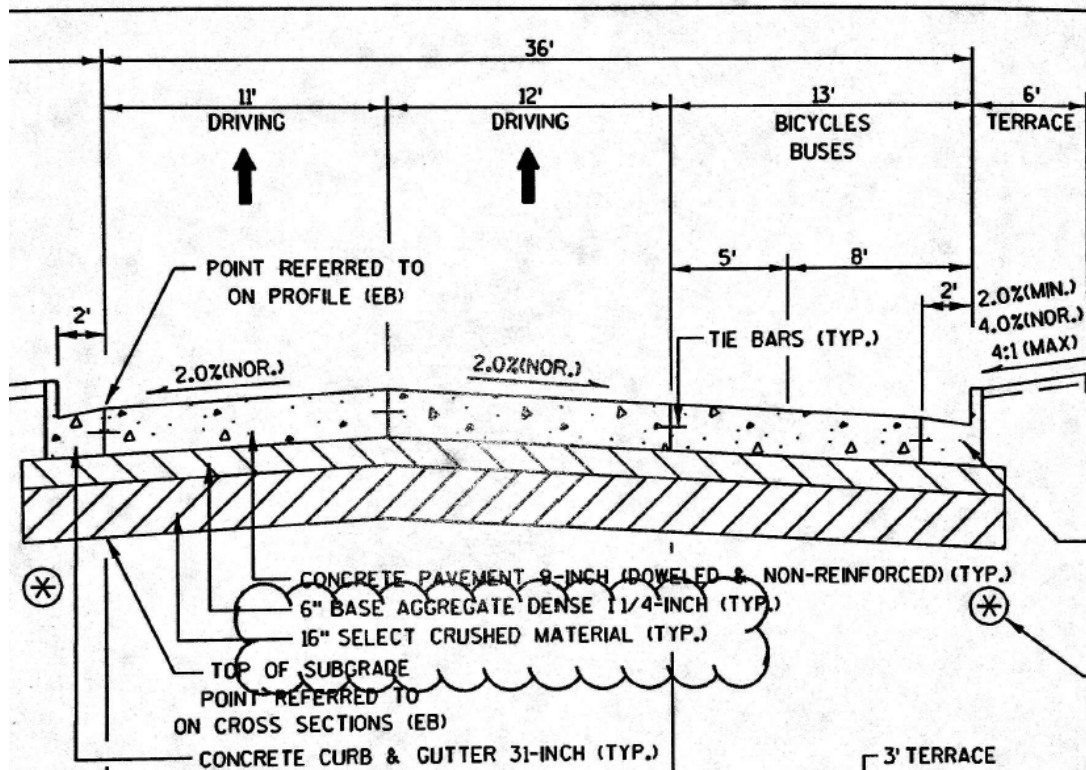


Figure 5.16. Cross Section of Pavement Structure at Greenfield Avenue. The contractor was unable to push the rigid pipe through the 40.6 cm (16 in.) crushed rock layer until a small backhoe excavated application points along the trench.

Because the two UPI workers were unable to push the 5 cm (2 in.) diameter cast iron pipe through the crushed concrete layer, even with the water on full bore from the nearby fire hydrant, another UPI operator dug holes with a small backhoe through the crushed concrete and spaced about 3 m (10 ft.) apart to serve as jetting application points. This operation can be seen in Figure 5.17. There appeared to be little coordination between the City of West Allis inspectors and the contractor as to the suitability of these subbase and subgrade materials for the jetting application.



Figure 5.17. Pictures of Jetting Operation at Greenfield Avenue. Excavated Application Points (top left). Truck Compaction Treads After Filling Application Points (top right). Rigid Cast Iron Pipe Jetting Below Top of Subgrade (bottom).

It is clear that contrary to expectation, during the Greenfield Avenue jetting, the backfill around the pipe itself was not subjected directly to the flow of water from the rigid pipe. Initially the compaction mechanism of jetting was thought to be derived from the physical action of the water jet carrying the backfill particles into place, where the final density of the backfill was dependent on the drainage capacity of the backfill, and the energy with which the water drains away from the pipe. However, in this case, the water jet was emitted about 1.8 m (6 ft.) above the elevation of the sewer. Upon questioning the contractor as to their understanding of the compaction mechanism, they described that the water is expected to percolate down to the pipe, to the point where water pressure builds up around the pipe, displacing the loose backfill. The contractor stated that the jetting instrument is generally left at the application point until water starts ponding on the surface, supposedly indicating the water has reached the pipe. As the backfill around the pipe is suspended in water, when the instrument is removed, the backfill particles can fall through the water column and surround the pipe. With minimal capillary forces acting at the curved grain-water interface to bulk the backfill into clumps, the grains are able to fill the void spaces more fully and achieve greater relative density.

The contractor indicated that in the past this type of jetting operation has been observed to produce subsidence at the surface of up to 12.5 cm (5 in.), certainly indicating that the compaction mechanism was working. However on this day, no subsidence was observed at the surface; the contractor predicted this was because rains at the site a few days earlier had already washed the backfill into place around the pipe. Besides observing subsidence at the surface, no quality control measures were, or are typically, implemented to check compaction of the backfill after a jetting application. For example, the holes remaining after the application were loosely filled with excess backfill. The backfill was then compacted by driving the truck over the holes along the trench profile, as seen in Figure 5.16. However, a few strength profiles with the dynamic cone penetrometer were collected at a selection of excavated application

points, and after the jetting was performed. Between 12 and 15 blows were needed to reach a penetration depth of 40 cm at all the application points. For a general comparison, the recycled concrete at Greenfield Avenue was slightly weaker than the sandy backfill compacted by the large vibratory roller at Highway 51, which required 15 to 20 blows to reach penetration depth of 40 cm (16 in.).

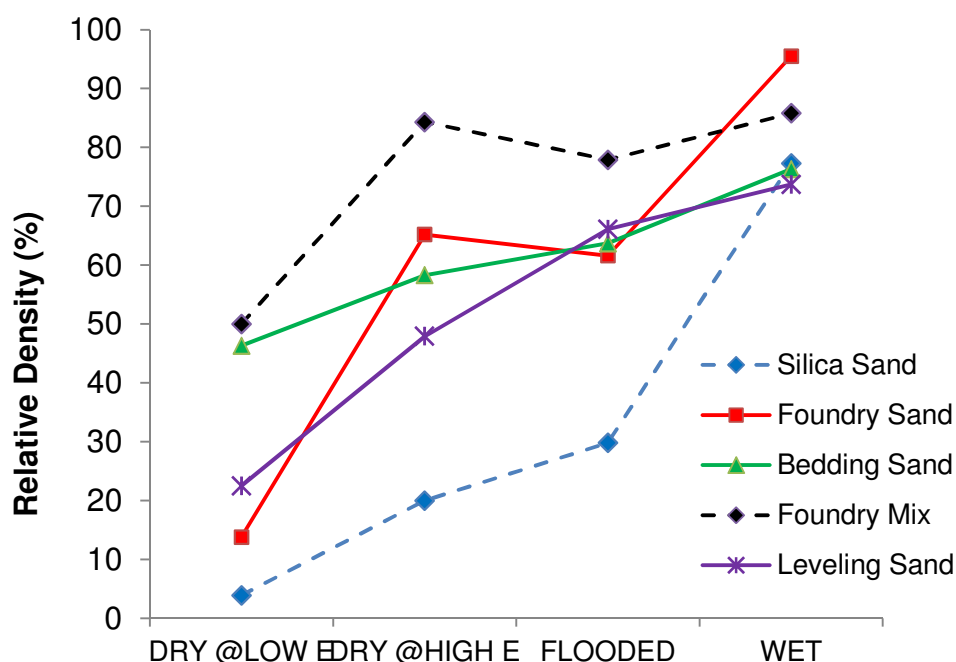


Figure 5.18. Comparison of Deposition Techniques for Sandy Soils Subjected to Flooding, or Compaction by Drainage in the Tank in the Lab.

It is noted here that the jetting operation performed at the Greenfield Avenue site creates a compaction mechanism that is nearly identical to the flooded deposition tests performed in the lab. During flooded deposition, the soils were dropped into a column of water in the tank; as such, the soil column builds up through the accumulation of individual grains falling through the water with low energy. As seen in Figure 4.18, which depicts the results from the final lab testing program conducted on backfills used by WisDOT, flooded deposition was generally the second most effective method next to wet deposition, where soils fell into the tank in slugs with high energy. This is promising as the field application includes the added benefit of a large thickness

of overburden pushing down on the jetted backfill as it falls into place through the water around the pipe. Additionally, the water would be expected to drain slowly through the native soils surrounding the trench, providing plenty of time for the individual grains to fall through the water and around the pipe. Both of these considerations would be expected to produce more compact backfill around the pipe in the field.

This particular application of jetting was no doubt hampered by the layer of large crushed concrete rocks preventing the contractor from inserting the pipe more deeply into the trench. Nonetheless their cast iron pipe jetting instrument was only about 91 cm (3 ft.) long, not nearly long enough to reach the sanitary sewer. It is particularly disconcerting that no quality control is implemented for a compaction operation dependent on water seeping toward a deeply buried pipe, 2.4 m (8 ft.) beneath the surface in this case. Perhaps in a more typical jetting application, if a sandy backfill with high drainage capacity is used to fill the utility trench, water would preferentially flow towards the pipe, instead of into the native soil surrounding the trench. Finally, when questioned as to the situations when jetting has been performed in the past, the contractor indicated it is almost exclusively applied to deeply buried pipes, instead of shallower storm sewer or electrical utilities. This may provide two advantages: 1) the thick overburden pushes down on the hydrated backfill, or 2) more practically, at such a great depth, just a moderate level of compaction is adequate to prevent acute settlement along the trench profile and subsequent rutting of pavement structures at the surface.

SECTION 6 – HYDRAULIC MODELING OF FIELD SCALE JETTING TESTS

The USGS finite difference algorithm Modflow is commonly used to model groundwater flow through aquifers, but its fundamental flow equations allow it to be used to model the flow processes produced during jetting. For this reason it is a great tool to be able to visualize in a general sort of frame how the jetting application should proceed to make things as smooth as possible in transitioning from the lab to the field. The models consider a variety of flow conditions and implications of materials with different conductivities and especially flow rate and timing of the jetting application. In this report, Modflow is used with the Groundwater Vistas graphical interface to evaluate expected flow processes created by hydraulic jetting at bridge abutments like those at the Highway 51 project site. The modeling may be used to make recommendations for best practices in jetting at a bridge abutment, and in the future may be compared to observations gathered in the field.

6.1 Context and Justification of Modeling

Performance of jetting in the field requires the specification or at least the recommendation of a wide variety of parameters including jetting probe length, diameter, and flow rate, three-dimensional spatial location of each jetting point, duration of jetting at each point, and possibly even the number of men operating a jetting instrument at a given time near the highway structure. To go into the field with no idea of suitable recommendations for each of these parameters would invite unexpected consequences and poor performance of the jetting application. For this reason, a model has been created with the Groundwater Vistas interface for Modflow. The program Modflow is widely used and freely distributed by the United States Geological Survey (USGS) to model groundwater flow through aquifers. However it also has a number of stress packages, such as the drain tile boundary condition, that allow for a reasonable adaptation of the program to the problem at hand.

The expectation is to use the model results to obtain *rough estimates* of all the jetting application parameters mentioned above to improve the jetting performance. The model will not be able to directly simulate compaction of the soil solid matrix due to jetting. However, there may be a coupled relationship between both the amount of water ponded on the surface of the backfill, as well as the amount of water exiting the system through the drain tile at the base of the abutment, against the effectiveness of the compaction. A large amount of water ponding on the surface during the model run indicates that flow is backed up, water is likely pushing the grains apart, and the downward seepage force is likely negated producing less effective compaction. Additionally, a greater amount of water exiting the system through the drain tile may indicate more effective compaction. It is hypothesized that there may be some additional pore pressure suction as water leaves the backfill through the drain, as opposed to entering the native soil and staying within the pore structure. It seems logical that a more effective drainage system would produce better compaction. These two benchmarks found in the results of the model will be the basis of recommendations for the aforementioned jetting application parameters.

It is important to remember during the modeling process that the model is not nearly an exact representation of the actual field system. It is a calculated representation of the actual system, and it will produce errors that are difficult to quantify without field scale results. At this point in the modeling process, every effort must be made to not only ensure accuracy of the model but to identify significant limitations. The most important limitations of this model are the inability to simulate unsaturated flow and the inability to account for disturbance to the soil solid matrix during jetting, or the very process of compaction itself. For example, backfill is often placed much closer to a dry condition, or its natural moisture content, rather than saturated, and Modflow does not provide a methodology for the incorporation of unsaturated flow equations into the model. Furthermore, a constant porosity and specific yield for the backfill must be specified throughout the model run, thereby ignoring the effect a changing solid matrix would

have on the nature of water flow through the system. Other limitations of the model include artificial no flow boundary conditions, and the inability to specify the direction of the source of water. Flow out of the jetting probe is represented by a source well in Modflow, and this source injects water uniformly in each of the three space dimensions, instead of downward as would occur in the field. When possible, every effort was made to decrease the effect of these limitations on the model results such that practical inferences may be made about how to improve the application and performance of jetting in the field.

6.2 Details of Modflow with Groundwater Vistas

In the following pages, a wide variety of jetting cases are simulated in Modflow. Among other things, each case seeks to investigate the effects of steady state vs. transient runs, jetting injection rate, jetting network and timing, hydraulic conductivity of the backfill and native soil, and even location and number of drain tiles present in the system. A typical model representation of the abutment-backfill-native soil system in Groundwater Vistas can be seen in

Figure 6.1. Some important points to note in the figure include:

- rows and columns are shown in the plan view; layers increase with depth and can only be seen in the cross-section view. rows, columns, and layers are the y-,x-, and z-dimension in Groundwater Vistas, respectively
- radius of each source well is 0.1 m (4 in.), simulating a jetting probe with diameter of 0.2 m (8 in.); source well locations are represented by the red boxes
- width of each drain is 0.2 m (8 in.); drains are represented by the yellow boxes and set to a stage equal to elevation head
- a constant head boundary, specified on the opposite side of the abutment wall, allows water to leave the system through its horizontal plane; this boundary is shown in blue in row 7
- the abutment wall is represented as a no flow boundary; this boundary is represented by the black boxes in layer 1-6 and column 1-7
- the water level on the surface is contoured in the cross-section view; this is represented as the thin blue line

- orange cells indicate locations where water has drained and the cell has gone dry; blue shaded cells indicate locations where the water has flooded above the surface of the backfill
- the height of the wall is 4.5 m (15 ft.)
- the backfill slopes away from the base of the abutment wall at 1.5H:1V; this is not shown in the figure but different hydraulic conductivities may be specified for the backfill and native soil
- the initial water level of the system is set to the top of layer 2; this is not shown in the figure but may simulate backfill placed in a wet condition

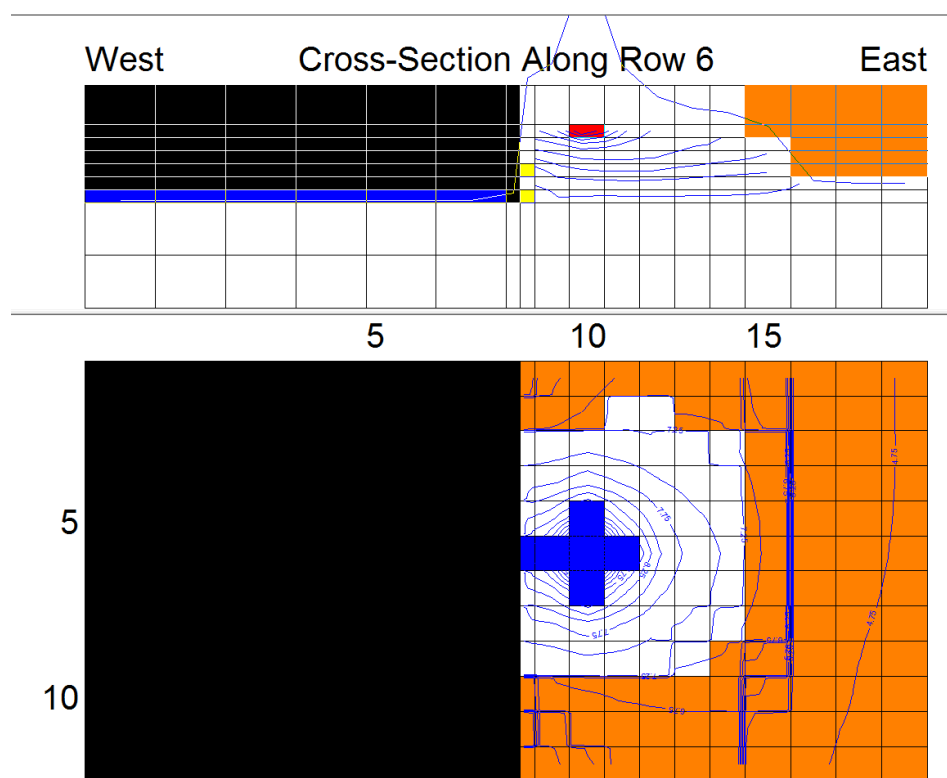


Figure 6.1. Jetting Case 1: Single Injection Well in Layer 2.

6.3 Steady State Models for Compaction by Drainage

Case 1: Single Well, Steady State

In this first steady state model, there is a single well injecting water into layer 2 at a rate of $0.1 \text{ m}^3/\text{s}$ (26 gal/s). The conductivities of the backfill and the native soil are set to 0.01 m/s and 0.001 m/s , respectively. These values are higher than what would be expected based on

lab tests, but for now the focus is to simply compare results when the conductivity of one material is much higher or lower than the other, and to ensure the model is yielding results that make sense. Note the sharp peak in the water level above the well in this case along with the flooded cells in layer 1. The additional thin blue lines below the water level denote equipotential contours. By definition, water in the system will flow perpendicular to these lines. Note in the cross-section view how a good portion of the water flows toward the drains in this case. This may also be checked in the mass balance dialog shown in Figure 6.2. At steady state, $0.029 \text{ m}^3/\text{s}$ (7.6 gal/s) is leaving the system through the constant head boundary on the other side of the wall, and $0.071 \text{ m}^3/\text{s}$ (18 gal/s) is leaving the system through the drains.

In each of the following cases, the type of results depicted in Figure 6.1 provide the basis for evaluating the effectiveness of the jetting in terms of the performance criteria. The concept of the transient simulation and the mass balance hydrograph will be introduced, and finally some recommendations about the various jetting parameters will be made in light of all the cases.

MODFLOW Mass Balance

From Column: 1 To Column: 18
 From Row: 1 To Row: 12
 In Layer: 0

OK
 Graph
 Export...

	INFLOWS	OUTFLOWS
Storage	0	0
X min	0	0
X max	0	0
Y min	0	0
Y max	0	0
Top	0	0
Bottom	0	0
Well	0.100000001490116	0
C.H.	0	0.0288779026013799
GHB	0	0
River	0	0
Drain	0	0.0711684410343878
Stream	0	0
Recharge	0	0
ET	0	0
Lake	0	0
TOTAL	0.100000001490116	0.100046343635768

Percent Error: -0.0463314094765561

Figure 6.2. Mass Balance Dialog for Jetting Case 1.

Case 2: Single Well, Steady State, Low Conductivity of Native Soil

In Case 2 (Figure 6.3) the effect of the native soil having a much lower hydraulic conductivity than the backfill is examined. The conductivity of the native soil is 10^{-5} m/s, and the conductivity of the backfill is still the same at 0.01 m/s. Now the surface flooding above the well is more extensive, and there are no dry cells in the surface layer. Interestingly, a much larger volume of water is leaving the system through the drain in this case. That makes sense since the native soil has much lower conductivity. In fact water actually enters the system through the constant head boundary in this case.

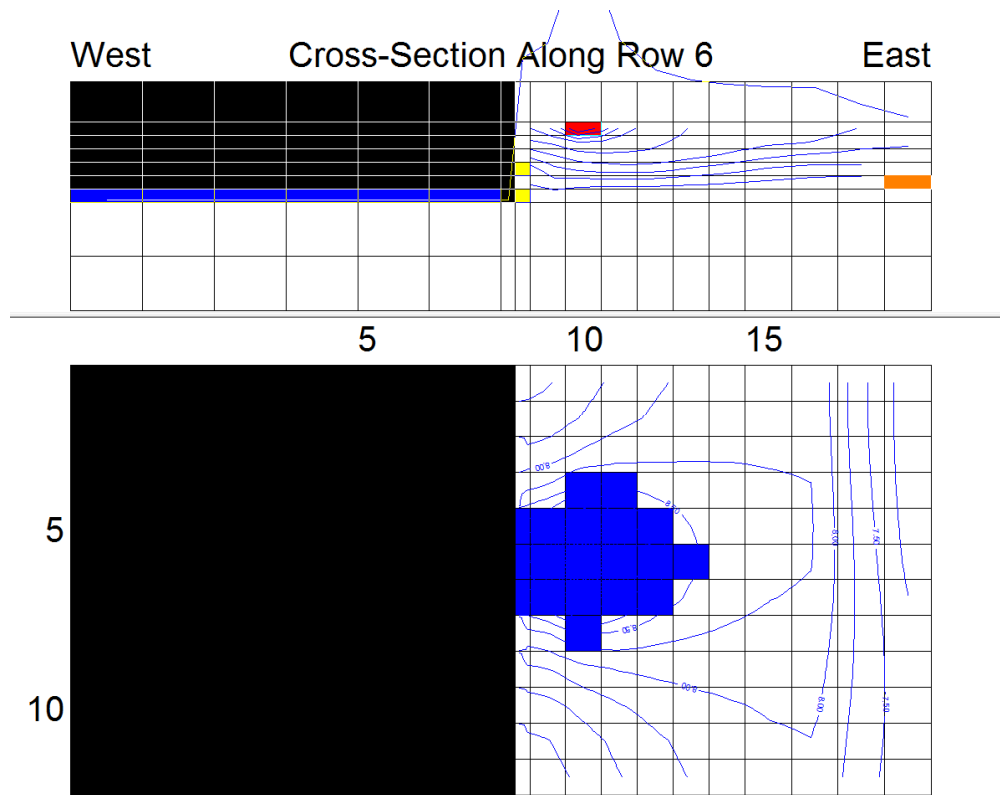


Figure 6.3. Jetting Case 2. Single Injection Well in Layer 2 with Low Conductivity Native Soil.

MODFLOW Mass Balance

From Column: 1 To Column: 18
 From Row: 1 To Row: 12
 In Layer: 0

OK
Graph
Export...

	INFLOWS	OUTFLOWS
Storage	0	0
X min	0	0
X max	0	0
Y min	0	0
Y max	0	0
Top	0	0
Bottom	0	0
Well	0.100000001490116	0
C.H.	0.000277672173126575	0
GHB	0	0
River	0	0
Drain	0	0.100310856476426
Stream	0	0
Recharge	0	0
ET	0	0
Lake	0	0
TOTAL	0.100277673663243	0.100310856476426

Percent Error: -0.0330854542483809

Figure 6.4. Mass Balance Dialog for Jetting Case 2.
Case 3: Single Well, Steady State, Low Conductivity of Backfill

The effect of the backfill having a much lower conductivity than the native soil is examined in Case 3. The conductivity of the backfill is now 10^{-5} m/s, and the conductivity of the native soil is 0.01 m/s. Note how all the cells are flooded in the surface layer, shown in Figure 6.5 below. The mass balance shown in Figure 6.6 indicates there is still a fair amount of water leaving the system through the drains. There is $0.067 \text{ m}^3/\text{s}$ (17.7 gal/s) leaving the drains here compared to $0.071 \text{ m}^3/\text{s}$ (18.8 gal/s) of water leaving the drains in the first case. This case highlights the importance of having a conductive backfill material to limit the amount of water backing up above the surface during the jetting application.

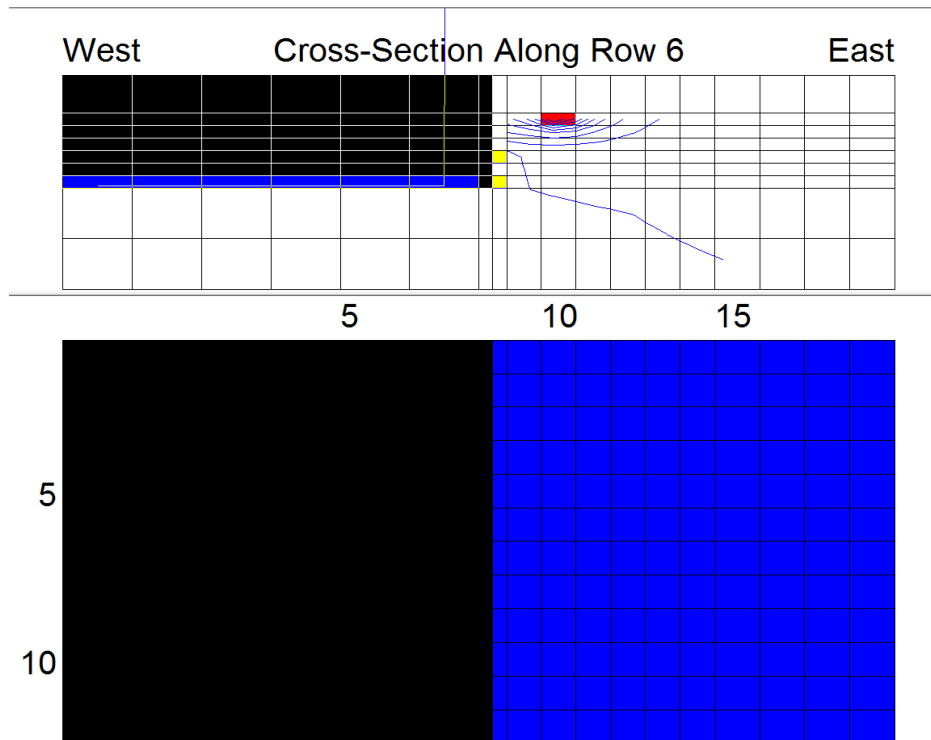


Figure 6.5. Jetting Case 3. Single Injection Well in Layer 2 with Low Conductivity Backfill.

From Column	1	To Column	18	OK Graph Export...
From Row	1	To Row	12	
In Layer	0			
	INFLOWS		OUTFLOWS	
Storage	0		0	
X min	0		0	
X max	0		0	
Y min	0		0	
Y max	0		0	
Top	0		0	
Bottom	0		0	
Well	0.100000001490116		0	
C.H.	0		0.0332671058567939	
GHB	0		0	
River	0		0	
Drain	0		0.0667808926664293	
Stream	0		0	
Recharge	0		0	
ET	0		0	
Lake	0		0	
TOTAL	0.100000001490116		0.100047998523223	Percent Error -0.0479855165799148

Figure 6.6. Mass Balance Dialog for Jetting Case 3.

Now with these steady state cases it is possible to model the process of flooding. Flooding is similar to jetting in that the downward flow of water is designed to compact the backfill, but it is less intensive in nature. During flooding, water is simply fan sprayed gently above the surface of the backfill. Again the key performance criteria are the extent of ponded water on the surface and the amount of water exiting the system through the drain. The conductivity of the backfill is set to 0.01 m/s and the conductivity of the native soil to 0.001 m/s as in the first case. There are ten injection wells each pumping water into the system at 0.01 m³/s (2.6 gal/s). Then the sum of all the flow rates in the wells is actually equal to each of the above cases. Note the water level contour in layer 1, shown in Figure 6.7 below. There is no water backed up on the surface in this case. The ratio of water leaving the system through the drain to water leaving the system through the constant head boundary on the other side of the wall here is very similar to the first case. Additionally, the grid of injection wells is located close to the wall to simulate the greater need for compacting the backfill in this area where heavy equipment cannot operate. The flow rate and flooding grid specified here would be a great starting point for the field application of flooding.

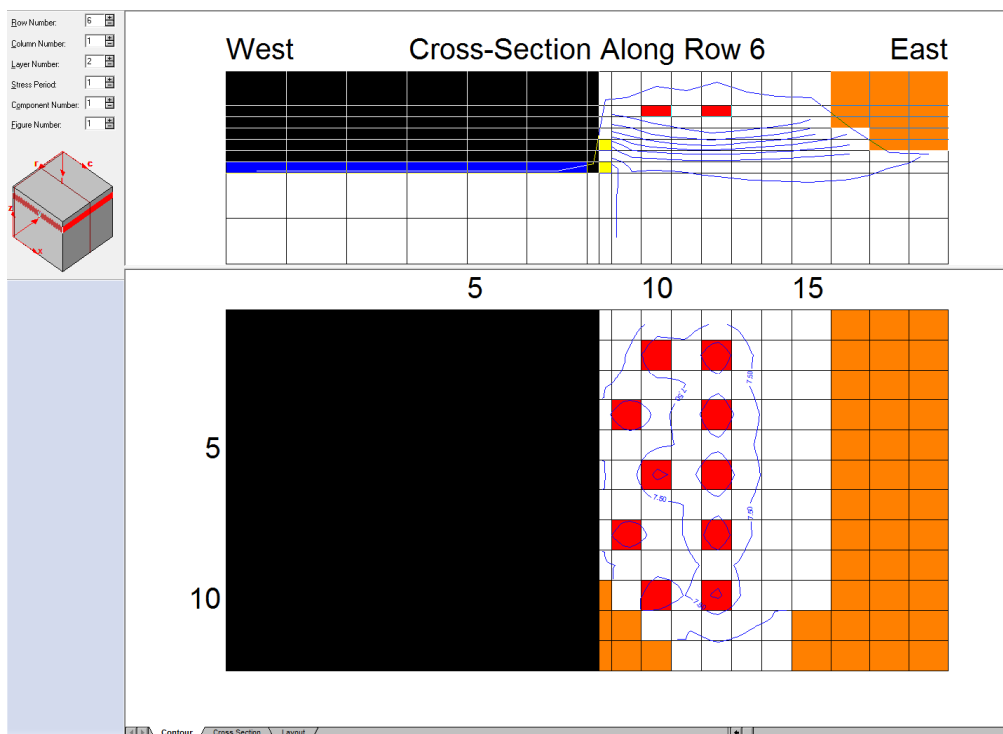


Figure 6.7. Flooding Case with Ten Injection Wells Near the Surface.

6.4 Transient Models for Jetting

At this point it is desirable to get a sense of the effect of varying time scales on the effect of the jetting application. Steady state runs imply that the energy of the water is independent of time, but not how long it would take to reach the steady state condition after the injection wells, or jetting points, are turned on in the system. To investigate time scales, transient runs may be made with Modflow.

Case 4: Jetting the Surface

For jetting application Case 4, shown in Figure 6.8 below, five stress periods are introduced. The stress periods last 100 s, 500 s, and 1000 s for each of the last three periods; this adds up to a total run of 1 hour of jetting. Additionally, a monitoring well has been added to the model for the purpose of monitoring pressure head at a given location throughout the transient run. The hydrograph from the monitoring well is shown in Figure 6.10. The well is

screened through layers 6 and 7, right in the center of the system, and is shown in the cross-section view where the two sets of thin blue lines intersect at the 'X' marker.

The cross-section in Figure 6.8 details the extent of the surface flooding 1 hour after the first injection wells were turned on. The water ponded on the surface is more extensive in area, but less so in magnitude. The highest head in layer 1 is 11.5 m (37.7 ft.) in layer 1 for this case. Notice also that only a single row of cells in layers 1 to 3 becomes dried out in this case. The scenario detailed here as jetting Case 4 would actually represent a good injection rate to use given the timing and spacing of jetting events.

The jetting grid is shown in Figure 6.9 below. In this figure, each circled number represents a source well injecting water during that corresponding stress period. The field implementation of this model would require three men each operating a jetting instrument. The decision to model three wells operating at a given time was made to both speed up the jetting process and in theory provide for a more even compactive effort in the field. Note also how the grid of jetting points is located entirely in layer 2 in this case (Figure 6.8). This is a very simple case where the compactive effort of the jetting would be focused near the surface, but it may prove to be a good starting point to examine the results in the new transient model setting. The flow rate out of the jetting instrument at each of the 15 injection points is $0.05 \text{ m}^3/\text{s}$ in this case.

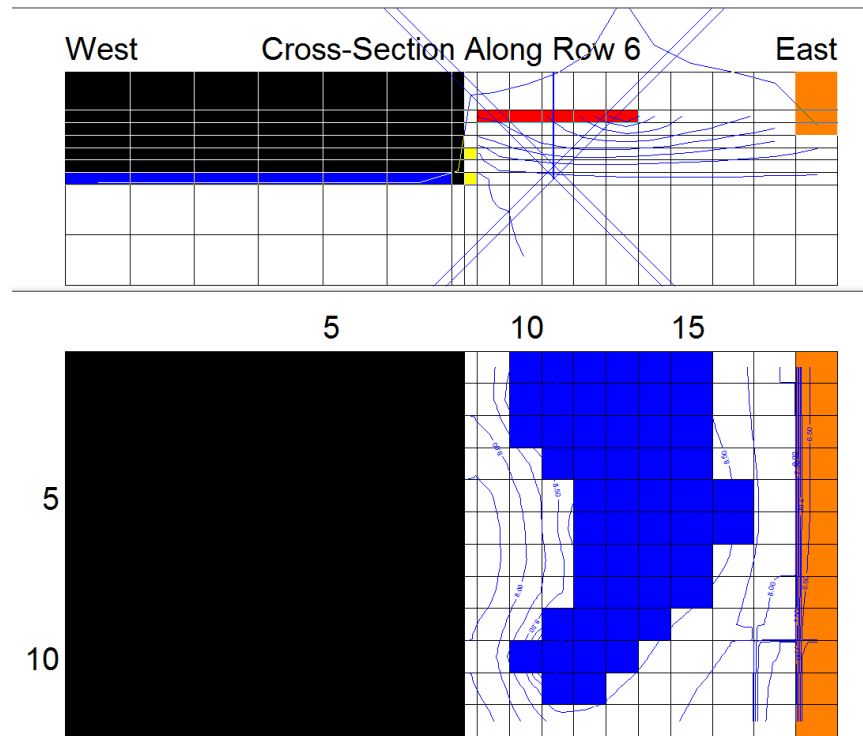


Figure 6.8. Jetting Case 4. Note the ponded water on the surface.

Row / Column	8	9	10	11	12	13	14
1							
2		1(1)		1(5)			
3			1(3)				
4		1(2)		1(4)			
5							
6		1(1)	1(2)	1(3)	1(4)	1(5)	
7							
8		1(2)		1(4)			
9			1(3)				
10		1(1)		1(5)			
11							
12							

Figure 6.9. Grid for Jetting Case 4. Layer numbers are shown as a function of the stress period, e.g. 1(5) represents an injection well turned on in layer 1 during the 5th stress period.

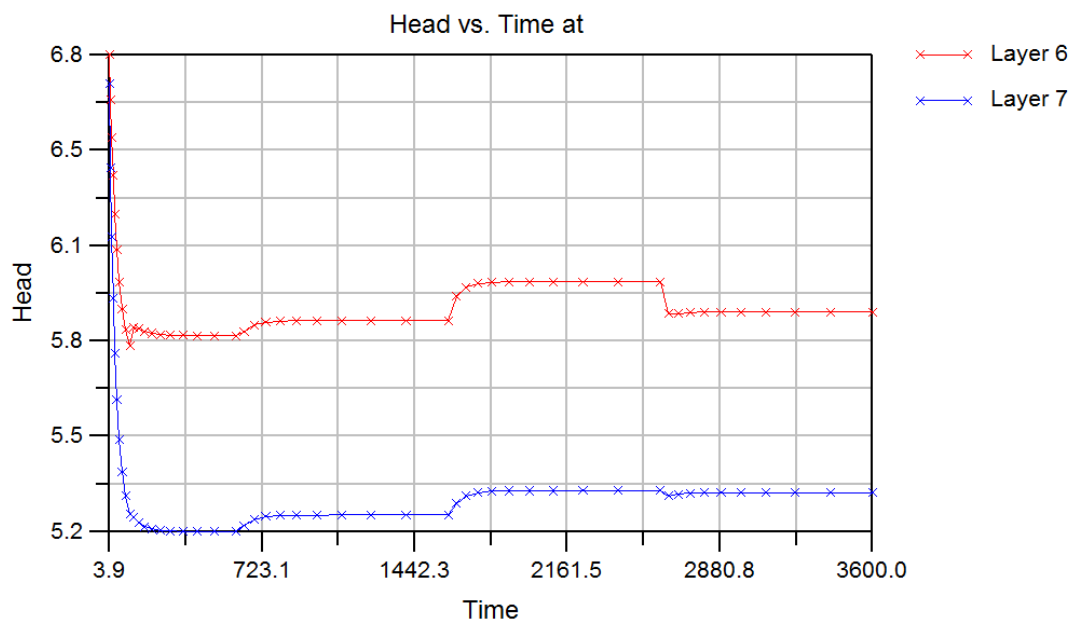


Figure 6.10. Hydrograph of Pressure Head (in meters) at the Monitoring Well for Jetting Case 4. Note the system response when an injection well is turned on near the monitoring well.

The results for Case 4 show that the drainage capacity of the system is largely sufficient for the given flow rate and jetting grid. The minimal ponding developed by the end of the run is limited in extent and likely would not inhibit the compactive effect of jetting.

Case 5: Jetting into the Backfill

Now in the following case a more advanced stress period setup and three-dimensional jetting network will be specified. Emphasis is now placed on advancing the model toward a more realistic and accurate solution for the field jetting application. There are now 25 stress periods, with each period lasting 216 seconds. This adds up to a total run of 90 minutes of jetting, a reasonable amount of time for three men to be working in the field. The hydraulic conductivity of the backfill and the native soil are set to $2.84 \cdot 10^{-4}$ cm/s and $8.95 \cdot 10^{-4}$ cm/s, respectively. Both of these estimates were determined in simple falling head tests in a rigid wall permeameter in the lab. Each material was sampled from the Highway 51 project site at Bear Tree Parkway. Both the backfill and the native soil were specifically compacted to a fairly dense

state in the permeameter before performing the conductivity tests in the lab to better simulate the field condition. The backfill-native soil interface can be seen in Figure 6.11.

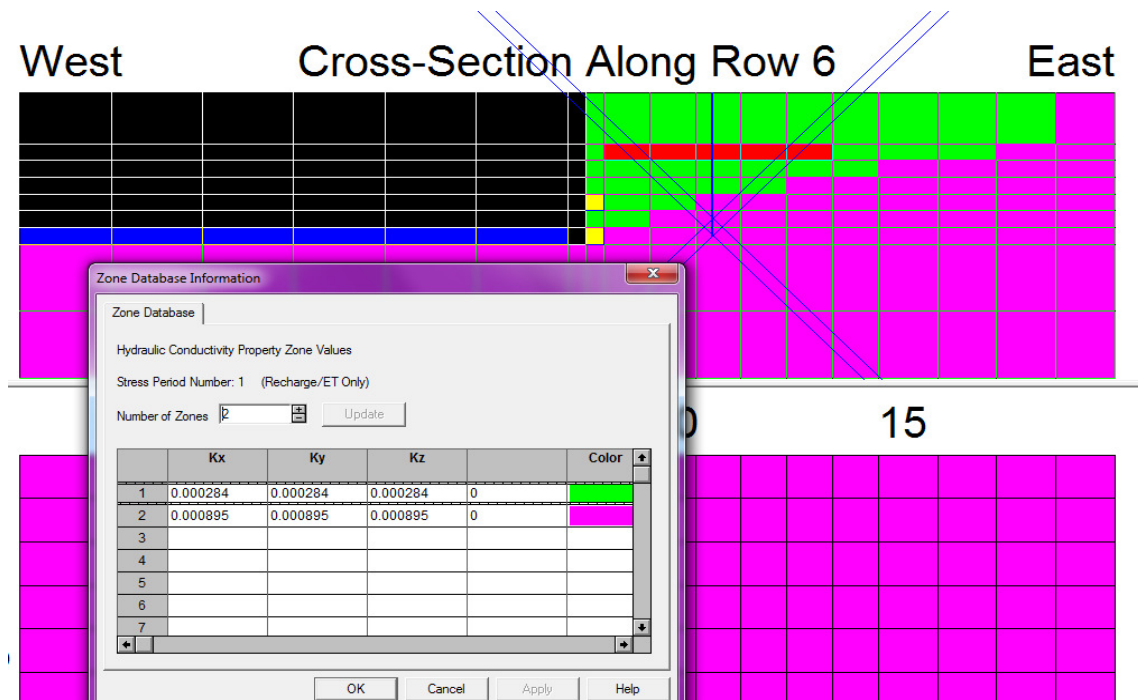


Figure 6.11. Backfill-native soil interface. The backfill is bright green, and the native soil is bright pink.

The results for Case 5, the new three-dimensional jetting network, the hydrograph of head at the monitoring well, and the mass balance are shown in Figures 6.12 through 6.15, respectively. The flow rate for all the injection wells is reduced to $0.02 \text{ m}^3/\text{s}$ (5.3 gal/s) in light of the new specified conductivities of the backfill and native soil. The cross-section shown in Figure 6.12 represents the results at 90 minutes, the end of the simulation; note the extensive flooding in the surface layer. Clearly the drainage system does not have adequate capacity to drain the large amount of water entering the system. A quick calculation reveals that over the entire run, with three wells operating continuously at $0.02 \text{ m}^3/\text{s}$ (5.3 gal/s) for 90 minutes, a total of 324 m^3 (11440 ft^3) of water is being injected into the system. That is an impractical amount of water to bring to the site. To acquire that quantity of water the construction crew would need to

tap into a nearby fire hydrant. Based on the results of this model, the injection rate of and duration of each jetting point is too large.

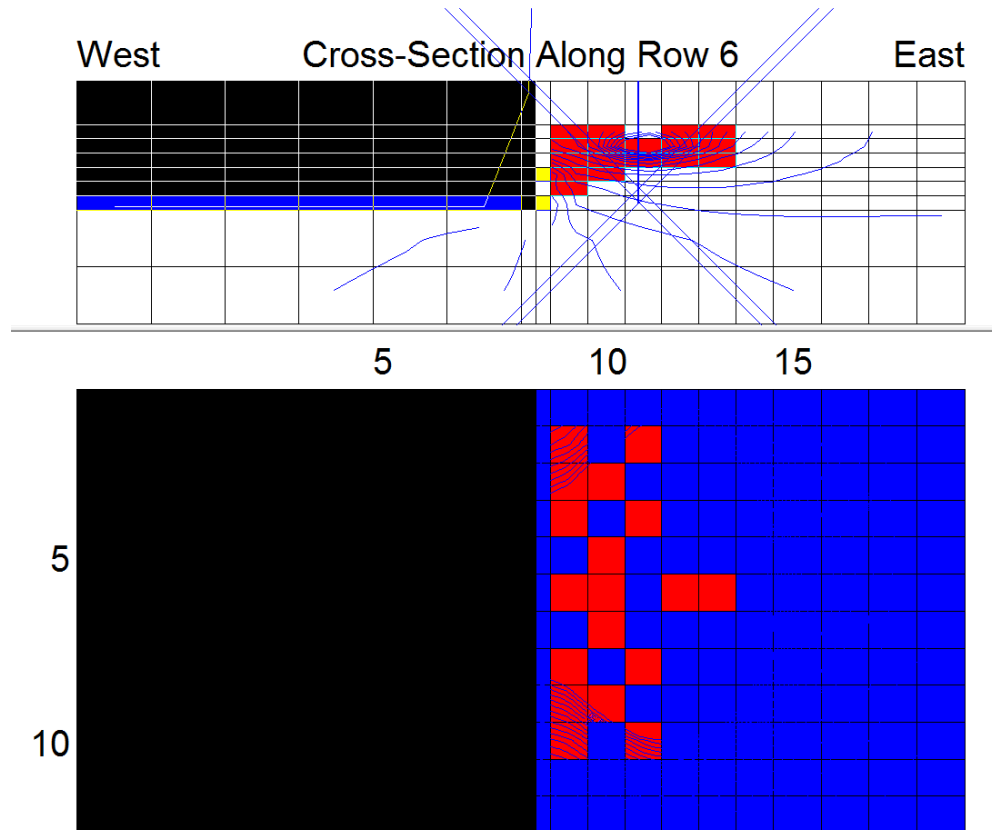


Figure 6.12. Jetting Case 5.

Row / Column	8	9	10	11	12	13	14
1							
2		2(1) to 6(5)		2(22) to 4(24)			
3		2(18) to 5(21)	2(14) to 5(17)				
4		2(9) to 6(13)		2(6) to 4(8)	3(25)		
5			2(18) to 5(21)				
6		2(1) to 6(5)	2(9) to 5(12)	3(25) to 4(13)	2(6) to 4(8)	2(22)	4(24)
7			2(14) to 5(17)				
8		2(9) to 6(13)		2(6) to 4(8)	3(25)		
9		2(18) to 5(21)					
10		2(1) to 6(5)		2(22) to 4(24)			
11							
12							

Figure 6.13. Grid for Jetting Case 5. Layer numbers are shown as a function of the stress period. Note how the jetting network is designed to simulate a given instrument being inserted down into deeper layers with each passing stress period. For example, 2(1) to 6(5) means the instrument was jetting layer 2 during the 1st stress period, layer 3 during the 2nd stress period, and so on. Once the instrument reaches the bottom-most layer, the instrument is quickly removed from the backfill and inserted into the next point near the surface at a new areal location in plan view.

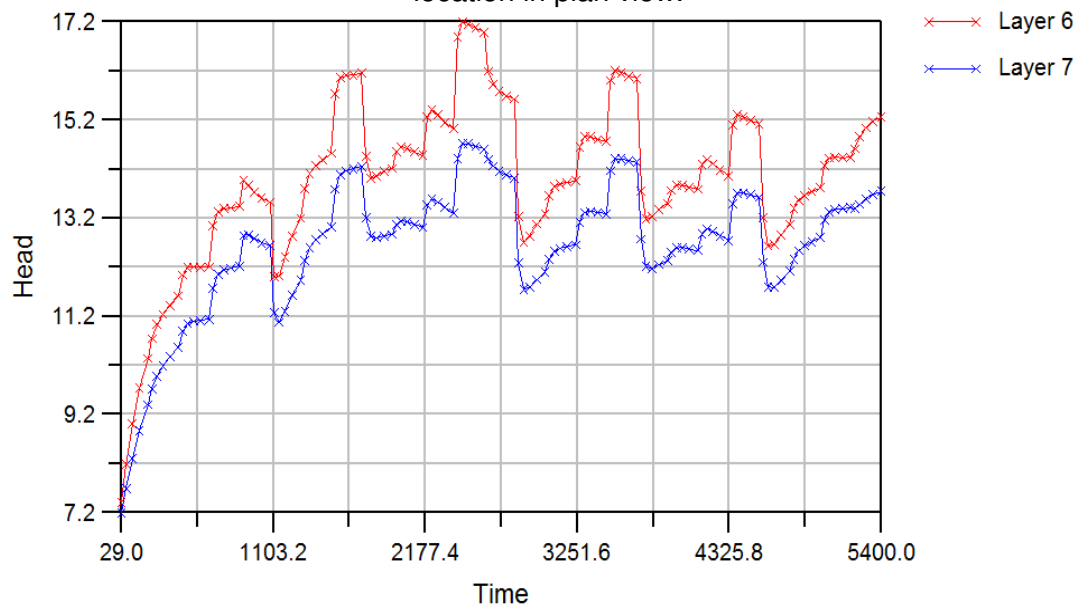


Figure 6.14. Hydrograph of Pressure Head at the Monitoring Well for Jetting Case 5. The system floods, and stays flooded, from a very early stress period. It is interesting to see the water levels fluctuating as the various injection wells are turned on and off. Note also how the water levels do eventually level off after about 30 minutes of jetting. This may indicate the geometric network is conducive to a successful operation, but the flow rate is too high.

From Column	1	To Column	18	OK Graph Export...
From Row	1	To Row	12	
In Layer	0			

	INFLOW/S	OUTFLOW/S	
Storage	1.9245791223893e-006	0.00218893240838591	
X min	0	0	
X max	0	0	
Y min	0	0	
Y max	0	0	
Top	0	0	
Bottom	0	0	
Well	0.0599999986588955	0	
C.H.	0	0.0342782154621091	
GHB	0	0	
River	0	0	
Drain	0	0.0236037044087425	
Stream	0	0	
Recharge	0	0	
ET	0	0	
Lake	0	0	
TOTAL	0.0600019232380179	0.0600708522792375	Percent Error -0.114812106112575

Figure 6.15. Mass Balance Dialog for Jetting Case 5. Shown here is the mass balance at the end of jetting. Note that the drain only accounts for 40% of the total system outflows. Upon examination of the mass balances of each of the last five cases, a trend may be observed where a smaller portion of water leaving the system specifically through the drains corresponds to a greater extent of backed up water on the surface layer.

Case 6: Jetting into the Backfill, with Reduced Flow Rate and Wall Application Points

The following case represents a sound strategy for implementing jetting in the field. Two subtle changes have been made to the model to reduce the extent of water ponded on the surface, and to increase the volume of water exiting through the drains: the flow rate of all the injection wells is reduced to $0.01 \text{ m}^3/\text{s}$ (2.6 gal/s), and three injection wells that were previously operating some distance from the abutment wall have been moved directly adjacent to the wall. The reduced flow rate increases the practicality of acquiring the volume of water necessary to perform the jetting operation. Furthermore, placing wells adjacent to the wall would likely increase the compactive effort in the area that needs it the most. The results for Case 6, the hydrograph of head at the monitoring well, and the mass balance are shown in Figures 6.16

through 6.18. The hydrograph in particular reveals the reduced extent of backed up water in the system throughout the transient run. The maximum pressure head reached 17.2 m (56.4 ft.) in Case 5; here the maximum pressure head is only 10.7 m (35.1 ft.), a significant improvement. Also of note from the hydrograph is the marked difference in pressure between layer 6 and layer 7, especially when a well turns on in layer 6. This localized spike in pressure may be interpreted as a sign that lower jetting pressure should be used, while spreading out jetting locations over a greater space, and spending shorter amounts of time at each location, in order to avoid over-taxing the drainage capacity of the system.

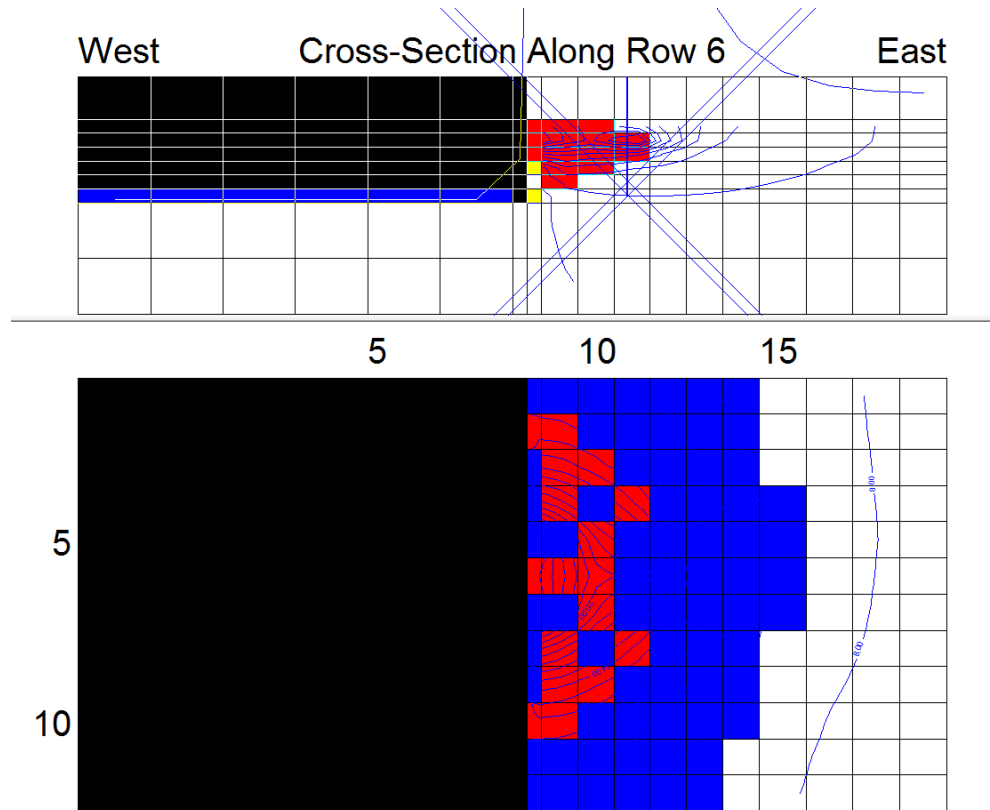


Figure 6.16. Jetting Case 6. There is still ponded water on the surface, but not to the extent seen in Case 5. The cross-section shown here represents the results at the end of the simulation.

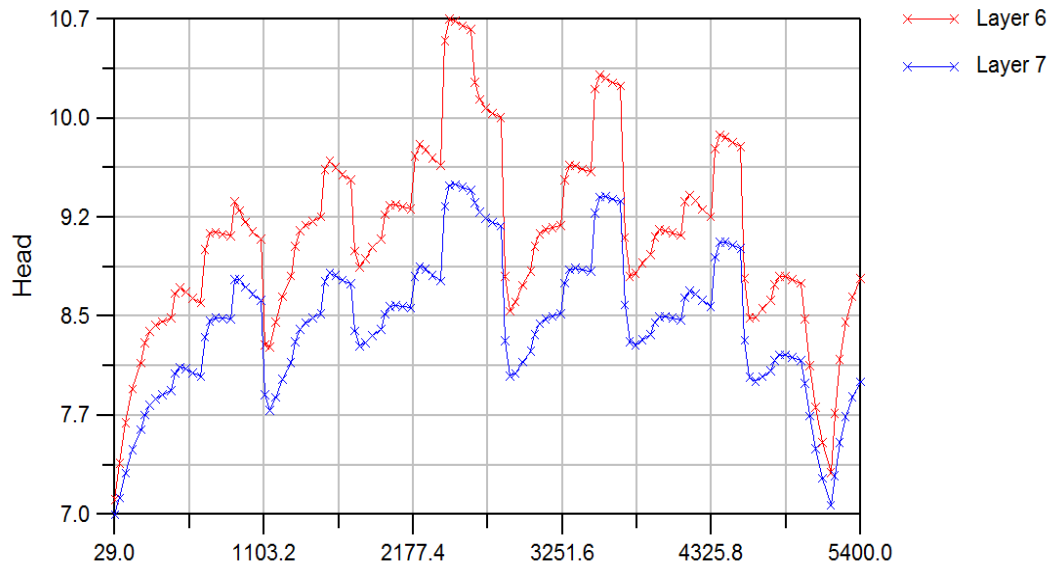


Figure 6.17. Hydrograph of Pressure Head (in meters) at the Monitoring Well for Jetting Case 6.

MODFLOW Mass Balance

From Column: 1 To Column: 18
 From Row: 1 To Row: 12
 In Layer: 0

OK
Graph
Export...

	INFLOWS	OUTFLOWS
Storage	3.17213574296815e-007	0.00403666533727431
X min	0	0
X max	0	0
Y min	0	0
Y max	0	0
Top	0	0
Bottom	0	0
Well	0.029999993294477	0
C.H.	0	0.0124938968656352
GHB	0	0
River	0	0
Drain	0	0.0135469086526427
Stream	0	0
Recharge	0	0
ET	0	0
Lake	0	0
TOTAL	0.030000316543022	0.030077470855522

Percent Error: -0.256848049407436

Figure 6.18. Mass Balance Dialog for Jetting Case 6. Note how 50% of the water is now leaving the system through the drain compared to only 40% in Case 5. This is a desirable effect to produce better compaction. The drainage capacity of the engineered system is utilized more effectively here, a desirable characteristic considering the uncertain drainage capacity that may be encountered in various native soils.

Now three extra cases are considered simply to demonstrate some of the capabilities of adjusting the model in response to different model setups as well as different jetting application strategies. The goal is to improve accuracy of the results, to further investigate some of the phenomena identified earlier in the paper, and to identify areas where the model may be sensitive to some of the artificial conditions imposed upon it.

Case 7: Jetting with Extra Drain Tile and Relaxation of Injection Points

An additional drain tile pipe is added right in the middle of the system at the backfill-native soil interface in column 12 for case 7. Drain tile is relatively inexpensive compared to the actual jetting operation and may significantly improve drainage capacity of the system. The drain tile is placed in this location to catch all that water that was observed in the previous cases to follow the long drainage path all the way to the constant head boundary on the other side of the wall. The second change to the model is the addition of a specified discharge out of the model. It would be most desirable to specify a discharge out of the bottom layer in the model to simulate water percolating down to greater depths below the wall in the field. However, Modflow only allows specified discharge out of surface layers. As such, a depth-integrated discharge of $10^{-5} \text{ m}^2/\text{s}$ is specified out of the right side of the model, in column 18 across the surface layer, to simulate the effect of water leaving the system through the native soil in a more direct manner.

The third change to the Case 7 model is the simplification of the jetting network to ease the implementation of a similar network by an actual crew in the field. From stress period 1 to 11, there are three injection wells operating as in the previous runs. However, from stress period 12 to 23, only two wells are turned on. During stress period 24 and 25, no wells are turned on. It is hypothesized that this 'relaxation' will reduce the extent of backed up water and improve jetting performance. Meanwhile less men will need to operate for the full length of the jetting application, and less water will need to be brought to the site, all desirable characteristics of a successful operation. Stress period 11 ends at 40 minutes, and stress period 23 ends at 80

minutes. To investigate the system sometime after jetting ends, stress period 24 and 25 are set to end at 90 minutes and 2.5 hours, respectively.

In addition to these time modifications, the spatial locations of each jetting point have been modified as well. Jetting performed with the instrument in the lower layers has been limited. It is hypothesized that water entering in the system at a higher elevation would have a greater compactive effect because the jet of water would exit with greater energy as it propagates down through the layers. On the other hand, when the probe is deeper in the backfill, the water would simply go into the drains, or worse get backed up from a lower layer all the way up to the surface. The result is a jetting network that is extended over greater space. Finally the observation well has been moved closer to the abutment wall. It is also screened a little shallower, in layers 4 and 5. Now the hydrograph will reveal the pressure heads where the worst ponding of water has taken place in the previous runs, near the injection wells and adjacent to the no flow boundary of the abutment wall.

The mass balance hydrograph for the entire system and the new three-dimensional jetting network are shown in Figures 6.19 and 6.20. Note how the system dries out entirely around 1100 seconds, or about 20 minutes after the initiation of jetting. This is a problem in Modflow, as injection wells automatically turn off when the cells around them go dry. Clearly the system is highly sensitive to the new specified discharge condition taking water out of the right side of the model. In light of this sensitivity, the no flow boundaries around the edges of the model should be far enough away from the drain and the injection points to limit their effect on flow through the system.

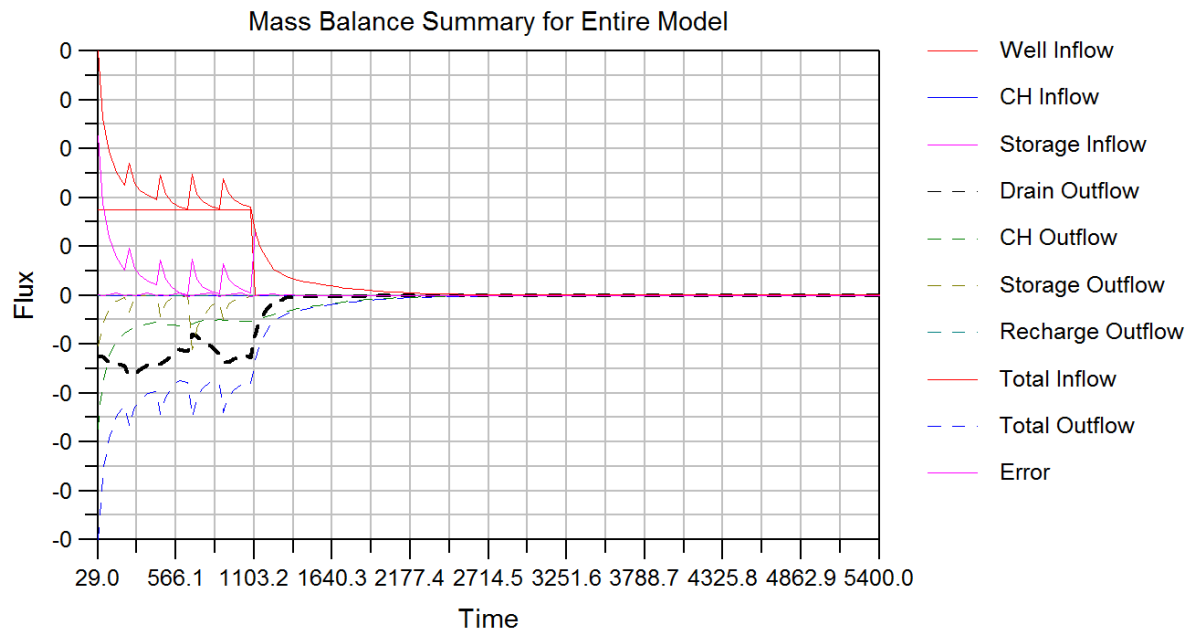


Figure 6.19. Mass balance Hydrograph for Case 7. The drain outflow is represented by the thick black dashed line.

Row / Column	8	9	10	11	12	13	14	15
1		3(14) + 5(15)		3(16) to 4(17)	2(21)			2(22)
2								
3		2(1)+4(2)+6(3)	3(8) + 5(9)	2(4) + 4(5)	2(11)	2(6)	2(10)	2(7)
4			3(20)					
5		3(12) + 5(13)		5(23)	2(18)		2(19)	
6		2(1)+4(2)+6(3)	3(8) + 5(9)	2(4) + 4(5)	2(11)	2(6)	2(10)	2(7)
7		3(12) + 5(13)		5(23)	2(18)		2(19)	
8			3(20)					
9		2(1)+4(2)+6(3)		2(4) + 4(5)	2(11)	2(6)	2(10)	2(7)
10			3(8) + 5(9)					
11					2(21)			2(22)
12		3(14) + 5(15)		3(16) to 4(17)				

Figure 6.20. Grid for Jetting Case 7-9 . Layer numbers are shown as a function of the stress period. The notation 3(12)+5(13) indicates a discrete application of the instrument to layer 3 during the 12th stress period and layer 5 during the 13th stress period.

Case 8: Jetting with No Flow Condition Far From the Abutment Wall

In Case 8, only one new change is made to the previous Case 7; the specified discharge out of the right side of the model is removed and changed back to a no flow boundary condition. This removes a sensitivity of the cells to dry out which may or may not represent what would happen in the field. The decision to remove the discharge is made simply for the sake of further analysis. The results for Case 8 at 500 seconds, 800 seconds, and 1200 seconds after the initiation of the jetting operation are shown in Figure 6.21 through 6.23, respectively below. With the new jetting network, 71 m³ of water is injected through the first 11 stress periods, or 40 minutes, and 52 m³ (2510 ft³) of water is injected through the next 11 stress periods, or additional 40 minutes of jetting. That makes for a total volume of 123 m³ (4343 ft³), significantly less than the 324 m³ (11440 ft³) applied in Case 5.

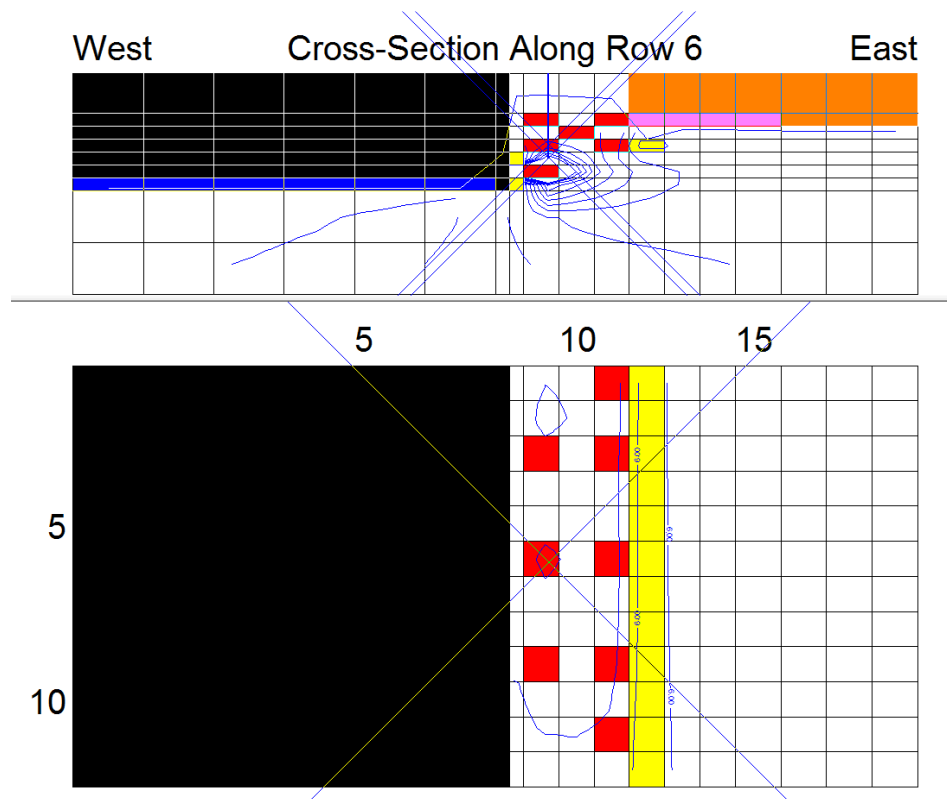


Figure 6.21. Jetting Case 8 at 500 Seconds.

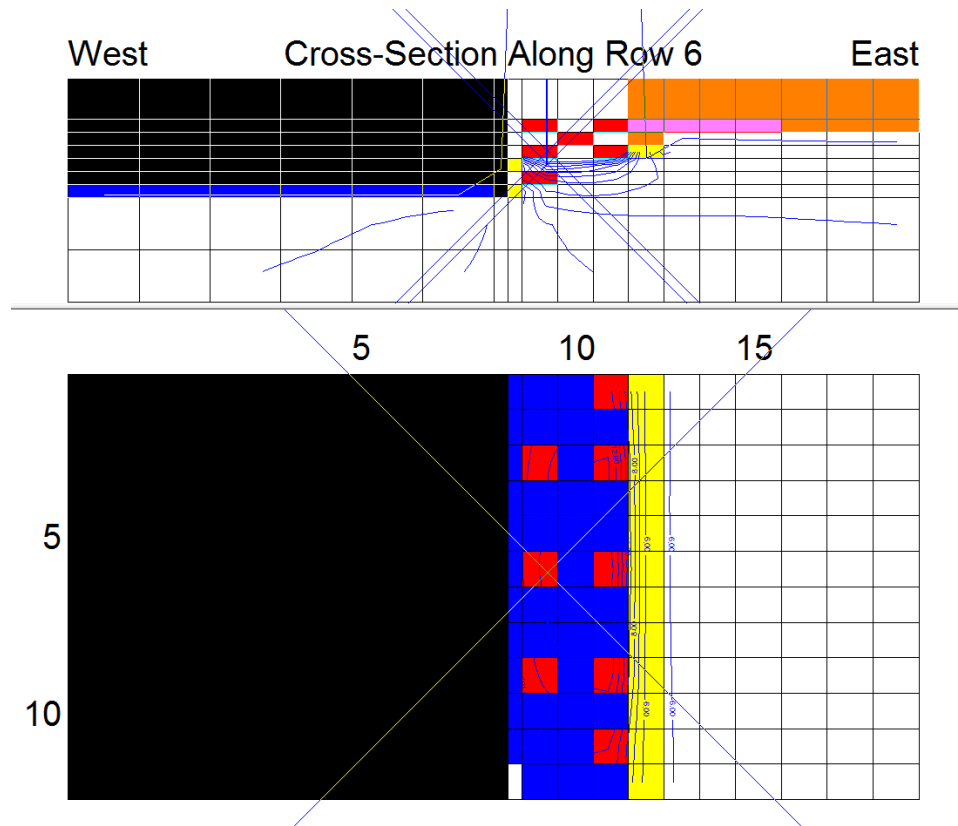


Figure 6.22. Jetting Case 8 at 800 Seconds.

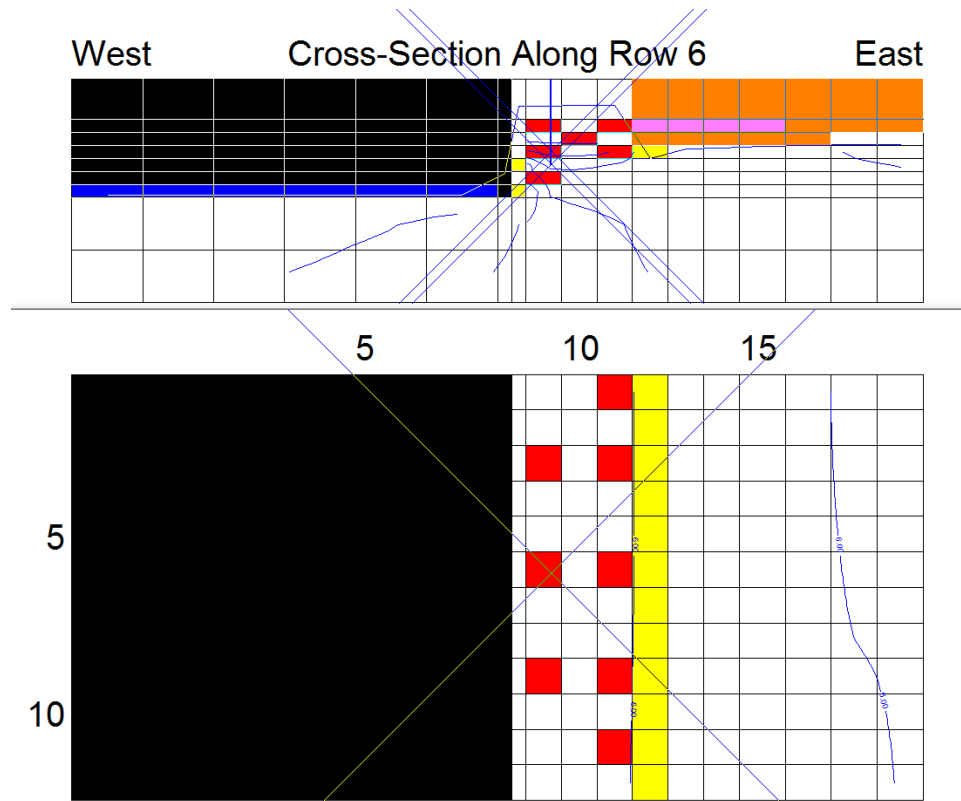


Figure 6.23. Jetting Case 8 at 1200 Seconds or 20 Minutes After Initiation of Jetting.

Note in this model run that the cells near the surface were flooded at 803 seconds, but then went dry shortly after 1200 seconds. Clearly placing the extra drain at the backfill-native soil interface greatly increases the drainage capacity of the system. In fact cells that are slowly drying out over time could be a sign the jetting is working well. It is hypothesized that the best compaction results are achieved when the drainage capacity of the system is not overwhelmed, and water exiting the jetting instrument can drain freely down through the layer.

Case 9: Jetting with Drain Tile Repositioned Against the Abutment Wall

The results of the last of the three extra cases, Case 9, can be seen in Figures 6.24 through 6.26. This case seeks to isolate the effect the previous case demonstrated where a drain placed at the backfill-native soil interface in the middle of the system greatly improved the drainage capacity of the engineered system. Now the drain is simply moved next to the abutment wall, such that there are now three drains against the wall. Placing an additional drain

higher up along the length of the wall may not only improve the capacity of the system, but it may actually passively direct more of the flow down through the backfill, instead of into the native soil, thereby increasing the compactive effect.

The extent of the ponding on the surface is minimal throughout the run. An example of this may be seen in the cross-section in Figure 6.26. The wells are spread out over a greater three-dimensional space, and they inject less water than in the previous runs. Additionally, the third drain tile gives the water another exit point next to the previously problematic no flow boundary of the abutment wall.

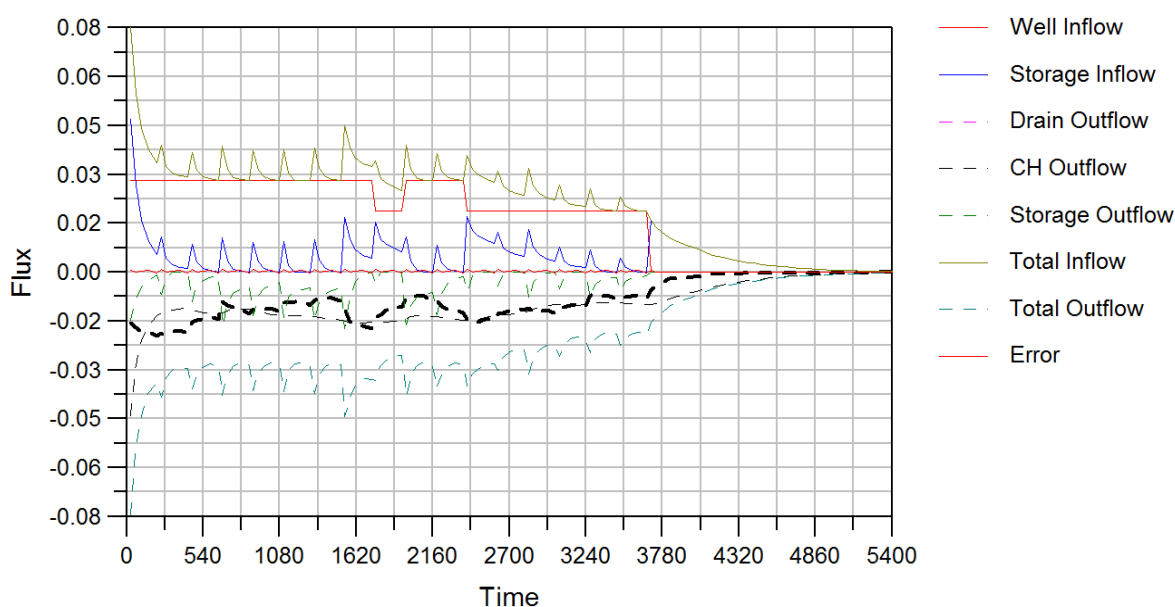


Figure 6.24. Mass Balance Hydrograph for Case 9. The drain outflow is the thick black dashed line. The units of flux are m^3/s .

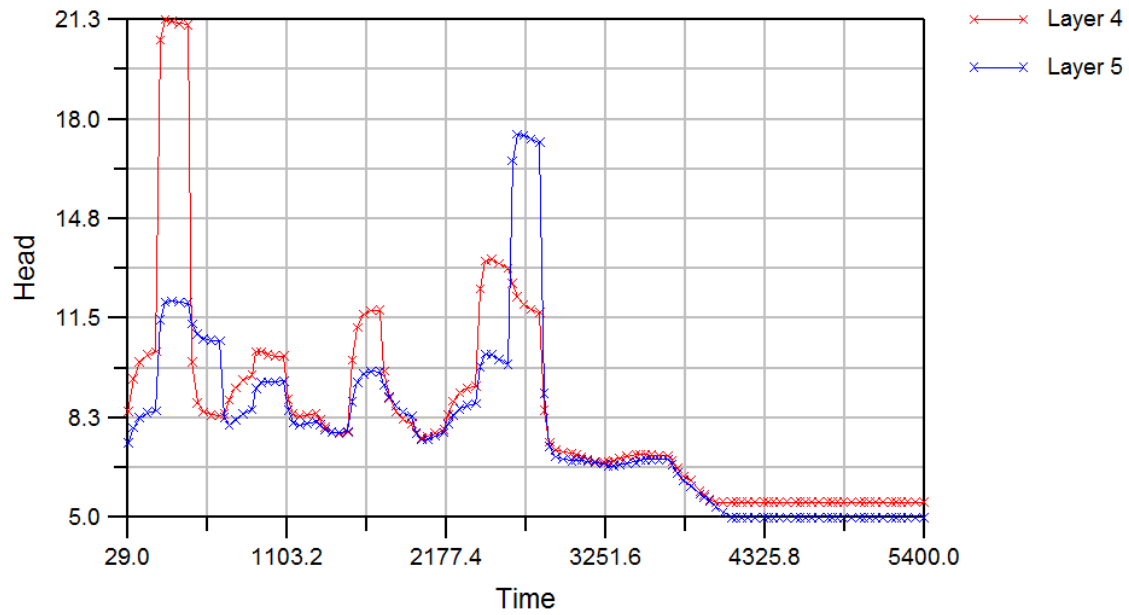


Figure 6.25. Hydrograph of Pressure Head (in meters) at the Monitoring Well for Case 9. Note the sharp increase in pressure head when an injection well is turned on next to the monitoring well near the start of jetting. Instrumenting the abutment wall with pressure transducers would be a great way to see the moment when the jet of water reaches a given depth in the backfill layer.

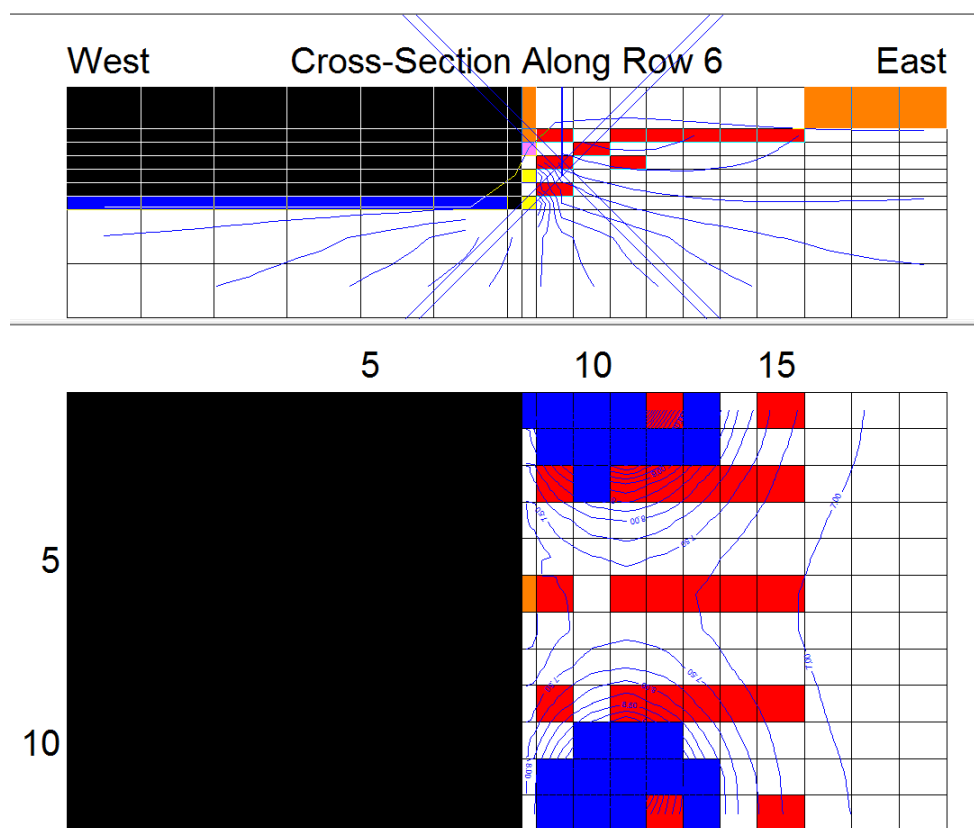


Figure 6.26. Jetting Case 9 at 54 Minutes.

6.5 Modeling Conclusions

The results of all the previous model cases may be used as evidence to make some conclusions regarding the application of jetting in the field setting:

- Injection wells (jetting points) need to be spread out over greater space and time with lower flow rates to reduce ponding on the surface. Having three men at the site to operate three instruments at the same time is beneficial to accomplishing this while reducing overall jetting time.
- The wall (the no flow boundary) tends to cause water to back up, so it will be worth the extra effort to place additional drains next to the wall in the fill provided the drains can be affixed to the same location against the wall.
- Placing a drain in the middle of the system at the backfill-native soil interface provided the greatest increase in drainage capacity of the system.
- A very large volume of water needs to be brought to the site to complete the jetting process. All the models simulated a 4 meter high abutment wall similar to the one at the Highway 51 project site. In Case 8 123 m³ (4343 ft³) of water was injected compared to 324 m³ (11440 ft³) in Case 5.

- The system is highly sensitive to changes in hydraulic conductivity of both the backfill and the native soil. It is very much necessary to determine the conductivity of each material at the site before jetting to be able to specify the flow rate out of the instrument.
- Allowing the system to relax with time greatly reduces the amount of water backed up in the system. This was observed in the three extra Cases 7-9.
- Some severe limitations were noted in the model which prevent it from making predictions of the jetting network and flow rate to an accuracy beyond a rough estimate:
 - disturbance to the soil solid matrix during jetting, i.e. changes in porosity
 - unsaturated flow, especially if the backfill were placed in dry condition
 - discharge of water out of the native soil at lower depths. Modflow does not allow a specified discharge boundary condition in anything but the top layer
 - the uncertainty inherent in these limitations is compounded by the absence of any field data in the literature or from this project

Overall the model allows for better initial estimates of a jetting network as well as flow rate and timing. Additionally recommendations can be made as to how to improve the drainage capacity of the system by strategically placing extra drains next to the wall or at the backfill-native soil interface. It has been identified that a determination of hydraulic conductivity of both the backfill and the native soils is critical before jetting is performed, and it is desirable to use coarser backfill materials to improve drainage capacity.

SECTION 7 - CONCLUSIONS

Hydraulic jetting and flooding has been investigated in the lab, in the liquefaction tank as well as the large plastic containers, and in the field at the Greenfield Avenue project site. The results from the liquefaction tank indicate that jetting produces a more compact soil structure when the energy of the water draining through the layer is increased. This is because jetting causes the soil to liquefy locally around the instrument, eliminating any capillary stress between the grains, thereby freeing them to move into a more compact arrangement. However, this comes at the expense of pushing water in between the grains, initially forcing them apart. From testing in the plastic containers, low pressure jetting has been found to produce a more compact, stiffer soil structure than dry deposition at high energy. Subsequently high pressure jetting has been found to improve the soil structure produced by low pressure jetting. Because jetting does introduce water between the grains, it is possible to create a viscous mixture with very low shear strength after jetting materials with low drainage capacity, such as the silty sand. However, each of the three sand-gravel mixtures, all clean materials with no fine particles, performed similarly in terms of density, strength, and stiffness when jetted.

At the Greenfield Avenue project site, an experienced contractor was observed jetting a buried utility pipe. The operation incorporated a unique advantage of jetting: it is possible to compact large thicknesses of backfill, as long rigid pipes may be used to introduce the jet of water deep into the layer. It was hypothesized that this type of jetting created a condition similar to the flooded deposition performed in the lab, because the water was forced into a confined space around the pipe, and beneath a large overburden. A testing program investigating flooded deposition of three natural sands currently used by the Wisconsin DOT proved that this deposition method, when combined with vibration energy, consistently produced dense soil structures, with relative densities ranging between 79% and 86%. This result was consistent

with the contractor's indication that this particular method of implementing jetting had been historically successful, despite a lack of quality control.

Meanwhile flooding, or compaction by drainage, has been investigated in the lab, in the liquefaction tank as well as the rigid wall permeameters, and in the field at the Highway 51 project site. The results from the liquefaction tank indicate that compaction by drainage has limited potential to improve a variety of soil structures, including those produced by flooded deposition, wet deposition, and dry deposition at low and high energy. The increase in effective stress, produced by the seepage force and residual matric suction following drainage, simply is not great enough to break the in situ particle contacts and move the grains into a more compact arrangement. However, uniform and rounded particles tended to form more compact soil structures upon deposition than angular particles, which exhibited greater interlocking. Falling head conductivity tests performed in the rigid wall permeameter essentially confirmed these observations.

At the Highway 51 project site, a contractor inexperienced with hydraulic methods of compaction performed compaction by drainage according to specifications developed by Wisconsin DOT personnel. The results indicated that the backfill compacted by drainage reached a greater density near the surface, and adjacent to the abutment wall, than the backfill compacted by traditional means, utilizing the steel drum vibratory roller. However, the backfill compacted by drainage beneath the surface exhibited very low shear strength during dynamic cone penetrometer measurements, and had to be dug out and recompacted by traditional means. The sandy backfill is a well-graded sand, and as such, when it is compacted to a dense condition it has a relatively low conductivity. This makes the backfill specified at Highway 51 a less than ideal candidate for compaction by drainage.

The need for a more restrictive material specification to perform flooding and jetting successfully is evident based on the results of this project. Current standards for structural backfill limit the fines in Grade 1 and Grade 2 structural backfill to no greater than 8% and 15%

passing by weight, respectively. The percent of fines in a flooding and jetting backfill should be limited to as close to zero as possible to ensure adequate drainage. A most relevant and supporting point to this recommendation is the evidence in the literature that finer natural sands are more prone to settlements and pore pressure buildup, resulting in erosion and premature damage to approach pavements and bridge structures. In this way the advantage of being able to perform flooding and jetting in confined spaces and the need for coarser materials to implement these methods are conveniently linked.

Flooding in particular should be considered a low energy compaction method that modestly improves soil structure. It is suitable for use in open country where traditional equipment is not available, and a high level of compaction is not necessary. Only a laborer, a source of water, and an instrument to fan spray the water are needed to perform flooding to induce drainage compaction. Jetting exerts much greater energy on the soil, and under the appropriate drainage conditions, can produce dense soil structures. As similar labor and equipment is needed for jetting as flooding, it is the more effective and practical method.

Finally, a compaction methodology using a free draining slurry is flooded into a backfill shows great promise. It is simple, provides a uniform compaction system and yields much better shear strength than traditional compaction equipment next to abutments. It created compacted lifts of uniform quality and shear strengths that are a greater than the shear strength and dry density of compacted lifts next to an abutment using traditional compaction equipment. However, engineers and contractors should control that the soil used to create the slurry must be both well graded (to obtain high dry density values), should have minimum to low percentage of fines (to allow free drainage and permit the generation of matrix suction) and have spherical particles to allow easy flowability..

REFERENCES

- ASTM Standard D1557, 2012, "Standard Test Methods for Laboratory Compaction Characteristics of Soil Using Modified Effort," ASTM International, West Conshohocken, PA.
- ASTM Standard D2216, 2010, "Standard Test Methods for Laboratory Determination of Water (Moisture) Content of Soil and Rock by Mass," ASTM International, West Conshohocken, PA.
- ASTM Standard D4253, 2000, "Standard Test Methods for Maximum Index Density and Unit Weight of Soils Using a Vibratory Table," ASTM International, West Conshohocken, PA.
- ASTM Standard D4254, 2000, "Standard Test Methods for Minimum Index Density and Unit Weight of Soils and Calculation of Relative Density," ASTM International, West Conshohocken, PA.
- ASTM Standard D5084, 2010, "Standard Test Methods for Measurement of Hydraulic Conductivity of Saturated Porous Materials Using a Flexible Wall Permeameter," ASTM International, West Conshohocken, PA.
- ASTM Standard D6758, 2008, "Standard Test Method for Measuring Stiffness and Apparent Modulus of Soil and Soil-Aggregate In-Place by an Electro-Mechanical Method," ASTM International, West Conshohocken, PA.
- ASTM Standard D6913, 2004, "Standard Test Methods for Particle-Size Distribution (Gradation) of Soils Using Sieve Analysis," ASTM International, West Conshohocken, PA.
- ASTM Standard D6951, 2009, "Standard Test Method for Use of the Dynamic Cone Penetrometer in Shallow Pavement Applications," ASTM International, West Conshohocken, PA.
- ASTM Standard D698, 2012, "Standard Test Methods for Laboratory Compaction Characteristics of Soil Using Standard Effort," ASTM International, West Conshohocken, PA.
- ASTM Standard D854, 2010, "Standard Test Methods for Specific Gravity of Soil Solids by Water Pycnometer," ASTM International, West Conshohocken, PA.
- Bareither, C.A.; Edil, T.B.; Benson, C.H.; Mickelson, D.M. (2008). Geological and Physical Factors Affecting the Friction Angle of Compacted Sands. *Journal of Geotechnical and Geoenvironmental Engineering*, Volume 134 (Issue 10), Pages 1476-1489.
- Berg, R.R.; Christopher, B.R.; Samtani, N.C. (2009). Design of Mechanically Stabilized Earth Walls and Reinforced Soil Slopes – Volume II. *Report No. FHWA-NHI-10-025*.
- Briaud, J.L.; Maher, S.F.; James, R.W. (1997). Bump at the end of the bridge. *Civil Engineering*, Volume 67 (Issue 5), Pages 68-70.
- Cai, C.S.; Shi, X.M.; Voyiadjis, G.Z.; Zhang, Z.J. (2005). Structural Performance of Bridge Approach Slabs Under Given Embankment Settlement. *Journal of Bridge Engineering*, Volume 10 (Issue 4), Pages 482-489.
- Cho, G.C.; Dodds, J.; Santamarina, J.C. (2006). Particle Shape Effects on Packing Density, Stiffness, and Strength: Natural and Crushed Sands. *Journal of Geotechnical and Geoenvironmental Engineering*, Volume 132 (Issue 5), Pages 591-602.
- Drnevich, V.; Evans, A.C.; Prochaska, A. (2007). A Study of Effective Soil Compaction Control of Granular Soils. *Report No. FHWA/IN/JTRP-2007/12*.

- Greimann, L.; Phares, B.; Faris, A.; Bigelow, J. (2008). Integral Bridge Abutment-to-Approach Slab Connection. *Report No. IHRB Project TR-530 & TR-539*.
- Krumbein, W. C. (1941). "Measurement and geological significance of shape and roundness of sedimentary particles." *Journal of Sedimentary Petrology*, 11(2), 64-72.
- Laba, J. T. (1983). Cohesive soil compaction by water jetting. *Canadian Geotechnical Journal*, Volume 20 (Issue 3), Pages 393-405.
- Massarsch, K.R.; Fellenius, B.H. (2005). Deep Vibratory Compaction of Granular Soils. Ground Improvement Case Histories (Chapter 19): Elsevier Publishers, B. Indranatna and C. Jian, Editors, Pages 633-658.
- Mayne, P.W.; Jones, J.S.; Dumas, J.C. (1984). Ground Response to Dynamic Compaction. *Journal of Geotechnical Engineering*, Volume 110 (Issue 6), Pages 757-774.
- Monahan, E.J. (1994). *Construction of Fills* (2nd Edition): New York, NY: John Wiley & Sons.
- Moser, A.P.; Folkman, S. (2008). *Buried Pipe Design* (3rd Edition): McGraw-Hill.
- Office of Radiation Safety, University of Wisconsin-Madison. (2005). *Radiation Safety for Radiation Workers*. Madison, WI: Board of Regents.
- Schaefer, V.; Suleiman, M.T.; White, D.J.; Swan, C.; Jensen, K. (2005). Utility Cut Repair Techniques – Investigation of Improved Cut Repair Techniques to Reduce Settlement in Repaired Areas. *Report No. IHRB Project TR-503*.
- Sladen, J.A.; Hewitt, K.J. (1989). Influence of placement method on the in situ density of hydraulic sand fills. *Canadian Geotechnical Journal*, Volume 26 (Issue 3), Pages 453-466.
- White, D.J.; Mekkawy, M.M.; Sritharan, S.; Suleiman, M.T. (2007). "Underlying Causes for Settlement of Bridge Approach Pavement Systems. *Journal of Performance of Constructed Facilities*, Volume 21 (Issue 4), Pages 273-281.
- Wisconsin Department of Transportation. (2013). *Standard Specifications for Highway and Structure Construction*. Section 209, Granular Backfill. Pages 108-109.
- Zhou, J.; Han, J.; Jia, M.C.; Lin, X. (2008). Laboratory Model Study on Densification of Hydraulically-Filled Fine Sands by Vibro-compaction. *Proceedings of Session of GeoCongress 2008: Geosustainability and Geohazard Mitigation*, Pages 700-707.

APPENDIX A

This section details the errors associated with each measurement made in the liquefaction tank tests described in Section 4, and the impact of those errors on the accuracy of subsequent void ratio calculations. A brief sensitivity analysis was conducted in Section 4.2.4, but this analysis did not consider specific, quantifiable errors together with the exact degree which the errors affect the calculated void ratios. Instead, two purely hypothetical situations were considered where the water content and total height of a soil column were mis-measured by 4% and 1 cm, respectively. The conclusion was made that if these measurements were incorrect by the hypothetical amount, then the relative density of the material between identical trials of dry deposition at high energy would have been the same. In fact, the results between the two identical trials were fairly consistent; five of the six soils exhibited changes in relative density of 10% or less, and all of the soils exhibited changes in post drainage water content of 5.5% or less.

With these preliminary results, the conclusion was made that relative density could confidently be used to indicate general performance trends of the materials, but strength and stiffness could be more reliable indicators of the physical processes at work. To validate (or refute) the use of relative density as a general indicator of performance, the errors during two different tests, flooded deposition and wet deposition followed by drainage compaction, are detailed herein. The mass of solids in the tank was calculated by different means during these tests, making them good candidates for this more thorough analysis. This difference in the measurement of solids was the only difference in measurement methods between all the tests, including both drainage compaction and jetting tests.

The material selected for this analysis is the silica sand. The silica sand has a minimum void ratio of 0.545 and a maximum void ratio of 0.800, yielding the sixth largest range between the minimum and maximum void ratio of the eleven materials tested. With the range near the

median of all the ranges, the silica sand will exhibit a moderate sensitivity of relative density to errors in the calculation of void ratio.

A.1 VOID RATIO CALCULATION FOR FLOODED DEPOSITION

The void ratio calculation for flooded deposition as well as the other dry deposition methods was simpler than that for wet deposition because the mass of solids placed into the tank could be measured directly before deposition. This is represented below in Table A.1, which shows the set of equations presented in Section 4: the mass of solids, m_s , seen in equation 4.6 was measured directly. During wet deposition the mass of solids had to be indirectly calculated after the test by measuring the water content of the soil column. This is represented in equations 4.4 and 4.5: here a uniquely determined system of equations is solved by relying on the water content after drainage to indirectly determine the mass of solids. Therefore the flooded deposition tests are expected to have smaller errors than the wet deposition tests. Further supporting this expectation is the observation that very smooth, flat surfaces on the soil column were produced during flooded deposition. During wet deposition, the slugs fell in such a way that the surface sloped and dipped against the tank walls.

Table A.1. Phase Calculations as Presented in Section 4.

$V_{total} = \frac{\pi}{4} d_{tank}^2 \bar{h}_{tank}$	(4.3)
$w = \frac{m_w}{m_s}$	(4.4)
$m_{solids} = \frac{m_{total}}{1 + w}$	(4.5)
$V_{solids} = \frac{m_s}{G_s}$	(4.6)
$V_{voids} = V_{total} - V_{solids}$	(4.7)
$e = \frac{V_{voids}}{V_{solids}}$	(4.8)
$D_R = \frac{e_{max} - e}{e_{max} - e_{min}}$	(4.9)

The measurements made in the tank used in the above calculations are detailed in Table A.2. The total height of the soil columns before and after drainage was measured by five meter sticks glued around the outside of the tank. Because a geotextile lay at the bottom of the inside of the tank, a separate meter stick was used to apply a height correction to each of the measurements made on the outside of the tank. Each of the meter sticks was accurate to 1 mm. The diameter of the tank was measured by a caliper accurate to 0.02 mm. The mass of solids was measured on a balance with precision to 0.1 g, but likely only accurate to 0.5 g, as the displayed value fluctuated up or down by about this amount. The specific gravity of solids, used to calculate the volume of solids from the mass of solids measurement, and shown in equation 4.6, was measured by the water pycnometer. The pycnometer method was likely highly accurate, as care was taken to remove all the bubbles by agitating the flask under the vacuum, and measuring its mass with a balance precise and likely accurate to 0.01 g.

With careful consideration of the nature of each of these measurements, quantifiable errors can be built in to the calculation of void ratio. These quantifiable errors, and their discrete as well as cumulative effect on void ratio and relative density, before and after drainage, are shown in Table A.3. The left half of the table shows the most important measurements made, or measurements that were made before drainage. Because the mass of solids could be measured directly before deposition during the flooded and dry deposition tests, the only additional measurements necessary after drainage to calculate the change in void ratio are the total heights used to determine the new total volume of the column. The same mass of solids are within the tank before and after drainage. The table shows each of the errors, here elaborated in detail:

- 1) average height of the soil column error, from the five meter sticks used to measure the flat surface produced during dry deposition
- 2) diameter of the soil column error from the caliper
- 3) height of the geotextile correction error, from a meter stick placed inside the tank on top of the geotextile, and outside the tank level against each of the five meter sticks

- 4) mass of the solids error, from the larger balance, which fluctuated slightly, and also from the possibility that a few grains spilled outside the tank during deposition
- 5) specific gravity error, from the smaller balance, and also from the possibility that a few air bubbles remained in the flask during vacuum agitation

These errors are quantified as 0.2 cm, 0.04 mm, 0.1 cm, 10.0 g, and 0.005, from one to five in the above numbering system. The errors are chosen such that each would reduce the void ratio from the as measured 0.730 before drainage. Even in this worst case scenario, with the accumulation of all the errors, the void ratio decreases by 0.023, and the relative density increases by 7.8%. While it is not prudent to report the void ratio to three decimal places, as was done in Section 4, the analysis here confirms that relative density is a good general indicator of performance for flooded deposited materials. It is unlikely that each of these errors, which were chosen as fairly large in magnitude based on reasonable expectation, would all have the sign (positive or negative) that decreases the measured void ratio. Finally, upon examining the right side of the table, the changes observed in the height of the soil column after drainage, which were on the order of 1 mm or possibly 2 mm, can be seen to change the void ratio by just a few thousandths. The error in the calculation of the change in void ratio is very small because the small changes in the height of the soil column could be observed by examining the meter sticks. The meter sticks remained in the same place against the side of the tank, and thus showed very well how the same soil column, which was only disturbed by drainage, subsided to a new height.

Table A.2. Measurements Made During Silica Sand, Flooded Deposition Test.

Silica Sand, Flooded Deposition test (detailed in Table 4.2)									
Before Drainage Measurements							After Drainage Measurements		
i	h_i (cm)	d_{tank} (cm)	$h_{\text{geotextile_corr.}}$ (cm)	m_s (g)	G_s	$e_{\text{before_drain}}$	i	h_i (cm)	$e_{\text{after_drain}}$
1	28.8	20.322	0.2	14047	2.662	0.730	1	28.7	0.724
2	28.3						2	28.3	
3	27.9						3	27.8	
4	27.6						4	27.5	
5	28.1						5	28.0	

Table A.3. Reasonable Estimate of Errors Made During Silica Sand, Flooded Deposition Test.

Accumulation of Errors in Silica Sand, Flooded Deposition test								
Before Drainage Measurements				After Drainage Measurements				
i	Error _{before_drain (i)}	e _{before_drain (i)}	D _{R (i)}	i	Error _{after_drain (i)}	Original Δ height (cm)	e _{after_drain (i)}	$\Delta e_{(i)}$
0	--	0.730	27.5	0	--	-0.1	0.701	-0.006
1	Average height error = 0.2 cm	0.718	32.2	1	Avg. Δ height error = -0.1 cm		0.694	-0.013
2	Diameter of tank error = 0.04 mm	0.717	32.5	2	Avg. Δ height error = +0.1 cm		0.707	0.000
3	Height of geotextile error = 0.1 cm	0.711	34.9					
4	Mass of solids error = 10.0 g	0.710	35.3					
5	Specific gravity error = 0.005	0.707	36.5					

A.2 VOID RATIO CALCULATION FOR WET DEPOSITION

As mentioned earlier, the void ratio calculation for wet deposition was more involved than the other test methods because the mass of solids could not be measured directly. During wet deposition, the solids were first mixed in a bucket to a qualitative wetness or viscosity before being deposited. For this reason, new errors were introduced in the form of using the total weight of the tank and water content of the soil column *after* drainage to determine the mass of solids. The measurements made before and after drainage are detailed in Table A.4, and the errors associated with these measurements are shown in Table A.5.

The errors numbered one to four in the left half of Table A.5 represent the same measurements as those made during flooded deposition. Because the nature of the errors are the same, the magnitude of the errors are quantified the same in this analysis. However, two new errors are introduced during wet deposition, here elaborated in detail:

- 5) total weight of tank error, from placing the tank on an old style Toledo counterweight scale accurate to 0.045 kg (0.1 lbs)
- 6) water content error, from dumping the entire soil contents within the tank into an empty bucket, thorough mixing the contents, then taking three samples to the oven from different depth within the bucket

These two errors are 0.091 kg (0.2 lbs) and 1.0%, respectively. The results show that the addition of these errors is significant, as they decrease the void ratio by 4.7% and 2.0%, respectively. Even more concerning is that the total change in relative density due to the accumulation of all the errors is 16.8%, from an as measured 62.4% to 79.2%. Fortunately the wet deposition tests were the only tests that utilized this method to calculate the volume of

solids in the tank, a critical component of determining the void ratio before and after drainage. At least for wet deposition tests, the void ratio should only be reported to one to two significant figures.

The increased magnitude of the error seen here may explain some of the more extremely high (and low) relative densities seen in the wet deposition tests in Section 4.2.2. For example, the relative density of the foundry sand during the less wet trials was measured to be 95.5% after drainage. It seems unlikely that simple wet deposition followed by drainage could produce a structure nearly as compact as that achieved by vibrating the sand for 15 minutes with a large lead weight surcharge.

Table A.4. Measurements Made During Silica Sand, Wet Deposition Test.

Silica Sand, Wet Deposition test (detailed in Table 4.3)											
After Drainage Measurements								Back-calculated Before Drainage Void Ratio			
i	h_i (cm)	d_{tank} (cm)	$h_{\text{geotextile_corr.}}$ (cm)	w (%)	w_{total} (lbs)	G_s	$e_{\text{after_drain}}$	i	h_i (cm)	m_s (g)	$e_{\text{before_drain}}$
1	29.0	20.322	0.2	23.0	39.9	2.662	0.641	1	29.1	14714.2	0.647
2	27.7							2	27.8		
3	27.1							3	27.3		
4	27.7							4	27.8		
5	28.3							5	28.3		

Table A.5. Reasonable Estimate of Errors Made During Silica Sand, Wet Deposition Test.

Accumulation of Errors in Silica Sand, Wet Deposition test								
After Drainage Measurements				Back-calculated Before Drainage Void Ratio				
i	Error _{after_drain (i)}	$e_{\text{after_drain (i)}}$	$D_{R (i)}$	i	Error _{before_drain (i)}	Original Δ height (cm)	$e_{\text{before_drain (i)}}$	$\Delta e_{(i)}$
0	--	0.641	62.4	0	--	-0.1	0.592	-0.006
1	Average height error = 0.2 cm	0.629	67.1	1	Avg. Δ height error = -0.1 cm		0.587	-0.011
2	Diameter of tank error = 0.04 mm	0.628	67.5	2	Avg. Δ height error = +0.1 cm		0.598	0.000
3	Height of geotextile error = 0.1 cm	0.622	69.8					
4	Specific gravity error = 0.005	0.619	71.0					
5	Total weight of tank error = 0.2 lbs	0.611	74.1					
6	Water content error = 1.0 %	0.598	79.2					

A.3 CONCLUSIONS FROM MEASUREMENT ANALYSIS

The analysis shows that for every deposition method besides wet deposition, relative density is reliable as a general indicator of performance, consistent with the way it was used in the body of this report. However, the errors for wet deposition have been shown to produce larger variations in the measured void ratio and calculated relative density. For these tests especially, relative density must be used with caution in evaluating the results. However, the analysis in this appendix should be considered conservative, as it is unlikely that all of the errors would have the sign (positive or negative) that decreases the measured void ratio.



WHRP

Wisconsin Highway Research Program
University of Wisconsin – Madison
1415 Engineering Drive
Madison, WI 53706
<http://wisdotresearch.wi.gov/whrp>